NCHRP Web Document 50 (Project D10-37C): Contractor's Final Report

Repair and Rehabilitation of Bridge Components Containing Epoxy-Coated Reinforcement

Prepared for:

National Cooperative Highway Research Program
Transportation Research Board
National Research Council

Submitted by:

Ali Akbar Sohanghpurwala
CONCORR, Inc.
Sterling, Virginia

William T. Scannell
ConcorrFlorida, Inc.
Merrit Island, Florida

William H. Hartt
Florida Atlantic University
Boca Raton, Florida

August 2002

ACKNOWLEDGMENT

This work was sponsored by the American Association of State Highway and Transportation Officials (AASHTO), in cooperation with the Federal Highway Administration, and was conducted in the National Cooperative Highway Research Program (NCHRP), which is administered by the Transportation Research Board (TRB) of the National Research Council.

CONTENTS

ACKNOWLEDGMENTS

The work reported herein was performed under NCHRP Project 10-37C by CONCORR, Inc. and the Department of Ocean Engineering, Florida Atlantic University. CONCORR, Inc. is the contractor for this study. Work at Florida Atlantic University is being conducted under a subcontract with CONCORR, Inc.

The principal investigators and authors of this report are: Ali Akbar Sohanghpurwala principal of CONCORR, Inc., William T. Scannell former principal of CONCORR, Inc., now principal of ConcorrFlorida, Inc. and Dr. William H. Hartt, professor of the Department of Ocean Engineering, Florida Atlantic University.

The authors express their sincere gratitude to the following individuals for all their assistance in identifying bridge structures for the field validation studies: Mr. Rodney G. Powers and Mr. Ivan R. Lasa, Florida Department of Transportation; Mr. William J. Winkler and Mr. Gerald R. Perregaux, New York State Department of Transportation; and Mr. Gerald J. Malasheskie, Pennsylvania Department of Transportation.

The authors are indebted to Mr. Donald R. Jackson, Federal Highway Administration, for making valuable information, obtained under Demonstration Project 84, available to this project.

The authors also wish to thank Dr. Yash P. Virmani, Federal Highway Administration, for authorization to utilize existing concrete slabs at the Turner Fairbanks Highway Research Center. Thanks are also extended to Mr. and Mrs. Kenneth C. Clear, TMB Associates, Inc. for generously donating numerous concrete specimens and providing the necessary historical information of these specimens.

SUMMARY OF FINDINGS

The primary goal of this effort was to address the anticipated need for premature repair and rehabilitation of concrete bridge elements containing epoxy-coated rebar (ECR). Laboratory, test yard, and field studies were conducted to evaluate and validate applicable strategies. The performance of each strategy was judged by the level of corrosion protection afforded in and outside the repair area. Based on the results of this effort, credible information available in literature, and the collective experience of the research team, a decision matrix was developed. The decision matrix matches appropriate repair and rehabilitation strategies to the damage mode, present condition, environmental exposure, and future propensity of corrosion. The evaluation of strategies was subdivided into two categories, one applicable to the mitigation of corrosion in cracks and the other to delaminations and spalls.

Several possible combinations of an epoxy injection material and two corrosion inhibitors were evaluated for corrosion mitigation in both corrosion and non-corrosion induced cracks. Injection of cracks was accomplished using bisphenol A and polyamine curing agent. Of the two surface applied (migrating) corrosion inhibitors used, one contained water based amine and an oxygenated hydrocarbon and the other contained calcium nitrite as the active agent. None of the repair strategies evaluated in this category exhibited any ability to provide protection against corrosion in the two spheres of interest; that is, 1) directly at the crack and 2) area adjacent to the cracks.

Various combinations of three patch materials (pre-bagged Portland cement concrete, pre-bagged polymer modified silica fume concrete, and Class III Portland cement concrete), three rebar

coatings (epoxy coating, water based epoxy resin/Portland cement coating, and water based alkaline coating with corrosion inhibitor), and four corrosion inhibitors (water based amine and an oxygenated hydrocarbon migrating corrosion inhibitor, water based amine and an oxygenated hydrocarbon admixture, calcium nitrite admixture, and a multi-component corrosion inhibitor and concrete densifier admixture) were used in the evaluation of repair strategies applicable to delaminations and spalls. No benefit was discernable from the use of admixed and migrating corrosion inhibitors in repair areas and/or areas adjacent to the repair. The best response from a corrosion protection standpoint was demonstrated by a high resistance, low permeability silica fume modified patch material and an epoxy rebar coating compatible with ECR in the repair area. The water based alkaline coating with corrosion inhibitor showed promise in providing protection in the repair area.

Impressed current cathodic protection applied to slabs for over 7.2 years successfully mitigated corrosion. The control slabs continued to corrode and experience corrosion induced damage, whereas, the cathodically protected ones did not suffer corrosion induced damage. Also, the current densities used to protect black reinforcing steel were found to be adequate to protect ECR.

CHAPTER 1

INTRODUCTION AND RESEARCH APPROACH

INTRODUCTION

Early research by the National Bureau of Science (now National Institute of Standards and Technology) and the Federal Highway Administration indicated that reinforcing bars that were cleaned and then coated with select powdered epoxies using an electrostatic spray process performed well in salt contaminated concrete (1). Such coated rebars were determined to be resistant to corrosion, such that premature deterioration of concrete due to the pressures generated by expansive corrosion products was minimized.

Epoxy resins are thermosetting poly-addition polymers and have, for the most part, been reported to have good long-term durability in concrete and to be resistant to solvents, chemicals and water (2). In addition, epoxy resins generally possess the necessary mechanical properties for such service including good ductility, small shrinkage upon polymerization and good heat resistance (3). Further, test results have indicated that the oxygen and chloride ion permeabilities of epoxy coatings are relatively low, even in worst case exposures (1, 2, 4). Epoxy coatings are, on the other hand, permeable to moisture (water); and it has been known for years, although not highlighted within the highway community, that the adhesion of epoxy based coatings to steel is reduced upon exposure to moisture (5). Thus, the fundamental attribute by which an epoxy coating affords corrosion protection to substrate steel arises from its barrier nature which retards ingress of chloride ions and oxygen. Also, by increasing the electrical resistance between neighboring coated steel locations, these coatings reduce the magnitude of macroscopic

corrosion cell action, the latter being generally considered as responsible for premature bridge deck deterioration (6).

By 1975 ten U. S. State Highway Departments had constructed bridge decks with epoxy-coated bars; and during the next decade the use of this product became widely adopted by highway agencies with freeze-thaw climates or coastline exposures (or both). Also, life cycle cost analyses utilizing epoxy-coated rebars (ECR) performance assumptions which were considered appropriate indicated that the increased initial cost of this material (ECR) in lieu of black steel would be recovered because of reduced latter life maintenance expense (7). That this technology has been widely accepted is exemplified by the fact that most state highway agencies now have a considerable inventory of bridges with ECR (8). In Canada, Ministry of Transportation, Ontario standardized the use of epoxy-coated steel for the top mat of bridge decks and in curb and lane barrier walls in 1978; and in 1981 epoxy-coated rebars were specified for some substructure components. Other provinces and agencies in that country have also used epoxy coated reinforcing steel.

The initial developmental and field investigations of ECR performance were generally positive with regard to the protection afforded to embedded steel and the utility of this methodology for corrosion control (3, 6, 7, 9-23). Subsequent laboratory and outdoor exposure studies were also generally positive (24, 25). Beginning with the disclosure that the splash zone region of ECR substructure elements in Florida Keys bridges exhibited corrosion induced concrete cracking and spalling after only six to nine years exposure (8, 26-29), many questions pertaining to the corrosion resistance of ECR in concrete were raised, however, they have been readdressed by several recent comprehensive studies (30-32). It was the general conclusion from these that, although concrete damage from ECR corrosion is not presently widespread, this corrosion

control alternative is not likely to provide the relatively maintenance free service life that was forecast earlier and that extensive repairs and rehabilitations will ultimately be required during the anticipated service life of many structures. In support of this, the ECR corrosion induced distress that has been observed in the field (8, 26-31,33-34) has been reproduced in the laboratory and test yard and mechanisms for its occurrence identified (30-32). The overall North American experience with the corrosion performance of ECR to the mid 1990's has been summarized by Manning (35).

RESEARCH OBJECTIVE

NCHRP Project 10-37C was developed to address the anticipated need for premature repair and rehabilitation of concrete bridge structures containing ECR. Laboratory, test yard, and field studies were deemed necessary in order to evaluate and validate ECR bridge member repair and rehabilitation strategies. The main objective of this research was to identify short-, medium-, and long-term strategies for repair and rehabilitation of distressed concrete bridge components containing ECR. The anticipated final product was a decision matrix that defines repair and rehabilitation strategies as a function of the bridge component, environment severity, condition of the component, life expectancy of the technique, and the post-repair life expectancy of the bridge member.

RESEARCH APPROACH

To accomplish the goals of the project, all possible damage modes for ECR were first defined, followed by the identification of all possible repair and rehabilitation strategies applicable to these modes of damage. Several pre-qualifying criteria for inclusion in the study were then

applied to the large number of candidate repair and rehabilitation strategies so that the project objectives could be met within the existing fiscal and time constraints.

The performance of the qualified repair and rehabilitation strategies were evaluated over periods from 13 to 31 months on new specimens constructed in this study (25 beams), new specimens that incorporated old specimens (5 beams using 15 old specimens), old specimens available from previous studies (10 slabs), a northern bridge deck (5 test areas), and select columns of a marine bridge structure (39 columns). Sufficient numbers of new specimens were constructed and appropriate damage modes artificially generated to allow the implementation of all pre-qualified strategies. Due to the limited availability of old specimens and the presence of limited damage modes on the bridge deck and the columns of the bridge, only select pre-qualified strategies were evaluated on them.

These evaluations were performed under accelerated chloride ion exposure with the new and the combination of the old and the new specimens exposed to the southern Florida climate and the old specimens exposed to the northern Virginia climate. The strategies implemented on the bridge deck and the marine substructure elements were evaluated under normal exposure conditions.

Limited laboratory evaluations of the effect of cathodic protection on the epoxy coating were also performed.

Based on the findings of this study and information available in literature, a decision matrix was developed. The decision matrix matches appropriate repair and rehabilitation strategies to the damage mode, present condition, environmental exposure, and future propensity of corrosion.

CHAPTER 2

FINDINGS

IDENTIFICATION OF REPAIR AND REHABILITATION STRATEGIES

The damage modes experienced by a reinforced concrete element can be categorized based on the cause(s) of deterioration, namely non-corrosion induced, corrosion induced, or damage induced by the combination of both (i.e. combined). The combined category is an example of damage that initiates due to one or more factors not related to corrosion and renders the area more susceptible to corrosion induced damage. Subsequently, corrosion is initiated and further propagation of the damage is controlled by the original cause and/or corrosion of the ECR. The damage that results from one or more of the causes manifests itself in one of two forms, concrete cracking and delamination of concrete. With time delaminations fail, and a spall is generated. However, no delineation is made between delaminations and spalls as they both require the same repair.

The following categories were selected for evaluation from the combination of causes and types of damage:

1. Non-corrosion Induced Cracking
2. Corrosion Induced Cracking
3. Corrosion Induced Delaminations

The analysis that resulted in the selection of these categories for inclusion in the project is described in detail in Appendix A.

Repair strategies applicable to each category described above were identified from the collective experience of the industry as available in literature and from project team experience. Effort was made to insure that strategies with applications in marine, deicing, and combined environments were included for pre-qualification. In this report the term "repair" is defined as a remedial undertaking which is performed to 1) restore a concrete element to an acceptable level of service, 2) restore a concrete element to an acceptable level of service while simultaneously also addressing the cause of corrosion, or 3) to mitigate corrosion only.

As the project fiscal and time constraints would not allow the evaluation of all strategies identified, the following pre-qualifying criteria were applied to filter out strategies for inclusion in the study:

1. The strategy should be expected to have a direct and positive impact on the future corrosion performance of the epoxy-coated reinforcing steel.
2. Each technique or material should not have any known adverse effects on epoxy-coated reinforcing steel.
3. Emphasis should be placed on strategies which have a history of success on bare reinforcing steel. Although new strategies were considered, none were identified.
4. In conjunction with item 3, each strategy should have some probability of success based on current knowledge even if adequate long-term performance information on bare reinforcing steel is not available (e.g. surface applied corrosion inhibitors).

This exercise resulted in the selection of the following strategies for inclusion in the project:

1. Non-Corrosion Induced Cracking
    a. no-repair
    b. epoxy injection of cracks
    c. flood cracks with corrosion inhibitor
    d. flood cracks with corrosion inhibitor and epoxy injection
2. Corrosion Induced Cracking
    a. no-repair
    b. epoxy injection of cracks
    c. flood cracks with corrosion inhibitor
    d. flood cracks with corrosion inhibitor and epoxy injection
    e. flood cracks with corrosion inhibitor, followed by epoxy inject and surface application of corrosion inhibitor
3. Corrosion Induced Delaminations
    a. no-repair
    b. patch repair
    c. recoat steel exposed in the delamination and patch
    d. recoat steel and patch with corrosion inhibitors admixed in the patch material
    e. recoat steel, patch, and apply corrosion inhibitor on the surface
    f. recoat steel, patch with corrosion inhibitors admixed in the patch material, and apply corrosion inhibitor on the surface

Tables 1 and 2 present the materials and specimen types used in the evaluation of the above strategies, respectively.

As cathodic protection is recognized as the only protection strategy available to stop corrosion on black steel, its application on ECR was also evaluated.

Table 1: Materials Used in the Implementation of Repair Strategies

Material	Description
Epoxy Injection	bisphenol A and polyamine curing agent
Patching Material A	pre-bagged Portland cement concrete
Patching Material B	pre-bagged polymer modified silica fume concrete
Patching Material C	Class III Portland cement concrete, Florida DOT standard specifications
Coating Material A	epoxy coating
Coating Material B	water based epoxy resin/Portland cement coating
Coating Material C	water based alkaline coating with corroion inhibitor
Corrosion Inhibitor A	water based amine and an oxygenated hydrocarbon for surface application
Corrosion Inhibitor B	calcium nitirite based inhibitor for surface application
Corrosion Inhibitor C	water based amine and an oxygenated hydrocarbon for use as admixture
Corrosion Inhibitor D	calcium nitirite based inhibitor for use as admixture
Corrosion Inhibitor E	multi-component admixture with corrosion inhibitor and concrete densifier

Table 2: Specimen Types Used in the Project

Specimen Type	Description
NCD Macrobeams	concrete beams with simulated cracks of various widths over ECR
G109 Macrobeams	concrete beams contaning ASTM G-109 specimens with ECR
FHWA Slabs	concrete slabs constructed with ECR in a previous FHWA study
Bent Bar Slabs	concrete slabs with straight and bent ECR from a previous study
PCS Beams	beams with sections manufactured using poor quality concrete and ECR
Cathodic Protection Slabs	concrete slabs with impressed current cathodic protection system installed
Duanesburg Bridge Deck	ECR bridge deck located in Daunesburg, New York
7 Mile Bridge	ECR columns of the 7 Mile Bridge located in the Florida Keys

With the exception of the bridge structures and cathodic protection slabs, the performance of the selected strategies and materials was evaluated under accelerated and aggressive chloride exposure. The test specimens were subjected to a two week wet, two week dry ponding cycle using a 15 % NaCl solution. Such an aggressive exposure condition was necessary to allow differentiation between strategies and materials within the project time constraints.

The primary goal of these evaluations was to ascertain the level of corrosion mitigation provided by each strategy and material evaluated. Any strategy or material used in corrosion mitigation has two spheres of impact, first, within the area of repair (i.e. crack or delamination) and second, the area adjacent to the area of repair. The application of repair itself can result in the development of additional corrosion cells outside the treated area, and thereby, limit the positive impact of the repair. Some strategies by design are limited to affect only the repair area and others are designed to impact both spheres.

Epoxy injection of cracks, patching of delaminations, and recoating of rebars are, by design, limited to mitigate corrosion only in the specific area of repair or application, whereas, all other strategies with corrosion inhibitors are designed to impact both spheres. Thus, the performance of the epoxy injection, patching, and steel recoating, should be judged by their ability to eliminate anodic sites in the crack or the delamination, as applicable, whereas, all strategies that include corrosion inhibitors should be judged by their ability to mitigate corrosion in both the repair and the surrounding areas. Cathodic protection of bridge decks is a special case, as this method is normally applied over the entire surface of the reinforced concrete element. As such, it is expected to protect all ECR in the subject element.

The strategies are so organized that they can reflect the incremental increase in improvement due to either a totally different strategy or an additional element to the previous strategy. The following examples are listed to clarify the organizational structure of the strategies:

Strategy 1 No-Repair

Strategy 2 Patch with Portland cement concrete

Strategy 3 Recoat steel with epoxy coating and patch with Portland cement concrete

Strategy 4 Recoat steel with epoxy coating and patch with Portland cement concrete admixed with a corrosion inhibitor

In this list of strategies selected for corrosion induced delaminations, Strategy 2 is very different from Strategy 1, whereas, Strategy 3 adds recoating to Strategy 2, and Strategy 4 adds admixed corrosion inhibitors to Strategy 3, and so on. This organization of strategies allows detection of incremental improvement, for example, better performance of Strategy 3 over Strategy 2 can be attributed to recoating. Similarly, the incremental performance improvement provided by each material can be identified. Although, more than one patch and coating materials were evaluated, in the actual organization of strategies, one patch material and the coating material was used in all strategies in which they were not the primary target of the evaluation. Findings of the performance of each material are presented below for each category.

REPAIR STRATEGIES FOR NON-CORROSION INDUCED CRACKING

The matrix of repair strategies, materials, and specimen types for this category is provided in Table 3 and a detailed description of the evaluation and a discussion of the results are presented in Appendix B.

Table 3: Matrix of Strategies, Materials, and Specimen Types for Non-Corrosion Induced Cracking

Strategy #	Repair Strategy	Materials		Specimen Types
		Epoxy Injection	Corrosion Inhibitor (Surface Applied)	
A	No-repair			NCD Macrobeams
B	epoxy injection of cracks	tested		NCD Macrobeams
C	flood cracks with corrosion inhibitor		A	NCD Macrobeams
D	flood cracks with corrosion inhibitor and epoxy injection	tested	A	NCD Macrobeams

Note: The alphabetic designation in the Corrosion Inhibitor column identifies the corrosion inhibitor used. A generic description of the corrosion inhibitor is provided in Table 1.

A total of four NCD Macrobeam specimens employed in this category were constructed with two mats of reinforcing steel. The top mat was comprised of nine equally spaced transverse ECR and two longitudinal ECR and the bottom mat was constructed with three longitudinal black bars. Concrete in these beams was poured in two lifts, where the bottom was chloride free and the top contained 11.88 kg/m^3 (20 pcy) of chloride ions. Steel shims of three different thicknesses were placed over each of the top mat transverse ECR to generate nine cracks (three of each width). After the repair strategies were applied, these beams were exposed to two weeks wet and two weeks dry ponding cycle using 15 % NaCl solution.

The results of 13 months of evaluation did not reveal any discernable difference between the repair strategies and materials evaluated. The variations observed in the specimens were small enough to be attributable to random scatter or variation by chance rather than to any improvement provided by the repair strategy. In addition, electrochemical impedance spectroscopy (EIS) data suggests that in general the quality of the ECR coating exposed in the cracks degraded with time as would be expected from such an exposure, thereby, indicating that the epoxy injection and corrosion inhibitor based repairs were not effective in protecting the coating on the ECR in the crack. The data indicates that none of the repair strategies provided any improvement over the No-Repair option.

REPAIR STRATEGIES FOR CORROSION INDUCED CRACKING

Three different types of specimens and a section of the bridge deck were used to evaluate various repair strategies for corrosion induced cracks. The matrix of repair strategies, materials, and specimen types for this category is provided in Table 4 and a detailed description of the evaluation and a discussion of the results are presented in Appendix C.

Table 4: Matrix of Strategies, Materials, and Specimen Types for Corrosion Induced Cracking

Strategy #	Repair Strategy	Materials		Specimen Types
		Epoxy Injection	Corrosion Inhibitor	
A	No-repair			G-109 Macrobeams, FHWA Slabs, Duanesburg bridge deck
B	epoxy injection of cracks	tested		G-109 Macrobeams, FHWA Slabs, Duanesburg bridge deck
C	flood cracks with corrosion inhibitor		A & B	G-109 Macrobeams, FHWA Slabs, Bent Bar Slab, Duanesburg Bridge
D	flood cracks with corrosion inhibitor and epoxy injection	tested	A & B	G-109 Macrobeams, FHWA Slabs, Duanesburg bridge deck
E	flood with corrosion inhibitor, epoxy injection, and surface application of corrosion inhibitor	tested	A	G-109 Macrobeams, FHWA Slabs, Duanesburg bridge deck

Note: The alphabetic designation in the Corrosion Inhibitor column identifies the corrosion inhibitor used. A generic description of the corrosion inhibitor is provided in Table 1.

In this category a total of four different types of specimens were used a) G-109 Macrobeams; b) FHWA slabs; c) Bent Bar Slab; and d) a portion of the Duanesburg bridge deck located in New York. A total of twelve beam type specimens termed G-109 Macrobeams were fabricated. These beams were constructed by embedding three G-109 specimens in the beam such that the top surfaces of the G-109 specimens were flush with the top surface of the beam. The G-109 specimens were fabricated in accordance with the standard test method ASTM G-109. Each G-109 specimen contained a top mat of steel comprised of an ECR and a black steel bottom mat. Adjacent to each G-109 specimen an ECR mat was embedded. The bottom mat of the beam was comprised of longitudinal and transverse black steel. The 1.52 x 0.61 x 0.15 m deep FHWA slabs were constructed in 1980 using non-specification bars. These slabs were fabricated with two mats of reinforcing steel. Of the five slabs used in this study, four had an ECR top mat and a black steel bottom mat and one had ECR in both mats. The top lift of concrete placed in these slabs contained 8.9 kg/m^3 (15 pcy) of chloride ions and the bottom lift was chloride free. These slabs had undergone 17 years of natural weathering and had experienced corrosion initiation and damage without any intervention or acceleration. The bent bar slab was also fabricated under another study in 1988 and had previously undergone accelerated exposure. The top mat of this 0.30 x 0.30 x 0.18 m deep slab was comprised of two straight and one bent bar and the bottom mat was comprised of black steel. For the field validation part of this category, the Schoharie Turnpike Bridge over I-88 in Duanesburg (Schenectady County) in New York was selected. This bridge was completed in 1981 and the deck was constructed with an ECR top mat and a black steel bottom mat. The structure has been subjected to salt application at the rate of 8 to 11 tons/lane kilometer per year (15-20 tons/lane mile per year). The deck had suffered concrete deterioration and it was believed to have resulted from corrosion of embedded steel.

Not all strategies could be tested on all specimens. With the exception of strategies associated with Corrosion Inhibitor B, all other strategies and materials were evaluated on the FHWA slabs. All FHWA slabs exhibited the first signs of ongoing corrosion as evidenced by generation of cracks and corrosion products and rust staining on the sides of the cracks associated with these. The slab treated with Strategy E exhibited rust staining within 5.2 months of evaluation; it was followed by slabs treated with strategies B, C, and D at 8.4 months of evaluation. The No-Repair slab was the last to exhibit rust staining at 13.9 months of evaluation. The driving voltage (potential difference between the two bar layers), macrocell currents (a measure of the magnitude of the corrosion cell), and half-cell potential data collected on the slabs for over 30 months were consistent with the visually apparent extent of corrosion deterioration. The magnitude of the macrocell currents reduced from its original corroding state when the repair strategies were implemented. Shortly after the implementation, the macrocell currents increased and remained high for the remainder of the evaluation. The no-repair strategy exhibited the least amount of macrocell activity and the most time to development of rust and rust staining. Driving voltage and half-cell potential data clearly indicated that the repair strategies applied to the FHWA slabs were of little or no benefit.

The strategy Flood with Corrosion Inhibitor using Corrosion Inhibitor A was evaluated on the Bent Bar Slab. Although, no visible physical deterioration of the specimen was observed, the macrocell current and half-cell potential data suggest that the repair did not mitigate corrosion on the bar exposed at the crack.

All strategies were evaluated on the G-109 Macrobeams. The results obtained are not as clear as those of the other specimen types discussed above. The variation in the macrocell data between strategies and between each strategy and the No-Repair option was insufficient to indicate any

positive impact of the repairs. Although, macrocell current data for all strategies suggests that the ECRs in the cracks become cathodic (i.e. were not corroding) to the bottom black steel or other steel in the specimen by at the time of the 10th data collection, the same was true for the No-Repair option. Thus, despite the finding that a reversal of macrocell current occurred subsequent to the repairs, this cannot be attributed to positive impact of the repairs per se. A decreasing-with-time trend was noted for the EIS impedance and AC resistance measurements. This indicates that the coating at the cracks is and perhaps elsewhere was deteriorating with time and that it continued to do so subsequent to the repairs.

All strategies with the exception of those associated with Corrosion Inhibitor B were evaluated on the Duanesburg bridge deck by visual inspection. After 34.5 months of monitoring, no visually observable difference in performance of the various repair strategies including the No-Repair strategy was discernable.

In summary, none of the repair strategies evaluated in this category exhibited any ability to provide protection in the two spheres of interest; that is, 1) directly at the crack and 2) area adjacent to the cracks.

REPAIR STRATEGIES FOR CORROSION INDUCED DELAMINATION

The matrix of repair strategies, materials, and specimen types for this category is provided in Table 5 and a detailed description of the evaluation and a discussion of the results are presented in Appendix D.

Three different types of specimens were used in this category a) PCS Macrobeams; b) bent bar slabs; and c) columns of the Seven Mile Bridge located in Key West, Florida.

Table 5: Strategies Evaluated for Corrosion Induced Delamination

Strategy #	Repair Strategy	Materials			Specimen Types
		Patch Material	Coating Material	Corrosion Inhibitor	
A	no-repair				PCS Macrobeams, 7 Mile Bridge
B	patch repair	A, B, & C			PCS Macrobeams, Bent Bar Slabs, 7 Mile Bridge
C	recoat and patch	A or C	A, B, & C		PCS Macrobeams, Bent Bar Slabs, 7 Mile Bridge
D	recoat and patch with admixed corrosion inhibitors	A or C	A	C, D, & E	PCS Macrobeams, Bent Bar Slabs, 7 Mile Bridge
E	recoat, patch, and apply corrosion inhibitor on the surface	A or C	A & B	A	PCS macrobeams, 7 Mile Bridge
F	recoat, patch with admixed corrosion inhibitor, and apply corrosion inhibitor on the surface	A or C		A, C, D, & E	PCS macrobeams, 7 Mile Bridge

Note: The alphabetic designation in the Materials columns identifies the materials used. A generic description of the materials is provided in Table 1.

The PCS Macrobeams were constructed similar to the G-109 Macrobeams, except that the G-109 specimen was replaced by a 0.36 x 0.36 x 0.10 m (14.0 x 14.0 x 4.0 inches) concrete slab fabricated using poor quality concrete. These slabs were labeled poor concrete specimens (PCS) and three slabs were embedded in each concrete beam. The entire beam was labeled PCS Macrobeam. Each slab was comprised of one mat of ECR with a series of coating defects introduced on the top surface and corrosion was initiated on the bars by the application of impressed current. The construction of the beam was similar to that of the G-109 Macrobeams. Concrete slabs similar to the bent bar slab described in the non-corrosion induced cracking category were also used in this category. Both the PCS Macrobeams and the bent bar slabs were subjected to two week wet-dry cycling after the repair strategies were applied to them. The Field evaluation studies were performed on 39 columns of the Seven Mile Bridge located in Key West, Florida. This structure was constructed in 1980 and is exposed to severe marine environment. The columns were constructed with ECR and within 8 years of construction started to exhibit corrosion induced concrete deterioration. The damage was observed to be increasing with time. A total of 13 repair strategies were installed and evaluated on these columns.

All strategies were evaluated on the PCS Macrobeams. After approximately two years of evaluation, the No-Repair strategy beam exhibited the most advanced deterioration based on visual inspection compared to all other strategies. It also exhibited the largest macrocell currents.

Use of Patch Materials A, B, and C reversed the macrocell currents and mitigated corrosion within the areas of repair. A reversal in current between the repair area and the adjacent ECR mat indicated that the steel in the repair areas was serving as a cathodic site to steel outside the repair area and this is supported by the macrocell current attributed to the adjacent ECR mat.

The use of Coatings A and C resulted in further improvement in performance, in that the macrocell current was reduced and, hence, the corrosion activity in the adjacent ECR mat was reduced. Inclusion of Coating B into the repair did not result in any reduction in corrosion activity compared to simply patching the delamination.

The use of corrosion inhibitor admixtures and surface applied migrating corrosion inhibitors in all combinations did not provide any improvement in performance when used in conjunction with Coating A and Patch Material A. As the combination of Patch Material A and Coating A was quite effective in controlling the macrocell current, it may be argued that no further incremental improvement could be accomplished by the corrosion inhibitors. However, the inclusion of Corrosion Inhibitor A in repairs using Patch Material A and Coating B did not exhibit any incremental improvement, thereby suggesting that the corrosion inhibitors were ineffective.

Patch Material A, Coatings A and C, and Corrosion Inhibitor C were evaluated on the Bent Bar Slabs. In general, these strategies did not provide sufficient reduction in macrocell currents. With time, however, macrocell currents increased indicating that the steel in the repair areas was corroding. Coating C with Patch Material A resulted in the smallest macrocell currents in the Bent Bar Slabs. Half-cell potential data for all slabs also indicated corrosion activity in the repair areas.

In the case of the Seven Mile Bridge, Patch Material C was used in all strategies requiring the use of Patch Material A. Here, a test area of fixed elevation was established on all test columns. Delaminations within this zone were treated according to the strategy that was to be applied on the column, and in the remaining area monitoring of the impact was performed. In an attempt to

measure macrocell currents, probes were installed inside and outside repair areas. For the No-Repair option, the probes were installed both within and outside of delaminated areas. Reference electrodes were also installed in the repair areas to facilitate measurement of half-cell potentials. Delamination surveys were performed twice after the installation of the repairs during the two plus years of evaluation. On the No-Repair columns, delaminations continued to form with time. Delaminations outside of the repair areas were also observed on columns associated with all materials of Strategy B, two materials of Strategy C (using Coatings A and C), one material of Strategy E (Corrosion Inhibitor A), and one material of Strategy F (Corrosion Inhibitor C). As Strategies B and C, by design, do not impact areas outside the repair, the observed delaminations do not necessarily reflect on their performance of the repair itself. On the other hand delaminations outside of repair areas in columns treated with corrosion inhibitors do indicate an inability to provide protection. Strategy B with Patch Material B and Strategy C with Coating A exhibited probe currents closest to desirable level (zero macrocell current). Whereas, Strategy B with Patch Material B, and Strategy C with Coating A, and Strategy E with Corrosion Inhibitor A exhibited very low macrocell currents for probes located outside the repair area.

In summary, there was no indication that the use of admixed and migrating corrosion inhibitors provided corrosion protection. The best response from a protection standpoint was accomplished with a high resistance, low permeability silica fume modified patch material such as Patch Material B and an epoxy coating compatible with ECR. The water based alkaline coating with corrosion inhibitor also showed promise.

IMPRESSED CURRENT CATHODIC PROTECTION

Results of experiments designed to evaluate the impact of impressed current cathodic protection system demonstrated that this corrosion protection method was the primary cause of disbondment on ECR. Localized areas that have undergone anodic polarization prior to cathodic polarization were less susceptible to coating disbondment. It is hypothesized that the level of cathodic reaction at previous anodic sites is somewhat diminished, hence the lower level of disbondment.

Impressed current cathodic protection applied to slabs for over 7.2 years successfully mitigated corrosion. The control slabs continued to corrode and experience corrosion induced damage, whereas, the cathodically protected ones did not suffer corrosion induced damage. Also, the current densities used to protect black reinforcing steel were found to be adequate to protect ECR.

CHAPTER 3

APPLICATIONS

INTRODUCTION

Although corrosion induced damage on ECR structures is presently not prevalent, there are indications that failures can be expected in the future. No methodologies, protocols, or guidelines are presently available to guide the practitioner in implementing repair and rehabilitation on ECR structures suffering corrosion induced damage. One of the goals of this effort was to develop a decision matrix that would provide a practitioner with a starting point for making the necessary decisions.

Past research effort has addressed materials and technologies suitable for repair and rehabilitation of concrete structures with black reinforcing steel. The present study is one of the first attempted to identify technologies and materials for repairing and rehabilitating ECR structures.

This was done based upon the results of this study, information available in literature, and the experience of the project team were used to develop a decision matrix that a practitioner can use as a guideline for making repair and rehabilitation decisions.

DECISION MATRIX

The scope of this decision matrix encompasses 1) different types of concrete elements reinforced with epoxy coated rebars, 2) various exposure conditions, 3) existing condition of the reinforcement and concrete, and 4) future corrosion propensity. It also includes treating damage

that was not induced by corrosion of the epoxy coated rebar. As with time, corrosion can initiate on the epoxy coated rebars exposed to the environment in damaged areas. Because of the complexity, the matrix has been divided into two tables to effectively present options for various elements, in various exposure environments, and with varying degrees of damage and propensity for corrosion. One of these tables deals with structures exposed to the marine environment and the other to deicing salt environments.

The repair options presented in the decision matrix are on based on technical viability and the damage categories are based on the cost effectiveness of the approach to allow more practical and reasonable solutions for each instance. This decision matrix is designed to identify solution(s) that will provide maximum extension in service life (i.e. time to next repair). However, in practice, maximum extension in service life may not constitute the best approach. For example a structure may become functionally obsolete prior to it becoming physically deficient. In this case, a lesser life and, presumably, reduced repair or rehabilitation cost are more appropriate. The decision matrix does not attempt to provide such information as it would unduly increase the complexity of the matrix. The decision matrix also does not include preventive measures that may be implemented to increase the service life by delaying or preventing the initiation of corrosion. It is only applicable to structures that have already suffered corrosion or non-corrosion induced damage.

The optimum choice of a repair and/or protection system for any reinforced concrete component is dependent on the condition of the component (i.e. the amount of damage accumulated) and the probability for continuation of corrosion and further accumulation of damage related thereto. A field and laboratory evaluation must be performed to quantify the damage that has accumulated and to categorize the probability for continuing corrosion. The existing protocol developed

under NCHRP 10-37B for evaluating the condition of and the propensity for corrosion on epoxy coated rebars is not particularly suited for this decision matrix. Therefore, the probability definitions developed for the decision matrix are based on exposure to chloride ions and observable failure of the epoxy coating on rebars extracted from the concrete element.

For each cell in the decision matrix, many options for repair and protection have been excluded in order to reduce the complexity of the matrix and provide an optimal starting point for the selection of the repair and/or protection system. Many of the options listed in the matrix have a proven history on concrete elements reinforced with black steel. Some options, such as cathodic protection of epoxy coated reinforcing steel, have been evaluated under the NCHRP 10-37C effort and by other efforts, and found to provide adequate protection, if properly designed and installed.

Some options do not have a proven track record but are considered promising. For example, the use of a procedure whereby small galvanic zinc anodes are placed in repair areas was only recently developed. If it can be confirmed that this method is technically sound, then such an approach is considered promising, especially for epoxy coated rebars. Although electrochemical chloride extraction could also be considered promising for epoxy coated rebars, a lack of information pertaining to ECR structures precluded it from being considered in this study.

Table 6 and 7 present the Decision Matrix for bridge structures in the marine and the deicing salt environments, respectively. Definitions of terms and procedures for their use are provided in Appendix F

Table 6: Decision Matrix for Repair and Protection of Bridge Structures Exposed to Deicing Salt Environment

Element	Sub-environment	Damage Category	Probability for Corrosion			
			Low	Localized	Medium	High
Substructure						
Piles & Columns	Deicing Salt Splash or Contaminated Water Runoff	Negligible	Do Nothing			
		Crack	EI	Do Nothing		
		Partial	Patch, Patch+EC	Patch; Patch+Zn-Rep, Patch+barrier(1)		Patch+Zn-adh
		Full Surface	Shotcrete; Jacket		Jacket; Jacket+Zn-Rep; Ovelay+barrier(1)	Overlay+Zn; Overlay+Ti; Jacket+Zn; Jacket+Ti
Pile Caps, Struts, & Hammer Heads	Contaminated Water Runoff	Negligible	Do Nothing			
		Crack				
		Partial	Patch, Patch+EC		Patch; Patch+Zn-Rep	Patch +Arc-Zn; C-Paint or Zn-adh
		Full Surface	Shotcrete		Shotcrete+Zn-Rep; Shotcrete+barrier(1)	Shotcrete+Arc-Zn; C-Paint or Zn-adh; Replace
Superstructure Elements						
Deck Top Surface	Direct Application of Salt	Negligible	Do Nothing			
		Crack				
		Partial	Patch, Patch+EC	Patch+Zn-Rep; overlay; asp-mem		Overlay+Ti; Patch+asph-coke; Hydro
		Full Surface	Overlay; Patch+apsh-mem		Hydro; overlay+apsh-mem	Overlay+Ti; Hydro; Replace

Table 6: Decision Matrix for Repair and Protection of Bridge Structures Exposed to Deicing Salt Environment (continued)

Element	Sub-environment	Damage Category	Probability for Corrosion			
			Low	Localized	Medium	High
Deck Soffit	Contaminated Water Runoff	Negligible	Do Nothing			
		Crack				
		Partial	Full Depth Patch		Full Depth Patch+Zn-Rep	Full Depth Patch + overlay-Ti
		Full Surface	Replace entire deck or effected areas			
Primary & Secondary Members	Contaminated Water Runoff	Negligible	Do Nothing			
		Crack	EI	Do Nothing		
		Partial	Patch, Patch+EC	Patch+Zn-Rep	Patch+Zn-Rep	
		Full Surface	Shotcrete	Shotcrete+Ti		Replace

Notes:

1 Install some waterproofing breathable sealer or membrane to prevent future contamination from chloride ions.

Abbreviations

Rt-grt: Route and grout cracks.

barrier: Coatings, membranes, overlays, and sealers.

EC: Epoxy coating of the rebar prior to the installation of the patch.

EI: Epoxy injectin of cracks.

Zn-adh: Zinc sheet anode with adhesive for attachement to concrete surface.

Overlay+Zn: Zinc mesh anode in concrete jacket/overlay functioning as a galvanic anode.

Overlay+Zn: Titanium anode in concrete jacket/overlay functioning as an impressed current anode.

Jacket+Zn: Zinc mesh anode in fiber glass jacket filled with a cementious fill functioning as a galvanic CP system.

Jacket+Ti: Titanium anode in fiber glass jacket filled with a cementious fill functioning as an impressed current CP system.

Zn-Rep: Zinc anode installed in repair areas to serve as a galvanic CP system.

Arc-Zn: Arc sprayed zinc galvanic cathodic protection system.

C-Paint: Conductive paint cathodic protection system.

Hydro: Hydrodemolition of the top contaminated layer and replacement with a concrete layer.

apsh-mem: Ashpalt overlay with a waterproofing membrane.

Table 7: Decision Matrix for Repair and Protection of Bridge Structures Exposed to Marine Environment

Element	Sub-environment	Damage Category	Probability for Corrosion			
			Low	Localized	Medium	High
Substructure						
Piles and Columns	Splash Zone (elevation 0 to 6 feet)	Negligible	Not feasible due to severity of exposure.	Do Nothing		
		Crack		Jacket+Zn; Jacket+Ti; Overlay+Zn; Overlay+Ti; Patch+Zn-adh(1)		
		Partial				
		Full Surface				
	Above Splash Zone (elevation 6 to 12 feet)	Negligible	Do Nothing			
		Crack	EI	Do Nothing		
		Partial	Patch+Zn-Rep+EI		Patch+Arc-Zn; Zn-adh(1)	
		Full Surface	Jacket; overlay	Jacket or overlay + Zn-Rep	Jacket+Zn; Jacket+Ti; Overlay+Zn; Overlay+Ti	
	Above Splash Zone (elevation 12 feet and above)	Negligible	Do Nothing			
		Crack	EI	Do Nothing		
		Partial	Patch+Zn-Rep+EI; Patch+EC+EI			Patch +Zn-Rep
		Full Surface	Jacket; overlay			Jacket+Zn; Jacket+Ti; Overlay+Zn; Overlay+Ti
Pile, Caps, & Struts	Splash Zone (elevation 0 to 6 feet)	Negligible	Not feasible due to severity of exposure.	Do Nothing		
		Crack		Shotcrete+Zn-Rep; Arc-Zn		
		Partial				
		Full Surface				

Table 7: Decision Matrix for Repair and Protection of Bridge Structures Exposed to Marine Environment (continued)

Element	Sub-environment	Damage Category	Probability for Corrosion			
			Low	**Localized**	**Medium**	**High**
Pile, Caps, & Struts	Above Splash Zone (elevation 6 to 12 feet)	Negligible	Do Nothing			
		Crack	EI		Do Nothing	
		Partial	Do Nothing; Patch, Patch+EC	Patch+Zn-Rep+EI; Patch+Zn-adh		
		Full Surface	Shotcrete+Zn-Rep			Shotcrete+Arc-Zn; Zn-Rep
	Above Splash Zone (elevation 12 feet and above)	Negligible	Do Nothing			
		Crack	EI		Do Nothing	
		Partial	Do Nothing; Patch, Patch+EC	Patch+Zn-Rep+EI; Patch+Zn-adh		Patch+Arc-Zn; Zn-Rep
		Full Surface	Shotcrete	Shotcrete+Zn-Rep		Shotcrete+Arc-Zn; Zn-Rep
Superstructure Elements						
Deck Top Surface	All elevations	Negligible	Do Nothing			
		Crack				
		Partial	Patch		Patch+Zn-Rep	Overlay+Ti; asph-coke
		Full Surface	Overlay	Overlay; Hydro		Hydro; Overlay+Ti; asph-coke; Replace
Deck Soffit	All elevations	Negligible	Do Nothing			
		Crack				
		Partial	Patch, Patch+EC		Patch+Zn-Rep	Patch+Arc-Zn
		Full Surface	Replace Deck			

Table 7: Decision Matrix for Repair and Protection of Bridge Structures Exposed to Marine Environment (continued)

<table>
<tr><th rowspan="2">Element</th><th rowspan="2">Sub-environment</th><th rowspan="2">Damage Category</th><th colspan="4">Probability for Corrosion</th></tr>
<tr><th>Low</th><th>Localized</th><th>Medium</th><th>High</th></tr>
<tr><td rowspan="7">Primary & Secondary Members</td><td rowspan="4">Splash Zone (elevation 0 to 6 feet)</td><td>Negligible</td><td colspan="4" rowspan="2">Do Nothing</td></tr>
<tr><td>Crack</td></tr>
<tr><td>Partial</td><td colspan="2">Patch, Patch+EC</td><td>Patch+Zn-Rep</td><td>Patch+Arc-Zn</td></tr>
<tr><td>Full Surface</td><td colspan="2">Shotcrete</td><td colspan="2">Shotcrete+Arc-Zn</td></tr>
<tr><td rowspan="3">Above Splash Zone (elevation 6 feet and above)</td><td>Negligible</td><td colspan="4">Do Nothing</td></tr>
<tr><td>Crack</td><td>EI</td><td colspan="3">Do Nothing</td></tr>
<tr><td>Partial</td><td colspan="2">Patch, Patch+EC</td><td>Patch+Zn-Rep</td><td>Patch+Arc-Zn; Patch+Zn-adh</td></tr>
<tr><td></td><td>Full Surface</td><td>Shotcrete</td><td>Patch+Zn-Rep</td><td colspan="2">Shotcrete+Arc-Zn</td></tr>
</table>

Notes :

1 If and only if it can be sealed properly to prevent water infiltration into the adhesive. Manufacturer claims successful installation on one si

Abbreviations

Zn-adh: Zinc sheet anode with an ionically conductive adhesive for attachement to concrete surface functioning as galvanic anode.
Patch: Concrete removal using standard practice and patch with cementitious mix.
EC: Epoxy coating of the rebar prior to the installation of the patch.
Jacket+Zn: Zinc mesh anode in a fiberglass jacket filled with a cementitious mix functioning as a galvanic CP system.
Jacket+Ti: Titanium mesh anode in a fiberglass jacket filled with a cementitious mix functioning as an impressed current CP system.
Overlay+Zn: Zinc mesh anode in a concrete jacket/overlay functioning as a galvanic CP system.
Overlay+Ti: Titanium mesh anode in a concrete jacket/overlay functioning as an impressed current CP system.
Arc-Zn: Arc sprayed zinc galvanic CP system.
Zn-Rep: Zinc anodes installed in repair areas prior to patch or overlay placement to give localised cathodic protection against ring anodes.
EI: Epoxy injection.
Jacket: Fiberglass jacket filled with an epoxy or cementitious mix.
Overlay: Concrete overlay or a concrete jacket.
Hydro: Hydrodemolition of the top contaminated layer and replacement with a concrete layer.
asph-mem: Ashpalt overlay with a waterproofing membrane.
asph-coke: Coke breeze conductive impressed current CP system with asphalt overlay.

CHAPTER 4

CONCLUSIONS AND SUGGESTED RESEARCH

CONCLUSIONS

1. Neither admixed nor migrating corrosion inhibitors provided any corrosion protection when used to rehabilitate cracks on concrete elements reinforced with ECR that were exposed to an aggressive chloride environment.

2. Neither type of corrosion inhibitors, the admixed and or migrating, provided any corrosion protection when used to rehabilitate delaminations on concrete elements reinforced with ECR that were exposed to an aggressive chloride environment.

3. Neither epoxy injection nor application of a migrating corrosion inhibitor (or the two together) provided any corrosion protection to concrete elements with simulated cracks that were exposed to an aggressive chloride environment.

4. Use of high resitivity, low permeability, silica fume concrete to patch corrosion induced damage provided protection against corrosion in the repair area and minimized the development of macrocells around the periphery of the repair.

5. Use of epoxy coatings in conjunction with cementitious patch material provided protection against corrosion in the repair area and minimized the development of macrocells around the periphery of the repair.

6. Cathodic protection can be used to mitigate corrosion on ECR concrete elements provided the steel is or can be made electrically continuous.

RECOMMENDATIONS

1. Evaluation of the various repair strategies as applied to the two bridges that were studied in this project should be continued for several more years to obtain a better understanding of their longer-term performance.

REFERENCES

1. "Nonmetallic Coatings for Concrete Reinforcing Bars," Report No. FHWA-RD-74-18, Federal Highway Administration, Washington, D. C., Feb. 1974.

2. Pike, R. G., "Nonmetallic Coatings for Concrete Reinforcing Bars", Public Roads, US Bureau of Public Roads, Vol. 37, No. 5, pp. 185-197, June 1973.

3. Salparanta, L., "Epoxy-Coated Concrete Reinforcements", Finland Technical Research Center, Research Report VTT-RR-525-88, March, 1988, p. 17.

4. Clifton, J. R., Beehgly, H. F., Hugh F., and Mathey, R. G., "Nonmetallic Coatings for Concrete Reinforcing Bars", National Bureau of Standards, Building Science Series - 65, Federal Highway Administration, Washington, D. C., 1975.

5. Lee H. and Neville, K., Handbook of Epoxy Resins, McGraw-Hill, Inc., New York, 1967.

6. Clear K. C. and Virmani, Y. P., "Corrosion of Non-Specification Epoxy-Coated Rebars in Salty Concrete," paper no. 114, CORROSION/83, April 18-22, 1983, Anaheim.

7. Clear, K. C., "Cost Effective Rigid Concrete Construction and Rehabilitation in Adverse Environments", Federal Highway Administration FCP Annual Progress Report, Project No. 4K, Sept. 30, 1981.

8. Gustafson, D. P.,"Epoxy Update," Civil Engineering, Vol. 58 (10), pp. 38-41, 1988.

9. Pfeifer, D. W., Langren J. R. and Zoob, A., "Protective Systems for New Prestressed and Substructure Concrete", Wiss, Janney, Elstner Associates, Inc., Report FHWA/RD-86/193, April 1987.

10. Brown, R. P. and Poore, T. G., "Two Years of Corrosion Monitoring of Reinforced Concrete Piles at Matanzas Inlet", Interim Report, Report No. 82-1, Florida Department of Transportation, July, 1982.

11. Edgell, T. W. and Riemenschneider, J. A., "Epoxy-Coated Reinforcing Steel Performance in Marine Exposure - A Nine Year Observation", Pipeline & Construction Specialty Markets, 3M Austin Center, 130-4N-07.

12. Espelid, B. and Nilsen, N., "A Field Study of the Corrosion Behavior on Dynamically Loaded Marine Concrete Structures", Concrete in Marine Environment, Proceedings 2nd International Conference, St. Andrews by-the-Sea, Canada, 1988, Editor, V. M. Malhotra, ACI SP-109, pp. 85-104.

13. J. Satake, M., Kamakura, K., Shirakawa, N., Mikami and Swamy, N., "Long-Term Corrosion Resistance of Epoxy-Coated Reinforcing Bars", Chapter 21 in Corrosion of Reinforcement in Concrete Construction, Ellis Harwood Ltd., U. K., 1983.

14. Roper, H., "Investigations of Corrosion, Fatigue and Corrosion Fatigue of Concrete Reinforcement", paper no. 169, CORROSION/83, Anaheim, California, April 18-22, 1983.

15. Clear, K. C., "Eliminate Premature Deterioration of Portland Cement Concrete", FCP Annual Progress Report - Year Ending September 30, 1978, Project 4B Federal Highway Administration, April 1979.

16. Unpublished FHWA data and photographs by Clear, Virmani and Jones, 1981.

17. Virmani, Y. P., Clear K. C., and Pasko, Jr., T. J., "Time-to-Corrosion of Reinforcing Steel in Concrete Slabs, Vol. 5: Calcium Nitrite Admixture or Epoxy-Coated Reinforcing Bars as Corrosion Protection Systems", Report No. FHWA-RD-83-012, Federal Highway Administration, Washington, D. C.. September, 1983.

18. Unpublished FHWA data and photographs by Y. P. Virmani, 1989.

19. Manjal, S. K., "Evaluation of Epoxy-Coated Reinforcing Steel Bridge Decks", Report No. FHWA-MD-82-03, Maryland State Highway Administration, Brooklandville, March, 1981.

20. Hagen, M. G., "Bridge Deck Deterioration and Restoration - Final Report", Report No. FHWA-MN-RD-83-01, Minnesota Department of Transportation, St. Paul, November, 1982.

21. McKeel, Jr., W. T., "Evaluation of Epoxy-Coated Reinforcing Steel, Milestone Report", HPR Study No. 79, Virginia Highway and Transportation Research Council, Charlottesville, July, 1984.

22. Weyers R. E., and Cady, P. D., "Deterioration of Concrete Bridge Decks from Corrosion of Reinforcing Steel," Concrete International, Vol. 9 (1), 1989.

23. Hededal, P. and Manning, D. G., Field Investigation of Epoxy-Coated Reinforcing Steel", MTO Report MAT-89-02, Ontario Ministry of Transportation, Dec., 1989.

24. Scannell, W. T. and Clear, K. C., "Long Term Outdoor Exposure Evaluation of Concrete Slabs Containing Epoxy Coated Reinforcing Steel," Transportation Research Record No. 1284, Transportation Research Board, Washington, D.C., 1990, pp. 70-78.

25. Sohanghpurwala, A. and Clear, K. C., "Effectiveness of Epoxy Coatings in Preventing Corrosion of Reinforcing Steel," Transportation Research Record No. 1268, Transportation Research Board, Washington, D.C., 1990, pp. 193-204.

26. Powers, R. and Kessler, R., "Corrosion Evaluation of Substructure, Long Key Bridge", Corrosion Report No. 87-9A, Florida Department of Transportation, Gainesville, Florida, 1987.

27. Zayed, M. and Sagues, A. A., "Corrosion of Epoxy-Coated Reinforcing Steel in Concrete," paper no. 386 presented at CORROSION/89, April 17-21, 1989, New Orleans.

28. Powers, R., "Corrosion of Epoxy-Coated Rebar, Keys Segmental Bridges Monroe County," Corrosion Report No. 88-8A, Florida Department of Transportation, Gainesville, Florida, August, 1988.

29. Zayed, M., Sagues, A. A. and Powers, R. G., "Corrosion of Epoxy-Coated Reinforcing Steel in Concrete," paper no. 379 presented at CORROSION/89, April 17-21, 1989, New Orleans.

30. Clear, K. C., "Effectiveness of Epoxy Coated Reinforcing Steel," Final Report, Canadian Strategic Highway Research program, Ottawa, Canada, Dec., 1992.

31. Clear, K. C., "Effectiveness of Epoxy-Coated Reinforcing Steel", Final Report, Concrete Reinforcing Steel Institute, Dec., 1991.

32. Clear, K. C., Hartt, W. H., McIntyre, J. F. and Lee, S. K., "Performance of Epoxy-Coated Reinforcing Steel in Highway Bridges", NCHRP Report No. 370, National Cooperative Highway Research Program, Washington, D. C., 1995.

33. Griggs, R. D., "Use of Epoxy Coated Concrete Reinforcement Steel in Georgia Highway Construction and a Limited Field Evaluation of the Performance of Epoxy Coated Reinforcement Steel as Corrosion Protection System in Coastal Georgia Bridge Construction", report submitted to the Office of Materials and Research, Georgia Department of Transportation, Feb., 1993.

34. Pyc', W. A., 'Field Performance of Epoxy-Coated Reinforcing Steel in Virginia Bridge Decks," PhD. Dissertation submitted to Virginia Polytechnic Institute and State University, Blacksburg, Virginia 1998.

35. Manning, D. G. 'Corrosion Performance of Epoxy-Coated Reinforcing Steel: North American Experience." Construction and Building Materials, Vol. 10 No.5, 1996, pp. 349-365.

APPENDIX A

REPAIR OPTIONS, MATERIALS AND PROCEDURES

EXISTING TECHNIQUES FOR CORROSION CONTROL OF BARE REINFORCING STEEL

Corrosion control methodologies for reinforcing steel in concrete may be categorized as being Physical, Electrochemical or Other (neither physical nor electrochemical), according to the manner in which each functions. Physical techniques for reducing or eliminating embedded steel corrosion are based upon providing a barrier either upon the steel itself or upon or within the concrete which reduces the ingress of chlorides, moisture, or oxygen (or a combination of these) to the steel. An example in the former category (on steel itself) is an epoxy-coating applied to reinforcing steel, either in conjunction with initial construction (e.g., ECR) or as part of a repair or rehabilitation strategy. In the remediation case, the coating is applied to either bare reinforcing steel or ECR (after removal of the existing coating), and it serves to minimize post-repair corrosion cell(s) between steel in the patched area and in adjacent unrepaired concrete. In either case, the onset of corrosion subsequent to chlorides in the concrete reaching the critical concentration at the steel depth is extended. Examples in the latter category (upon the concrete) include admixtures such as high range water reducers, fly ash, silica fume, and combinations of these; such that a less permeable and higher electrical resistivity concrete than would otherwise be the case results. Also included in this category are sealers, overlays, and membranes which reduce the presence of water and chlorides at the concrete surface and, hence, limit the ingress of these species into the concrete.

Electrochemical methods, on the other hand, include cathodic protection and electrochemical chloride extraction and involve a supplementary electrochemical cell or reaction(s) in addition to

the naturally occurring one(s). The resultant potential and current are intended either to electromigrate chlorides away from the metal (electrochemical chloride extraction or ECE) or to polarize the metal to a more negative potential where corrosion rate is low or nil (cathodic protection or CP).

The Other category of repair and rehabilitation options includes 1) inhibitors which can be either surface applied (migrating) or admixed into patch and overlay materials (or both), 2) combinations of strategies, 3) new or yet-to-be-identified strategies, and 4) doing nothing. The last of these (doing nothing), while not technically gratifying, is in some instances the most viable alternative from the standpoint of life cycle cost optimization (in this case, remaining life cycle cost optimization).

POTENTIAL REPAIR AND REHABILITATION STRATEGIES FOR ECR

The approach employed for identifying key elements in development of the research work plan and in defining feasible, appropriate repair and rehabilitation strategies is presented below. The two terms, "feasible and appropriate", are intended to convey that a particular qualifying strategy is viable from technical, practical, and economic standpoints within the overall context of the specific situation that exists for a particular structure or structural component.

Identification and assessment of technically feasible candidate repair and rehabilitation strategies were accomplished in terms of the topical considerations and protocol that are diagrammed in Table A-1. This table presents an overview flow diagram of the process used to produce the list of viable repair and rehabilitation strategies. As a precursor to this, the various damage modes (left side of Table A-1) were defined and categories of candidate repair and rehabilitation options

(Existing, Combined, and New, see upper right of Table A-1) were listed and evaluated. In this discussion the term 'repair' is defined as a remedial function which is performed for the purpose of restoring a bridge component to an acceptable level of service, whereas 'rehabilitation' intends, in addition, to correct the cause(s) of the deterioration. The table also considers each of the three repair/rehabilitation categories according to the source of the corrosive(s) (marine, deicing, or combined exposure). Regardless of the source, however, it is assumed that the environment influence invariably reflects chlorides at the steel depth having achieved a critical concentration with adequate moisture and oxygen availability such that either macro - or micro-corrosion cells (or both) are able to function. Also, as indicated in Table A-1, appropriateness of a particular repair or rehabilitation option may be influenced by the cause(s) of the concrete damage (corrosion induced, non-corrosion induced, or a combination of the two (multi-mode)). Correspondingly, repair and rehabilitation strategies were identified according to which of the three damage modes apply. Table A-2 lists, categorizes, and provides commentary regarding various repair/rehabilitation options. In the discussion that follows, each of the three damage causes (corrosion induced, non-corrosion induced, or combined) and how these relate to different repair and rehabilitation strategies was developed and expanded upon in order to formulate the experimental plan.

CRITERIA FOR SELECTION OF REPAIR AND REHABILITATION STRATEGIES

In order to successfully accomplish the project objectives within existing fiscal and time constraints and in view of the large number of candidate repair and rehabilitation strategies that are available, prequalification of these for inclusion in the evaluation phase was considered

necessary. Therefore, the following pre-qualifying criteria were developed to assist in the strategy selection process:

1. The strategy should be expected to have a direct and positive impact on the future performance of the epoxy-coated reinforcing steel.

2. Each technique or material should not have any known adverse effects on epoxy-coated reinforcing steel.

3. Emphasis should be placed on strategies which have a history of success on bare reinforcing steel. Although new strategies were considered, none were identified.

4. In conjunction with item 3, each strategy should have some probability of success based on current knowledge even if adequate long-term performance information on bare reinforcing steel is not available (e.g. surface applied corrosion inhibitors).

Commentary on Table A-2

Note 1: Due to funding limitations and maintenance priorities, corrosion induced cracks are seldom repaired until the damage has progressed to the point where it is in the 3-D category (i.e. repairs are typically delayed until the concrete damage effects riding quality, safety, and/or structural integrity). However, it is considered probable that corrosion inhibitors may extend the time until damage progressed to the 3-D category. Early repair of cracks in the 2-D category is likely to be a short term solution since the adjacent concrete remains chloride contaminated. Determination of how damage of this type in ECR containing concrete can best be repaired requires additional study and was not evaluated.

Table A-1: Overview Flow Diagram for Development of Strategies.

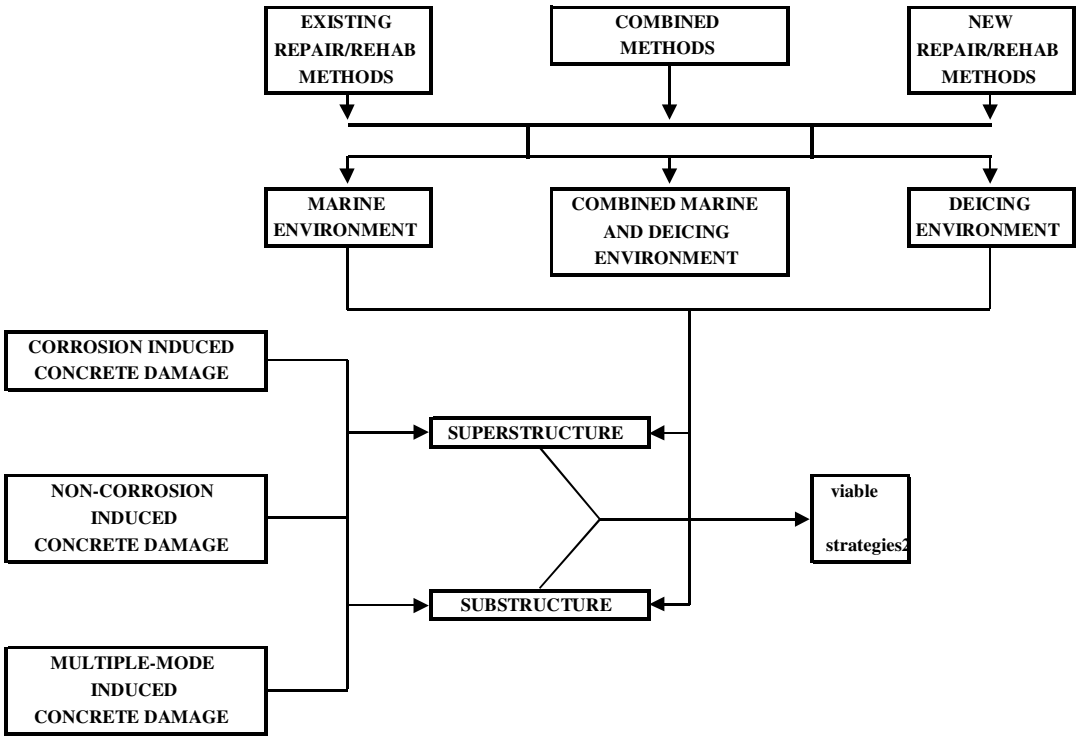

Table A-2: Repair and Rehabilitation Strategies.

REPAIR/REHABILITATION STRATEGY		CAUSE OF CONCRETE DAMAGE		
		CORROSION	OTHER	COMBINED
I. PHYSICAL	A. PATCHING*			
	1. 2-D	See notes 1 and 4	See notes 2 and 4	See notes 1, 3, and 4
	2. 3-D	See note 5	See note 6	See note 7
	B. OVERLAYS	See note 8		
	C. BARRIERS	See note 8		
	D. PARTIAL REPLACEMENT	See note 9		
II. ELECTRO-CHEMICAL	A. CATHODIC PROTECTION	See note 10		
	B. ELECTROCHEMICAL CHLORIDE EXTRACTION	See note 11		
III. OTHER	A. INHIBITORS	See note 12		
	B. COMBINATIONS OF STRATEGIES	See note 13		
	C. NEW STRATEGIES	See note 14		
	D. DO NOTHING	See note 15		

* A 2-D patch refers to crack repair whereas a 3-D patch pertains to delaminations and/or spalls.

Note 2: Structural cracking is one of the only probable examples of non-corrosion induced damage in the 2-D category. On bridge decks, this type of damage typically results in transverse cracks aligned with the embedded reinforcing steel. Impact damage, delayed ettringite formation, plastic shrinkage, etc. are other forms of non-corrosion induced damage. If corrosion has not occurred subsequent to the cracking, the same methods that are presently employed for repair of structural cracks in concrete containing bare reinforcing steel should also apply to concrete with ECR. Unlike the case of corrosion induced cracks (see note 1), repair of structural cracks can provide a long term solution. However, if structural cracks are left untreated, corrosion damage will ultimately result. Therefore, to realize the longest possible service life from repair of structural cracks, the repairs must be affected in a timely manner. Repair of non-corrosion induced cracks was included in this study.

Note 3: The prominent example in this category is non-corrosion induced cracks which have not been repaired, thus allowing some corrosion to occur but not to a degree that the concrete damage transcends from 2- to 3-D. Once corrosion commences, any repair must consider that the steel exposed at the crack is probably anodic to reinforcement in the adjacent, sound concrete, which serves as the corresponding cathode (the lower steel mat may also be a cathode in this cell). This should be the case irrespective of whether the steel is bare or epoxy-coated. For bare steel this cathodic region receives at least some protection from the anode, and attention need not focus upon it. For ECR, however, cathodic disbondment of the epoxy-coating within this adjacent concrete may result, thereby facilitating ingress of corrosives and rendering the steel at this location more susceptible to corrosion than would otherwise be the case. In this regard, repair of 'combined cause' cracks in concrete with ECR may have different implications and be distinctive compared to those in concrete containing bare steel.

Note 4: Strategies for repair of cracks in concrete containing ECR are listed below:

1. Flood with corrosion inhibitor.
2. Polymer application (epoxy injection and methyl methacrylate flooding).
3. Combination A-B.
4. Strategy A, B, or C followed by application of a sealer, overlay (w/ or w/o membrane), or barrier.
5. Strategy A, B, or C followed by application of a surface applied inhibitor.

Flooding cracks with methyl methacrylate (MMA) has limited application when one is considering all types of bridge components (i.e. this crack repair strategy is not applicable to vertical surfaces). It can be argued that the same is true for the strategy where cracks are flooded with a corrosion inhibitor, however, since a migrating inhibitor was to be used for this purpose, it was believed that methods of injecting this material even partially into cracks on vertical surfaces were worth pursuing in this project. Therefore, crack repair strategies which involve flooding with MMA were not included in this study.

Note 5: Two-D repairs differ from 3-D ones in that treatment of the steel per se is either more difficult or not possible in the former case but can be affected for the latter. Thus, in the 3-D case the exposed steel can be cleaned (sandblasted, including removal of the residual epoxy-coating) and recoated. A concern here, however, is the degree of cleaning and recoating that can be provided in a field setting, particularly upon the bar backside (this is a problem for both bare bar and ECR repairs). Unlike ECR in sound concrete adjacent to a repaired crack, which is likely to be a cathode, the ECR adjacent to a 3-D patch may be anodic, either to the steel within the patch or to the bottom mat. The possibility that cathodic disbonding of the coating may have

occurred here prior to the repair could accentuate the corrosion that arises from this. Repair/rehabilitation is likely to involve the following:

1. Removal of all unsound concrete,
2. Removal of concrete (sound or damaged) around the entire circumference of exposed bars,
3. Bar cleaning and recoating, and
4. Placement of the patch material.

Other factors to be considered are 1) use of corrosion inhibitors (surface applied, patch admixed, or both) and 2) type of bar coating and patch material. In this regard, surface applied (migrating) inhibitors could have particular utility, provided they prove to function as intended, in situations where reinforcement in a patch area is either not coated, is poorly coated after cleaning, or is inadequately cleaned prior to coating (or some combination of the three). Additionally, a criterion should be established regarding how far back into sound concrete the ECR should be exposed. For bare steel, such exposure is generally affected until no visible rust is apparent upon the bar. In the case of ECR, however, the coating may appear visually intact but be of low adhesion or disbonded due to this region having been a cathode, in which case corrosion could initiate here relatively soon after the repair/rehabilitation is completed. Additional study is needed in order to qualify methods for corrosion induced concrete damage repair/rehabilitation, and this topic was addressed. However, due to budgetary constraints, establishment of a criterion for concrete excavation along exposed bars was not addressed.

Note 6: Three-D, non-corrosion induced concrete damage is likely to result where:

1. Design, construction, or maintenance (or combinations of these) has been inadequate,

2. Construction materials do not meet specification, or
3. Service loadings have been excessive (or combinations of these).

For cases where post-damage corrosion has not transpired and no reinforcing steel is exposed, repairs can be affected according to established protocols for bare steel reinforced concrete structures. If reinforcing steel is exposed it is likely to be corroded and repairs would be affected in accordance with Note 7. Consequently, further study of damage in this category was not performed.

Note 7: Examples in this category involve occurrence of corrosion in association with one or more of the causality factors listed in Note 6. In addition, non-corrosion induced concrete cracks which are not repaired (see Note 2) will eventually lead to corrosion of the ECR (see note 3) to such a degree that delamination and spalling result and the damage becomes 3-D. Options in these cases are likely to be the same as cited above in Note 5, and these were addressed as tests pertaining to repair/rehabilitation of 3-D corrosion induced damage.

Note 8: Application of an overlay or barrier to an ECR concrete component is considered to affect subsequent corrosion performance according to the extent to which the rate of further chloride and water ingress is reduced. Based upon this and from information regarding the effectiveness of any patch type repair/rehabilitation (see Notes 1-7 above) that is performed either prior to or during the overlay or barrier application, it should be possible to project the service life extension that should result. The overlay and barrier experience that has been gained for concrete structures containing bare reinforcement should be directly applicable to situations where ECR is involved. Therefore, no tests involving overlay/barrier technology and methods

per se were addressed, but evaluations of this repair/rehabilitation approach based upon existing literature for bare bar and application of this information to ECR were included.

Note 9: Service experience that has been developed historically for concrete containing bare steel should be directly applicable to partial replacement of structures containing ECR. Therefore, no tests or analyses pertaining to this were included in this study.

Note 10: Cathodic protection is now generally recognized as appropriate for control of ongoing corrosion of bare steel in chloride contaminated concrete, and preliminary experiments have indicated its utility also for concrete containing ECR. However, two factors may complicate or limit its usefulness in the latter case. The first of these pertains to an anticipated lack of electrical continuity between ECR bars. This same problem can exist for bare reinforcement in concrete, but the extent to which continuity is a problem here is likely to be less than for ECR. However, it is considered that concerns regarding electrical continuity should not preclude consideration of cathodic protection as a strategy for corrosion control of ECR in concrete, since continuity, where it is lacking, can be established using existing technology. The question to be addressed for a particular structure is if establishing continuity is economically feasible. No experiments or analyses pertaining to ECR electrical continuity or to establishment of continuity, where it is lacking, were included, since decisions regarding this, as part of a particular repair or rehabilitation activity, are likely to be structure specific.

The second factor pertains to the fact that coating disbondment may accompany application of cathodic protection to ECR (alternately, disbondment may already be present) and that protection may not extend from bare areas along what could be a high resistivity electrolyte path beneath the coating. Corrosion of this type has historically been identified as an important failure mode

for cathodically protected epoxy-coated pipelines in buried applications. Specific experiments addressing the extent to which cathodic protection can be realized upon steel beneath a disbonded coating in concrete were included in the Task 3 work plan.

Note 11: Electrochemical Chloride Extraction (ECE) has recently become a demonstration technology for bare reinforced concrete transportation structures. As such, several trial projects are underway; but it may be years before long-term results are available and the method can be fully qualified. Specific difficulties that are considered important in the application of ECE to ECR structures and components, in addition to the two discussed above in conjunction with cathodic protection, are:

1. The coating is expected to be fully disbonded at the conclusion of the ECE treatment and can no longer be relied upon to provide corrosion protection,
2. The degree to which chloride is extracted may be highly variable from one location to the next since coating resistivity may be high at some places and low in others, and
3. Pathways for rapid remigration of corrosion reactants along the disbonded coating may result since the steel itself was not bonded directly to the concrete.

It was concluded that study of the application of ECE to ECR structures should wait until the learning experience for bare reinforcement is more complete. Consequently, no experiments specifically relevant to ECE were included in this study.

Note 12: Inclusion of corrosion inhibiting admixtures in concrete as a part of initial construction has now been adapted by numerous state DOT's as a corrosion control measure. Also, corrosion inhibitors are now available for surface application to concrete; however, the extent to which any

of these are effective has not been well documented to date. Possible alternatives for incorporation of corrosion inhibitors into repair/rehabilitation include the following:

1. Surface application as a corrosion prevention strategy (no repair/rehabilitation involved).
2. Surface apply in conjunction with patching (prior to and/or after patching; the former may be particularly applicable if no admixed inhibitor is used in the patch material and/or if bars are not recoated).
3. Admix in repair/rehabilitation materials (without surface applied inhibitor).
4. Surface application prior to placement of an overlay.
5. Admix in overlay materials (with or without surface application on existing concrete).

Option 1) was cited above as a means of corrosion control within existing cracks (see Note 4). Options 2) and 3) were mentioned in conjunction with both 2-D (see Note 4) and 3-D patch repairs (see Note 5) where inhibitors can be either surface applied or admixed (or both). Specific experiments were included to address the effectiveness of these approaches. However, since surface applied inhibitors may adversely impact the bond between patch material and existing concrete (unless additional cleaning steps are taken), these materials were applied only after all patching was completed. In addition, no cementitious materials were placed over concrete surfaces which received the inhibitor. Although surface applied inhibitors prior to placement of an overlay (option 4) and admixed inhibitors in overlays (option 5) are applicable, specific experiments pertaining to this were not recommended (see Note 8).

Note 13: Combinations of various corrosion control strategies for ECR in concrete are considered particularly appropriate, as noted above, where inhibitors plus patch or overlay

materials (or both) were discussed (see Notes 4 and 5, for example). As such, this approach was discussed in previously mentioned, specific cases.

Note 14: No new corrosion control strategies were identified for inclusion in the study. However, during the project, the research team did keep abreast of the corrosion control literature, specifically as this pertains to steel in concrete and to ECR in particular. A promising new strategy employing an embedded galvanic anode (Galvashield XP Anode) in patch areas was identified. This technology was only recently introduced and therefore, was not included in the subject research effort.

Note 15: The option of not repairing/rehabilitating is a viable one from the standpoint of optimizing the remaining life cycle cost. Experiments pertaining to this were included in the study in all categories for which testing was recommended as baseline or control specimens. It was thought that results from these, in comparison to those for the companion repair/rehabilitation strategies, would provide the necessary input from which appropriateness of the 'Do Nothing' option could be assessed for a particular situation.

Summary of Selected Repair/Rehabilitation Strategies for Evaluation in Task 3

Based on the above discussion, the following specific strategies were evaluated in this study. It should be noted that these strategies apply to asphalt covered ECR bridge decks only after the asphaltic layer is removed.

I. 2-D Patch Repair - Corrosion Induced and Combined:

   a. Epoxy injection.

   b. Flood with corrosion inhibitor.

c. Flood with corrosion inhibitor and epoxy injection.

d. Flood with corrosion inhibitor, epoxy injection, and surface application of corrosion inhibitor.

II. 2-D Patch Repair - Non-Corrosion Induced (corrosion has not yet occurred):

a. Epoxy injection.

b. Flood with corrosion inhibitor and epoxy injection.

c. Flood with corrosion inhibitor and surface application of corrosion inhibitor.

III. 3-D Patch Repair - Corrosion Induced and Combined:

Note that for all 3-D patch repair strategies, the extent of concrete removal (i.e., remove all unsound concrete and remove concrete (sound or damaged) around the entire circumference of exposed bars) and bar cleaning (i.e., sandblast to remove all existing coating and corrosion products) was the same.

a. Patch only (includes several different materials).

b. Recoating exposed steel and patching (includes numerous coating and patch materials).

c. Recoating exposed steel and patching with admixed corrosion inhibitors (includes numerous coating, patching, and corrosion inhibiting materials).

d. The same strategy as in C, but with surface inhibitors being applied subsequent to patching (with and without admixed corrosion inhibitors).

IV. 3-D Patch Repair - Non-Corrosion Induced:

For cases where post-damage corrosion has not transpired and no reinforcing steel is exposed, repairs can be affected according to established protocols for bare steel reinforced concrete structures. If reinforcing steel is exposed, it is likely to be corroded; and repairs would be affected in the same manner as in the case of 3-D corrosion induced damage.

V. Overlays and Barriers - Corrosion, Non-Corrosion, and Combined (including 2-D and 3-D patching):

The overlay and barrier experience that has been gained from concrete structures containing bare reinforcement should be directly applicable to situations where ECR is involved.

This strategy also includes use of surface applied inhibitors prior to placement of an overlay and admixed inhibitors in overlay materials (with or without surface application on existing concrete). However, activities pertaining to these were limited to analyses as opposed to experiments per se.

VI. Partial Replacement:

No experiments in this category were included.

VII. Cathodic Protection:

Experiments in this category focussed upon the extent to which cathodic protection can be realized upon steel beneath a disbonded coating in concrete.

VIII. Electrochemical Chloride Extraction:

No experiments specifically relevant to ECE were included.

IX. Combined Strategies:

This approach is represented in the above categories where two or more strategies have been combined.

X. New Strategies:

No new corrosion control strategies were included.

XI. Do Nothing Strategy:

Experiments pertaining to this were included in all categories for which testing was recommended as baseline or control specimens.

MATERIALS AND PROCEDURES

This section describes the procedures and materials used in performing repairs of test specimens and test areas on field structures. Where, deviations from the norm occurred, the deviations are noted in the appropriate Appendix where the test results for the specimens are reported.

Crack Repair

Flood with Corrosion Inhibitor

Prior to flooding the cracks with the corrosion inhibitor, the cracks were cleaned thoroughly using a supersonic pick which delivers an airstream velocity in excess of 2334 km/hr (1450 mph) and holds the airstream together up to 101 mm (10 inches).

Two corrosion inhibitors, Corrosion Inhibitor A (MCI-2020, a water based amine and an oxygenated hydrocarbon) and Corrosion Inhibitor B (Postrite, a calcium nitrite based inhibitor) were evaluated in this study. Corrosion Inhibitor A was applied at the following rates recommended by the manufacturer.

Crack Width (mills)	Lineal feet per gallon
10	275
15	262.5
20	250
40	200
60	150

It was applied in two coats. To ensure that the corrosion inhibitor was applied at the recommended application rate, the quantity of inhibitor required was measured out for each specimen based on the average crack width and total length of cracks. The measured quantity of inhibitor was then applied in the cracks with a narrow tip squirt bottle. A total of two coats of corrosion inhibitor were applied in the cracks at the recommended rate. The second coat was applied after the first coat had dried to touch and there was no standing solution.

Corrosion Inhibitor B was applied in three separate applications, and during each application, the crack was supersaturated with the inhibitor. Subsequent applications were applied after the previous application was dry to the touch and there was no standing solution on the concrete surface.

Epoxy Injection

Epoxy injection of cracks was accomplished by injecting Epoxy Injection A (Thermal-Chem Injection Resin, bisphenol A and polyamine curing agent) in the cracks using manufacturer recommended equipment and procedures. The injection was performed by a technician trained in the process. Prior to epoxy injection, the cracks were cleaned with the supersonic pick.

When epoxy injection was to be performed subsequent to flooding cracks with a corrosion inhibitor, the cracks were thoroughly rinsed with tap water to remove any residue left by the inhibitor. The rinsing operation was performed after the corrosion inhibitor was dry to touch and there was no standing solution.

Surface Application of Corrosion Inhibitor

The effectiveness of surface application of Corrosion Inhibitor A was evaluated. The inhibitor was applied at the rate of 6.1 m^2/L (250 square feet per gallon).

When surface application of the inhibitor followed flooding of the cracks by the same inhibitor, the inhibitor was applied immediately after the cracks were flooded; and if it followed epoxy injection, it was applied after the epoxy had cured.

Delamination and Spall Repair

A total of three concrete repair (patch) materials were evaluated in combination with three admixed corrosion inhibitors, three bar coatings, and one surface applied corrosion inhibitor. Due to financial and time constrains a total of 13 combinations out of the 27 combinations possible were evaluated in this study.

All damaged areas on the test specimens and the field structure were demarcated by acoustic methods and the perimeter of the repair areas were sawcut 25 mm (1 inch) deep without damaging the embedded rebars. Additional concrete was removed along exposed rebars until 25 to 50 mm (1 to 2 inches) of uncorroded rebars were exposed along their length in each direction. Sufficient concrete around exposed rebars was removed to provide a 19 mm (¾inch) clearance around the entire circumference of the bar. Concrete removal was accomplished using a 6.8 kg (15 lb.) (maximum) chisel hammer. All exposed rebars were sandblasted to a "hear white" condition in accordance with SSPC-SP10. All coating on the rebars exposed in the repair area were removed.

Surface preparation of repair areas included sandblasting with medium grade black beauty sand followed by extra fine (passing mesh # 30) black beauty sand. After sandblasting and immediately prior to applying bar coatings and/or patch material, the entire repair areas were cleaned with an air blast. Patch materials were applied the same day the cleaning operation was completed on a saturated surface dry concrete substrate, with no standing water at the time of the placement of the patch material.

All patch materials were wet cured for 7 days using wetted burlap and polyethylene sheets. For each type of patch material (patch material with corrosion inhibitor was considered a different mix), a total of three 76 mm by 102 mm (by 3 inch by 6 inch) cylinders were cast and cured the same way as the patch material. Compressive strength test was performed at 28 days of age.

All coatings on exposed rebars were installed in accordance with manufacturer's instructions.

Patch Repair Material

A pre-bagged, ultra high strength, air-entrained portland cement based concrete Patching Material A (Metro Mix 240 AE) and a pre-bagged, polymer modified, silica fume enhanced repair mortar Patching Material B (Sika Mono Top 615) were used on laboratory specimens and on a bridge structure. Patching Material C, a Class III concrete as specified by the Florida Department of Transportation Standard Specifications for Road and Bridge Construction was evaluated on a bridge structure.

Bar Coatings

Three bar coatings, Rebar Coating A (Scotchkote 306, ambient temperature cure, two part thermosetting liquid epoxy coating same color as Scotchkote 206N), Rebar Coating B (Armatec 110 Epochem, three component, water based epoxy resin/portland cement bonding agent), and Rebar Coating C (ECB, a single component, water based barrier with corrosion inhibitor) were included in the study for evaluation.

Rebar Coating A was applied as a single coat of 16 mil thickness. Whereas, Rebar Coatings B and C were applied as two coats of 508 μm and 177 μm (20 mil and 7 mil) thick, respectively.

Surface Application of Corrosion Inhibitor

The effectiveness of surface application of Corrosion Inhibitor C (MCI 2020) was evaluated by applying the inhibitor at the rate of 6.1 m^2/L (250 square feet per gallon).

When surface application of the inhibitor followed flooding of the cracks by the same inhibitor, the inhibitor was applied immediately after the cracks were flooded, and if it followed epoxy injection it was applied after the epoxy had cured.

Corrosion Inhibitor Admixture

The following three admixed corrosion inhibitors were evaluated in this study:

Corrosion Inhibitor C (MCI-2000, a water based amine inhibitor) was added to the mix water at the rate of one 0.6 L/m^3 (pint per cubic yard). Due to the small quantity of admixture, the mixing water was not adjusted.

Corrosion Inhibitor D (DCI-S, a calcium nitrite based inhibitor) was added to the mix water at the rate of 15 L/m^3 or 20 L/m^3 (3 gallons or 4 gallons per cubic yard). Mix water was adjusted to account for 0.83 kg/L (7 lbs. of water per gallon) of inhibitor.

Corrosion Inhibitor D (Catexol 1000 CL, multicomponent corrosion inhibitor and concrete densifier) was added to the mix water at the rate of 17.5L/m^3 (3.5 gallons per cubic yard) and the mix water was adjusted to account for 55% water content by volume of the inhibitor.

Cathodic Protection

Material and procedures for cathodic protection are discussed in Appendix E.

APPENDIX B

EVALUATION OF REPAIR STRATEGIES FOR NON-CORROSION INDUCED CONCRETE DAMAGE

EXPERIMENTAL PROCEDURE

The objective of this evaluation was to investigate and determine the effectiveness of various options for the repair of cracks in concrete that have not resulted from corrosion of ECR. Based on the discussion presented in Appendix A, the following repair options were selected for evaluation:

a. no repair
b. epoxy injection of cracks
c. flood with corrosion inhibitor and epoxy injection
d. flood with corrosion inhibitor and surface application of inhibitor

The following materials were used to implement the above repair options:

Epoxy Injection A: bisphenol A and polyamine curing agent

Corrosion Inhibitor A: water based amine and an oxygenated hydrocarbon

These repair options were applied to new specimens that were constructed to simulate a crack along each of the top mat transverse ECRs. Cracks of various sizes were simulated so that the limitations, if any, of each repair option with regards to crack width could be ascertained. Specimen preparation is discussed below and all details pertaining to the application of the repairs and materials are discussed in Appendix A. Table B-1 presents repair options and materials used in this study.

Specimens Preparation, Instrumentation, and Exposure

Experiments in this category utilized four non-corrosion damaged (NCD) macrobeam. Each of these consisted of, first, a bottom mat of three longitudinal (19 mm (#6 or (0.75 in)) nominal diameter) black bars (BB) and, second, a top mat of nine equally spaced transverse ECRs (Tecr) upon two longitudinal ECRs (Lecr). The ECR was Scotchkote 213 16 mm (#5 or 0.625 inches) bars that were acquired from a plant in Jacksonville, Florida. Clear cover of the outer bars was 25 mm (1.0 in) in all cases. Each of the transverse bars contained a single, central 3.2 mm (0.125 in) diameter coating defect positioned at the top of the bar. Longitudinal bars, on the other hand, had two similar defects equally spaced between each of the transverse bars. The concrete above each of the transverse ECRs contained a simulated crack to the depth of and parallel to the ECR. These "cracks" were formed by placing a stainless steel shim above each transverse ECRs prior to concrete pouring and then withdrawing this after one day of curing. The shim width for transverse ECR bar numbers T1-T3 was 0.51 mm (0.020 inches), for bar numbers T4-T6 1.02 mm (0.040 inches), and for bar numbers T7-T9 1.52 mm (0.060 inches). Figure B-1 presents a schematic illustration of a NCD specimen.

Concrete for the NCDs was poured in two lifts, where the bottom 100 mm (4.0 in) was Cl^- free and the top 51 mm (2.0 in) contained 11.88 kg/m^3 (20 pcy Cl^-) as NaCl. Concrete mix design is presented in Table B-2. Figure B-2 shows the end region of an NCD beam subsequent to concrete pouring and removing the forms and appearance of several of the simulated cracks. No accelerated corrosion was affected in the case of the NCDs, and these experienced natural weathering only subsequent to fabrication (January, 1997).

Table B-1: Repair Options and Materials.

Repair Option/Materials	Repair Option	Specimen/Test location Identification
		NCD Macrobeams
No Repair	NCD-A	NCD-1
Epoxy Injection	NCD-B	NCD-2
Flood with Corrosion Inhibitor A	NCD-C	NCD-3
Flood with Corrosion Inhibitor A and Surface Application of Corrosion Inhibitor A	NCD-D	NCD-4

Table B-2: Concrete mix design for new G109 specimens.

Material	Description	Specific Gravity	Amount
Cement	ASTM C-150, Type I	3.15	360.1 kg/m^3 (605 pcy)
Fine Aggregate	ASTM C-33	2.56	703.6 kg/m^3 (1182.0 pcy)
Coarse Aggregate	S.F.B.C. Pearock (3/8 in max)	2.46	910.7 kg/m^3 (1530.0 pcy)
Water	ASTM C-84	1.00	183.3 kg/m^3 (308.0 pcy)
Air Entrainer	ASTM C-260, MBVR	-	-

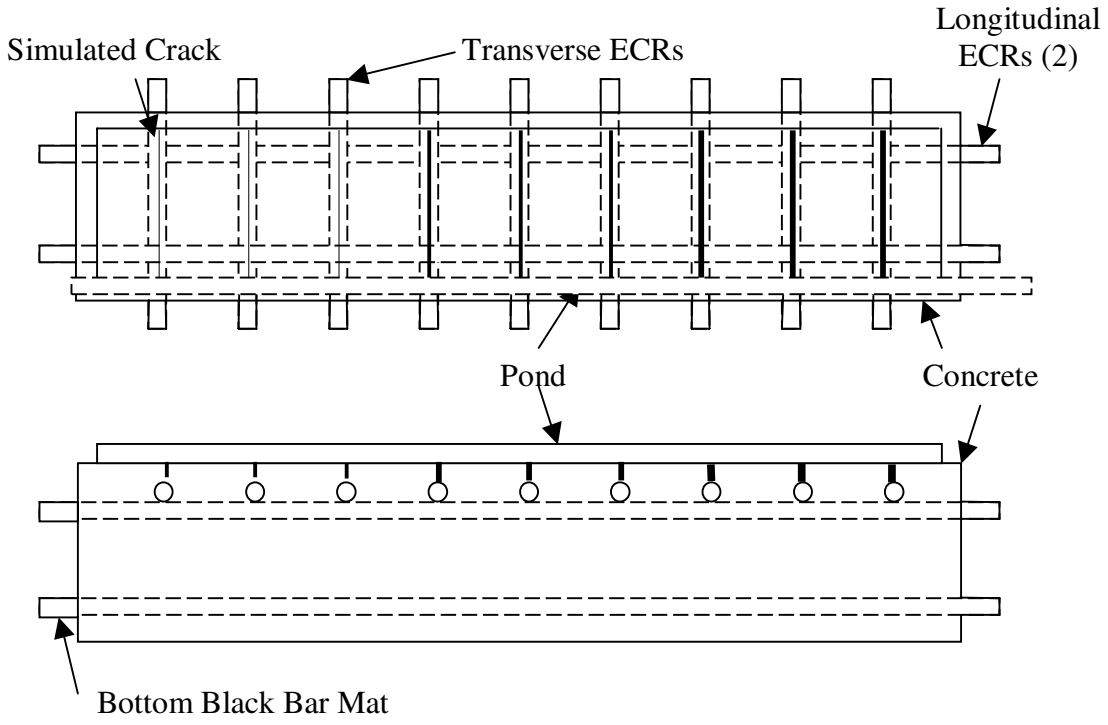

Figure B-1: Schematic illustration of Non-Corrosion Damaged (NCD) macrobeam.

Figure B-2: Top surface of an NCD macrobeam subsequent to concrete curing showing simulated cracks.

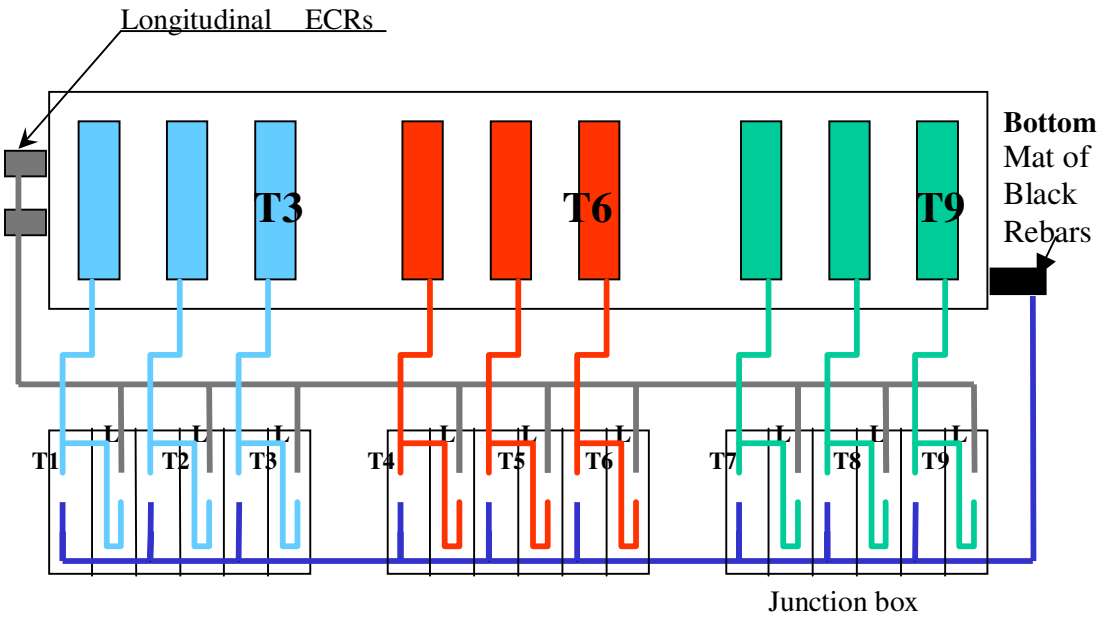

Figure B-3: Schematic illustration of a NCD macrobeam with electrical measurement circuitry.

Figure B-3 illustrates the external circuitry with which the macrobeams were instrumented for purposes of data acquisition. This consists of an electrical connection to 1) each of the nine Tecr, designated as Tx where "x" is the bar number (1-9), 2) the bottom black steel mat (B), and 3) the longitudinal top ECRs (L). Throughout the exposure, each terminal pair was shorted except for relatively brief periods during which connection to a zero resistance ammeter was made for the macrocell current measurements and during which resistance was measured across each terminal pair. The former parameter (current) was measured with all other terminal pairs (circuit legs) shorted, whereas resistance between two terminals of interest was measured with all other circuit connections open. Table B-3 lists the designation nomenclature for components between which current was measured in the case of each terminal pair, and Table B-4 does the same for resistance. Consequently, the measured current in the case of the T9-B was that between a particular Tecr (number 9 in this case) and the bottom mat black steel (I_{tb}) plus the current between the Lecr and the black mat steel (I_{lb}), whereas, the measured current in the case of the L-(T9+B) terminals was between the Tecr and the bottom black mat steel (I_{lb}) plus the current between the Lecr and the Tecr (I_{lt}). The data collection schedule for these specimens is listed in Table B-5.

The repair options were installed on the NCD macrobeams in December, 1998. After the repairs were affected and baseline post-repair data were acquired, the top surface of each macrobeam was subjected to a two week wet, two week dry ponding cycle using a 15 w/o NaCl solution. Subsequent data acquisitions were normally, but not always, taken during the dry portion of the cycle.

Electrochemical Impedance evaluation was also conducted 4 times during the entire test period.

Table B-3: Listing of the components between which current was measured for each terminal pair.

Terminals	Connection
Tx-B	Transverse ECR Number “x”to Bottom Black Bar Mat plus Top Longitudinal ECR to Bottom Black Bar Mat.
L-(Tx+B)	Top Longitudinal ECRs to Transverse ECR Number “x”Plus Bottom Black Bar Mat.

Table B-4: Listing of the components between which resistance was measured for each terminal pair.

Terminals	Connection
Tx-B	Transverse ECR Number 'x' and Bottom Black Steel Mat.
L-B	Top Longitudinal ECRs and Bottom Black Steel Mat.

Table B-5: Scheduling of the macrocell and resistance data acquisitions.

Data Acquisition Number	Timing
1	Baseline, Just Prior to Repair.
2	Baseline, Just After Repair.
3	Repair + One Month (wet).
4	Repair + One Month (dry).
5	Repair + Three Month (dry).
6	Repair + Four Month (wet).
7	Repair + Five Month (dry).
8	Repair + Eight Month (dry).
9	Repair + Thirteen Month (dry).

FINDINGS & DISCUSSIONS

Correlation between the T-B and T-L resistances at each of the measurement times was excellent in all cases. Figure B-4 shows a typical plot of these data, and Table B-6 lists the R^2 and Slope values for the different measurement times. This suggests that these resistances were controlled by the respective transverse bars, which is consistent in the former case (T-B connection) with the bottom bars being uncoated and, hence, of low resistance and in the latter (T-L connection) with the longitudinal bars being of relatively large surface area. Figure B-5 shows the average T-B resistance for each specimen at the time of the various data acquisitions. This indicates that this parameter (resistance) was relatively high for each specimen at the time of the two baseline and first two post repair data acquisitions and low thereafter. Also, during the latter period (low resistance), resistance tended to decrease with time for the repaired beams.

Resistance between the Lecr and BB was also measured, with the results being shown in Figure B-6. Thus, this resistance was approximately an order of magnitude less than that between the Tecr and the BB (or, alternatively, between the Lecr and Tecr). This presumably reflects the relatively large surface area of the longitudinal bars compared to the transverse one.

For the two sets of baseline and five of the seven sets of post repair data, a correlation was apparent between the T-B and L-(T+B) macrocell current data. Such correlation was poor for post-repair data acquisitions five and six, however. Figure B-7 shows an example where the correlation was good and Figure B-8 where it was less so. For cases where identical currents were measured for each terminal pair, the slope of the best fit line should be unity. A positive

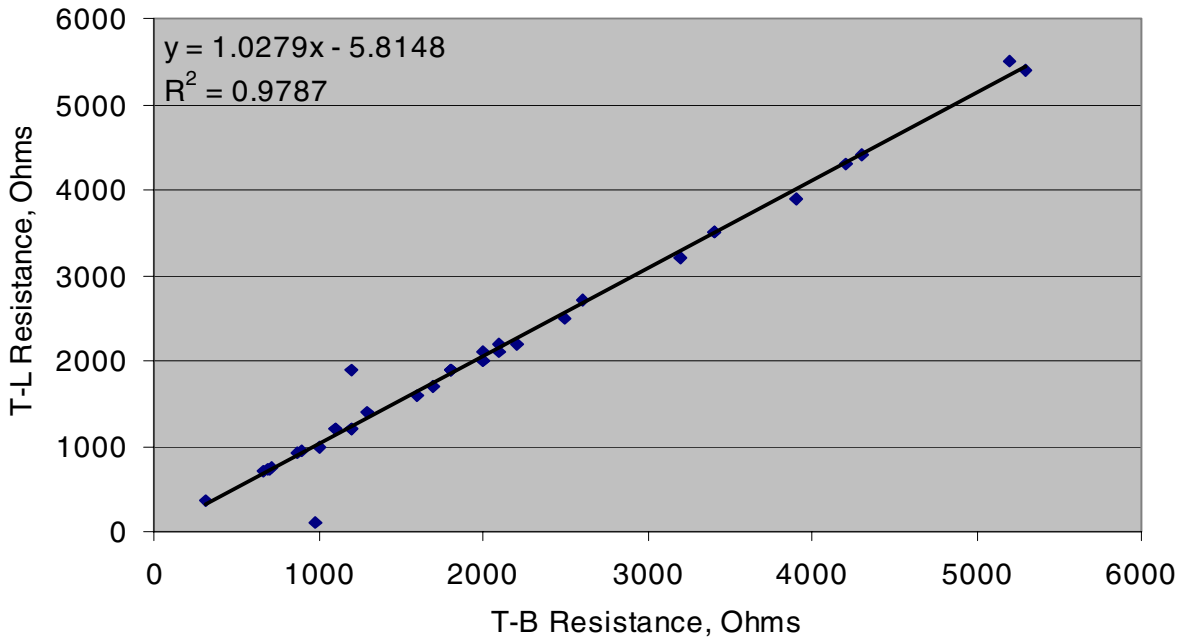

Figure B-4: Resistance between the T-B terminals plotted versus the corresponding values for the L-B terminals at the time of the Fifth Post Repair data acquisition.

Table B-6: R^2 and best fit line slopes for plots of the average T-B versus T-L resistances at the different measurement times.

Measurement	R^2	Slope
First Baseline	1.00	1.00
Second Baseline	1.00	1.00
First Post Repair	1.00	1.00
Second Post Repair	1.00	1.00
Third Post Repair	1.00	0.99
Fourth Post Repair	1.00	1.01
Fifth Post Repair	0.98	1.03
Sixth Post Repair	0.95	0.96
Seventh Post Repair	1.00	1.01

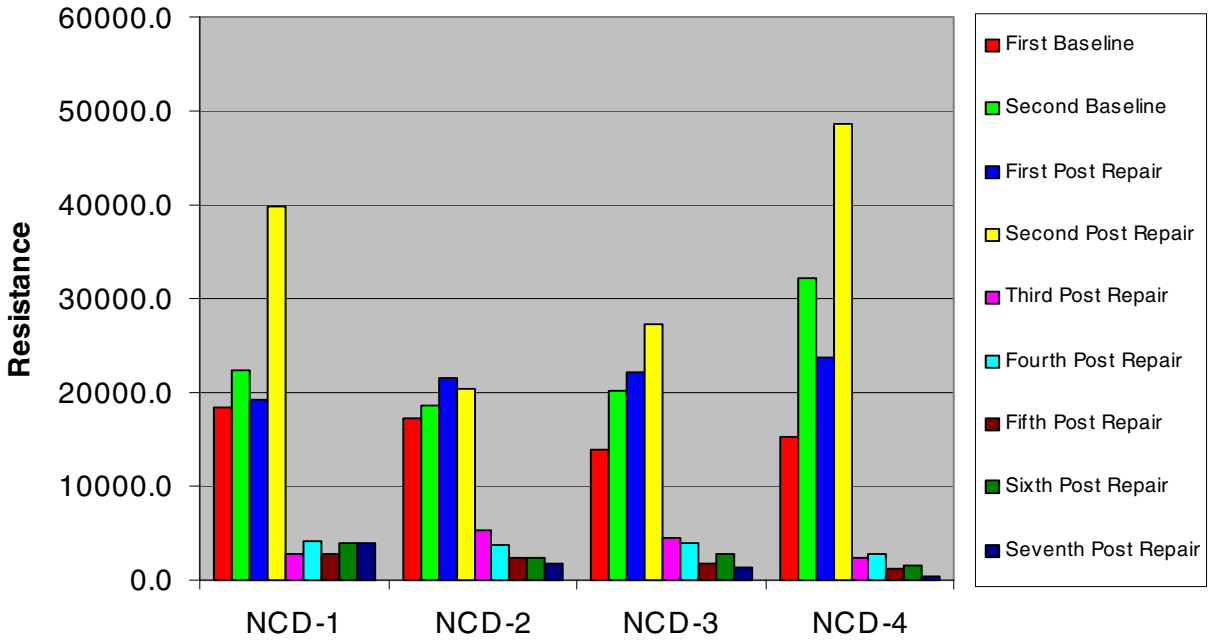

Figure B-5: Listing of the average T-B resistances at each of the data acquisition times for the four NCD specimens.

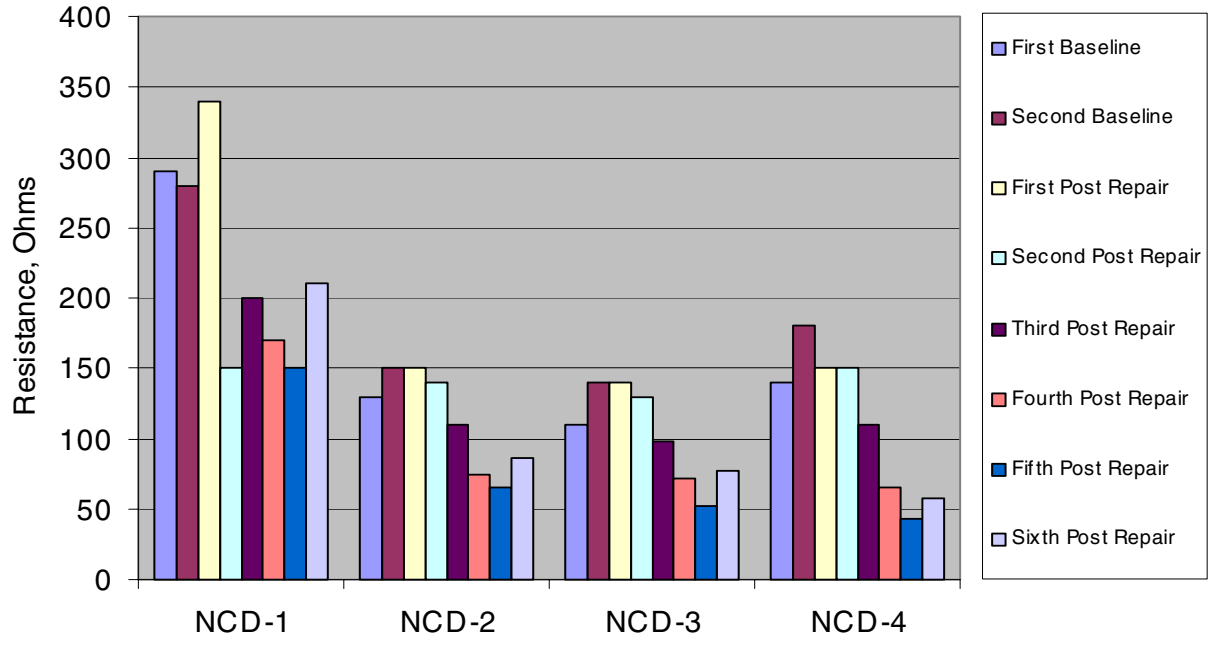

Figure B-6: Resistance between the bottom black steel mat and longitudinal ECRs at the time of each data acquisition.

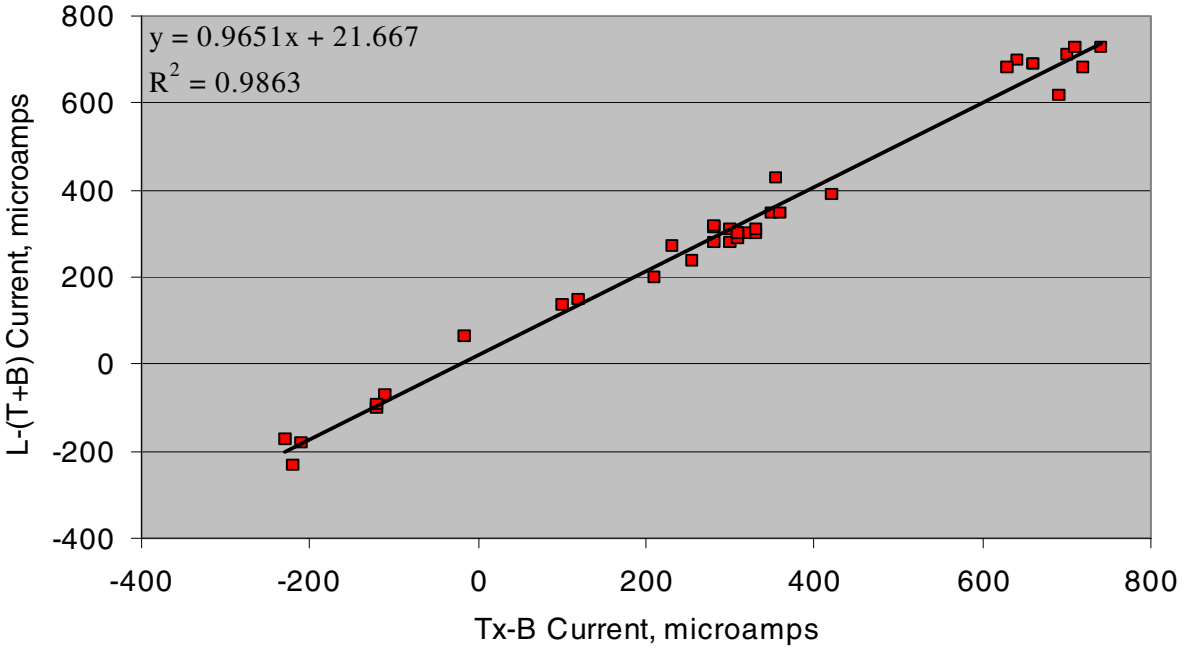

Figure B-7: Macrocell current between the Tx-B terminals plotted versus the corresponding values for the L-(Tx+B) terminals at the time of the First Baseline data acquisition.

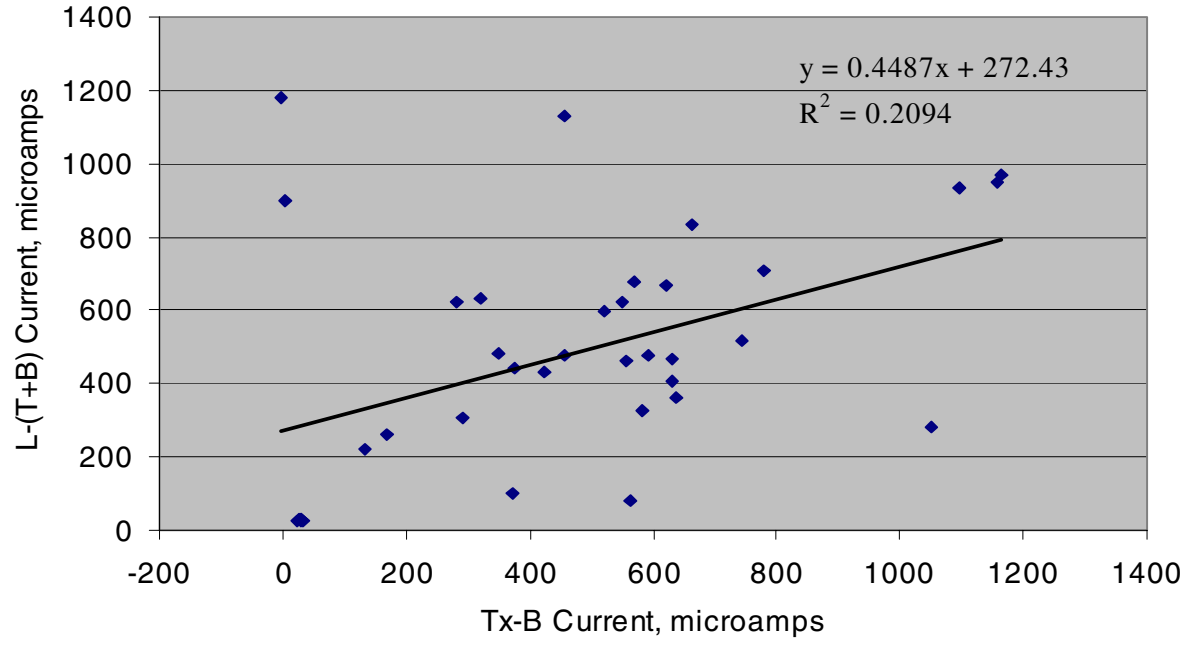

Figure B-8: Macrocell current between the Tx-B terminals plotted versus the corresponding values for the L-(Tx+B) terminals at the time of the Fifth Post Repair data acquisition.

current is indicative of the ECR being anodic to the black steel. Table B-7 lists the R^2 and Slope values for the best fit line for each of the nine data sets.

As the current through terminals Tx-B is a sum of I_{tb} and I_{lb}, and terminal L-(Tx-B) is the sum of I_{lb} and I_{lt}, the following equation determines the relationship between the various currents when the currents measured on terminal Tx-B and L+(Tx-B) are similar in magnitude and direction:

$$I_{tb} + I_{lb} \sim I_{lb} + I_{lt}$$

For this equation to be satisfied I_{tb} must be equal to I_{lt} which is also predicted by the resistance data presented above. This is possible if and only if the transverse ECR is anodic to both the longitudinal ECR and the black steel mat and the latter two are at the same potential. Such is expected as the transverse ECR was exposed in a crack and the chloride ion content in the surrounding concrete was higher than the threshold required for initiating corrosion from the time the macrobeams were constructed.

The variation of macrocell current Tx-B with time is presented in Figure B-9 and indicates that in general the macrocell current was somewhat variable, but by the seventh post repair evaluation the macrocell current in all macrobeams had reversed. The excellent correlation (see Table B-7) between Tx-B and L+(Tx-B) observed up to the fourth post repair evaluation dissipated during the fifth and the sixth post repair evaluations and regained much of the lost correlation during the last evaluation. These data can be explained by the Lecr becoming active with time due to the presence of large quantities of chloride ions in the surrounding concrete, continuous ingress of chloride ions due to the bi-weekly cycling, and the presence of intentionally created defects. The large surface area of the Lecr and the BB, is expected to generate a large current which could mask the currents generated by the transverse ECR. In such

Table B-7: R^2 and best fit line slopes for plots of the average Tx-B versus L-(Tx+B) macrocell currents at the different measurement times.

Measurement	R^2	Slope
First Baseline	0.99	0.97
Second Baseline	0.99	1.00
First Post Repair	0.87	0.87
Second Post Repair	0.84	0.96
Third Post Repair	0.94	0.92
Fourth Post Repair	0.96	0.98
Fifth Post Repair	0.20	0.45
Sixth Post Repair	0.24	-0.18
Seventh Post Repair	0.71	0.94

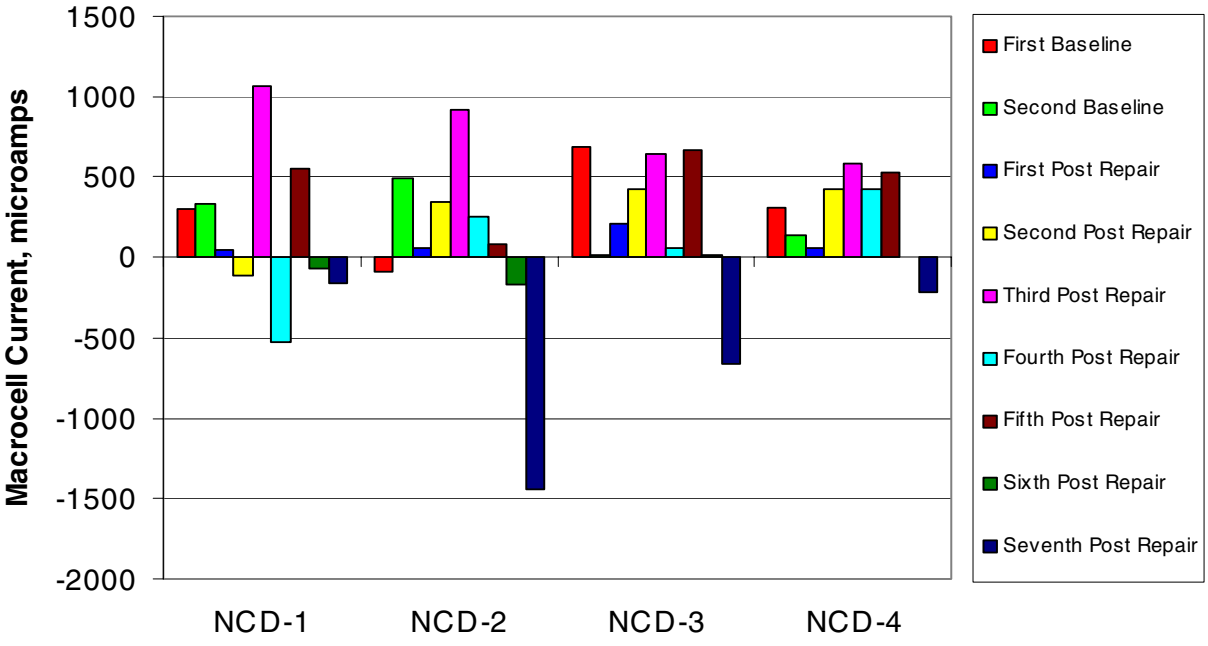

Figure B-9: Listing of the average Tx-B macrocell current at each of the data acquisition times for the four NCD specimens.

a situation, I_{tb} and I_{lt} are not expected to be similar in magnitude or direction and this is reflected by the not as perfect a correlation observed during the seventh post repair evaluation. There are other possible combinations of currents that can produce the results observed during the seventh post repair evaluation, but the one noted above is believed to be the most likely.

No consistent trend is apparent in the macrocell currents to indicate that corrosion performance of any of the repaired macrobeams was better than for the non-repaired one. Also, the transverse ECR exhibited anodic behavior at least up to the forth post repair evaluation and possibly continued to be anodic to the black steel mat during the remaining evaluations. With the exceptions noted below, none of the macrobeams, including the non-repaired one, exhibited any corrosion induced damage throughout the study.

Figure B-10 shows the results of impedance measurements that were performed upon the transverse ECRs. Here data were averaged for each crack width and for each specimen. Because of experimental problems, data was not collected for NDC-1 and NDC-2 during the second and third acquisitions. The data indicate that, subsequent to the repairs, impedance decreased with time, which is indicative of a progressive reduction in coating quality. The fact that this trend generally parallels that of the resistance data (see Figure B-8), suggests that coating quality controlled this parameter (resistance) also. The range of the impedance data generally covers about one order of magnitude (except for the third acquisition where only limited results are available). No clear effect of crack width upon impedance is apparent. However, it may be significant that impedance of the NCD-1 and NCD-2 ECRs was relatively high at the final data acquisition, whereas that for NCD3 and NCD4 it was relatively low. This suggests that the repairs had no effect upon coating quality.

A visual inspection of the NCD macrobeams at the time of the seventh data acquisition showed that no concrete damage had occurred at the simulated crack-transverse ECR region of any of the specimens. Figure B-11 shows the appearance of one of these specimens. Rust staining was apparent on the side specimen faces in conjunction either with a pond leak or seepage from the simulated crack. However, a relatively large corrosion induced crack was apparent upon the side face of Specimen NCD-3 at the level of the Bottom Black Bar Mat. Figure B-12 presents a photograph of this. No trends in the data for this specimen could be related to presence of this crack.

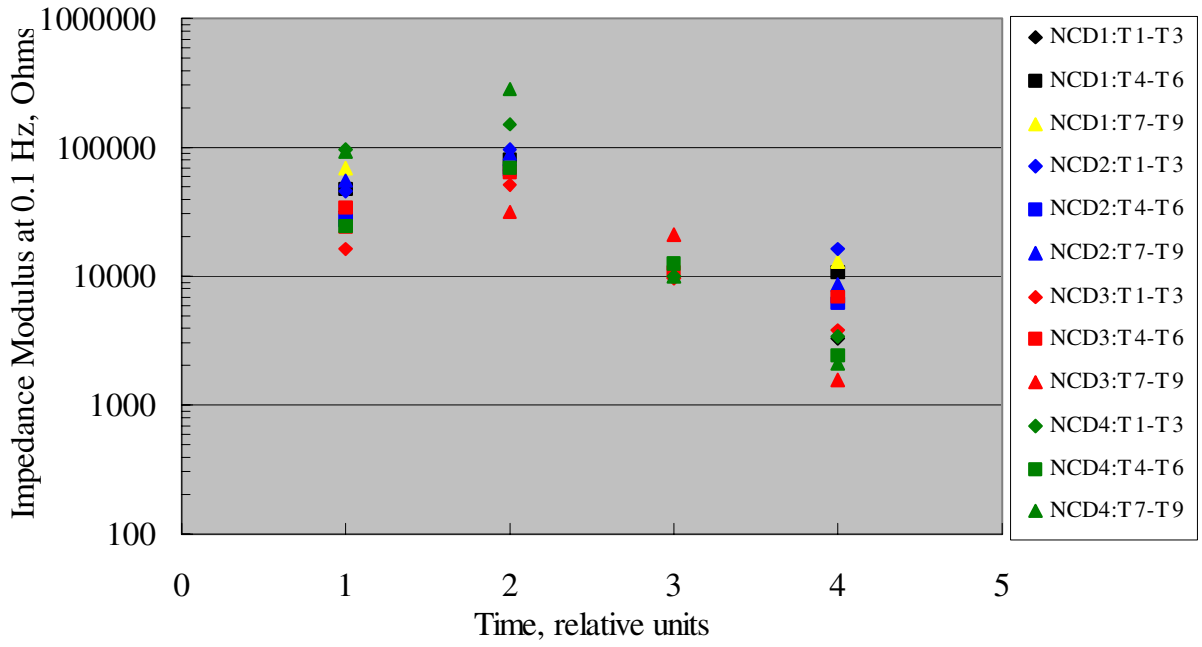

Figure B-10: Impedance data for the NCD macrobeams.

Figure B-11: Photograph of two NCD macrobeams under exposure testing.

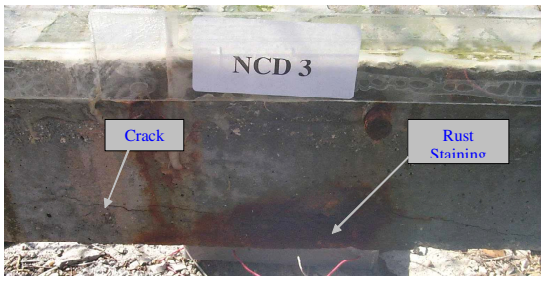

Figure B-12: Photograph of one side of Specimen NCD-3 showing a crack induced by corrosion of the bottom mat reinforcement and associated rust staining.

APPENDIX C

EVALUATION OF REPAIR STRATEGIES FOR CORROSION INDUCED CRACKING

EXPERIMENTAL PROCEDURE

The objective of this part of the program was to investigate and determine the effectiveness of various options for repair of cracks in concrete that result from ECR corrosion. Based on the discussions presented in Appendix A, the following repair options were selected for evaluation:

a. no repair (Control)

b. epoxy injection of cracks

c. flood with corrosion inhibitor

d. flood with corrosion inhibitor and epoxy injection

e. flood with corrosion inhibitor, epoxy injection, and surface application of corrosion inhibitor

and the following materials were used to implement the above repair options:

Epoxy Injection: bisphenol A and polyamine curing agent

Corrosion Inhibitor A: water based amine and an oxygenated hydrocarbon

Corrosion Inhibitor B: calcium nitrite based inhibitor

These repair options were applied on new specimens in which cracking was induced by forced initiation and acceleration of ECR corrosion, existing specimens ("old specimens") constructed in previous studies, and on an existing bridge deck suffering corrosion induced cracking. All details pertaining to the application of the repairs and materials are discussed in Appendix A.

The following specimens types were used in the laboratory evaluation:

1. **G-109 Specimens:** Specimens constructed in accordance with ASTM G-109, "Standard Test Method for Determining the Effects of Chloride Admixtures on Corrosion of Embedded Reinforcement in Concrete Exposed to Chloride Environments." Both, new specimens constructed in this study and old G109 specimens from a previous NCHRP study were used. The G-109 specimens were embedded in a beam to simulate bridge deck environment.

2. **FHWA Slabs:** Existing slabs from a previous FHWA study.

3. **Bent Bar Slab:** Existing slab from a previous study.

All repair options were applied on the newly constructed G-109 specimens, only select repair options were installed on all other specimens and the select bridge deck. Table C-1 tabulates the specimen types, and repair options installed.

Experimental procedure and tests results for each specimen type are presented below.

G109 MACROBEAM STUDY

Experimental Procedure

A total of twelve concrete beam type specimens, termed G-109 macrobeams, were fabricated, each of which was comprised of three primary components, as listed below:

1. Three standard size G-109 specimens embedded at the upper macrobeam surface. The topmost bar in each G-109 was epoxy coated and the bottom two were bare. These three G-109's were designated as "G-109L", "G-109M", and "G-109R" (left, middle, and right) according to their position in the macrobeam. Twenty-one of the G109s were

fabricated as a part of this program (these are designated as "new" G109s), while 15 were acquired from a previous study ("old" G109s) as explained below.

2. Three adjacent ECR mats. These were also positioned at the uppermost macrobeam surface with one being adjacent to each of the G-109 specimens. These mats were designated as "L-ADJ", "M-ADJ", and "R-ADJ" according to their position relative to a G-109.

3. A bottom mat of black steel. This consisted of three 16 mm (#5 or 0.625-inch) longitudinal bars and seven equally spaced 9.5 mm (#3 or 0.375-inch) transverse bars.

Fabrication and testing of the G109 macrobeams involved the following steps and procedures:

1. Preparation of the G109 specimens. The ECR in each G-109 specimen was in the as-received condition except that three equally spaced 3.2 mm (0.125 in) diameter coating defects were introduced along the top surface of the bars. The ECR was Scotchkote 213 16 mm (#5 or 0.625-inch) bars that were acquired from a plant in Jacksonville, FL. The concrete was poured in two stages with material for the bottom 100 mm (4.0 in) utilizing the mix design in Table C-2. The top 51 mm (2.0 in) was the same concrete as for the bottom but this was admixed with 11.88 kg/m^3 (20 pcy) Cl^- by adding additional water containing NaCl. This increased the w/c to 0.61. The 28 day compressive strength for the lower lift concrete was 42.2 MPa (6,120 psi) and for the upper 36.2 MPa (5,240 psi). Figure C-1a shows an 11 station G109 form after placement of the bottom concrete lift and installing the ECRs, and Figure C-1b shows this after completion of the pour. The new G109 specimens were cast in January, 1997.

The old G109s were fabricated in early 1992 as a part of NCHRP Project 10-37 and, subsequent to curing, underwent outdoors natural weathering in northern Virginia. The bars for these were acquired from several coaters and job sites in the United States and Canada; however, the coating was Scotchkote 213 in all cases. The concrete for the old specimens was placed in two lifts where the top 51 mm (2.0 in) contained 8.91 kg/m^3 (15 lbs. chloride per cubic yard) as NaCl, and the concrete below this was chloride free. The mix design, other than for chlorides, for both lifts is shown in Table C-3. Figure C-2 shows a photograph of several of the old G109 specimens as received.

2. Accelerated corrosion of the G-109 specimens. Subsequent to curing, a plastic bath with a mixed metal oxide (MMO) mesh was fitted to the top surface of all (new and old) G-109 specimens; and beginning in March, 1997, each ECR was subjected to an impressed anodic current of 0.5 mA in conjunction with salt water ponding. This current was subsequently reduced to 0.3 mA. Preliminary tests indicated that this should cause a corrosion induced crack to form in approximately one month. However, cracking had not occurred as of July, 1997; and so to expedite matters, fabrication of the macrobeams proceeded.

3. Casting of G-109 macrobeams. Concrete pouring for the macrobeams was performed in July, 1997. This involved mounting three G-109 specimens along with three adjacent mats and a bottom black bar mat into a plywood form. Figure C-3 illustrates the geometry of these specimens. The top 51 mm (2 in) of the adjacent mat concrete was prepared using the same concrete mix design with admixed chlorides as for the

Table C-1: Repair Options, Materials, and Specimen Types

Repair Option/Materials	Repair Option	Specimen/Test location Identification				
		New G109 Beams	Old G109 Beams	FHWA Slabs	Bent Bar Slab	Duanesburg Bridge
No Repair	CIC-A	1	3	206		C1 & C2
Epoxy Injection	CIC-B	2	4	207		C3 & C4
Flood with Corrosion Inhibitor A	CIC-C	8	5	208	X	C5 & C6
Flood with Corrosion Inhibitor A and Epoxy Injection	CIC-D	9	6	203		C7 & C8
Flood with Corrosion Inhibitor A, Epoxy Injection, and Surface Application of Corrosion Inhibitor A	CIC-E	10	7	210		C9 & C10
Flood with Corrosion Inhibitor B	CIC-F	11				
Flood with Corrosion Inhibitor B and Epoxy Injection	CIC-G	12				

Table C-2: Concrete Mix Design for New G-109 Specimens

Material	Description	Specific Gravity	Amount
Cement	ASTM C-150, Type I	3.15	360.1 kg/m^3 (605 pcy)
Fine Aggregate	ASTM C-33	2.56	703.6 kg/m^3 (1182.0 pcy)
Coarse Aggregate	S.F.B.C. Pearock (3/8 in max)	2.46	910.7 kg/m^3 (1530.0 pcy)
Water	ASTM C-84	1.00	183.3 kg/m^3 (308.0 pcy)
Air Entrainer	ASTM C-260, MBVR	-	-
Slump			100 mm (4 in)

Table C-3: Concrete Mix Design for Old G-109 Specimens

Material	Amount
Cement	356.7 kg/m^3 (599.3 pcy)
Water	178.4 kg/m^3 (299.7 pcy)
Coarse Aggregate	910.0 kg/m^3 (541.7 pcy)
Sand	823.5 kg/m^3 (1383.5 pcy)
Daravair, AEA	38.7 ml/m^3 (4.6 oz/gal)

(a) (b)

Figure C-1: Photographs of an 11 stations G-109 form with (a) lower lift of concrete in place and (b) completed pour.

Figure C-2: Photograph of old G-109 specimen as received.

upper 51 mm of the G-109s, whereas the lower concrete was chloride free (mix design per Table C-2). The 28 day compressive strength for both concretes was essentially the same as for the G-109s. The specimens were cured for seven days using wet burlap and a polyethylene sheet cover. Subsequently, they were exposed directly to the atmosphere. Figure C-4 shows a photograph of three macrobeams subsequent to demolding and installation of electrical lead wiring, and Figure C-5 is a close-up view of an embedded G109 with a concrete surface crack. Clear cover for all outer bars was 25 mm (1.0 in).

Continued impressed current accelerated corrosion of the G-109 specimens. Because no cracking had occurred as of January, 1998, the current was increased to 0.4 mA for some specimens. Current was increased for the other specimens two months later. As of the end of March, 1998, six of the G109 specimens exhibited hairline cracks, and rust stains were apparent on these and other specimens where the bars exited the concrete. As of July, 1998, impressed current testing of ten specimens was terminated since cracks of what was judged to be adequate size had developed; and current for the remaining ones, which were either uncracked or insufficiently cracked, was increased from 4.4 to 9.8 mA. Cracks developed upon all but two of the latter specimens at various times, and impressed current testing was terminated in June, 1999. Invariably, cracks developed in all of the new G109 specimens; and it was the old specimens that required the longer test times. Upon termination of impressed current testing for individual macrobeams, these continued under natural weather exposure in Southern Florida only.

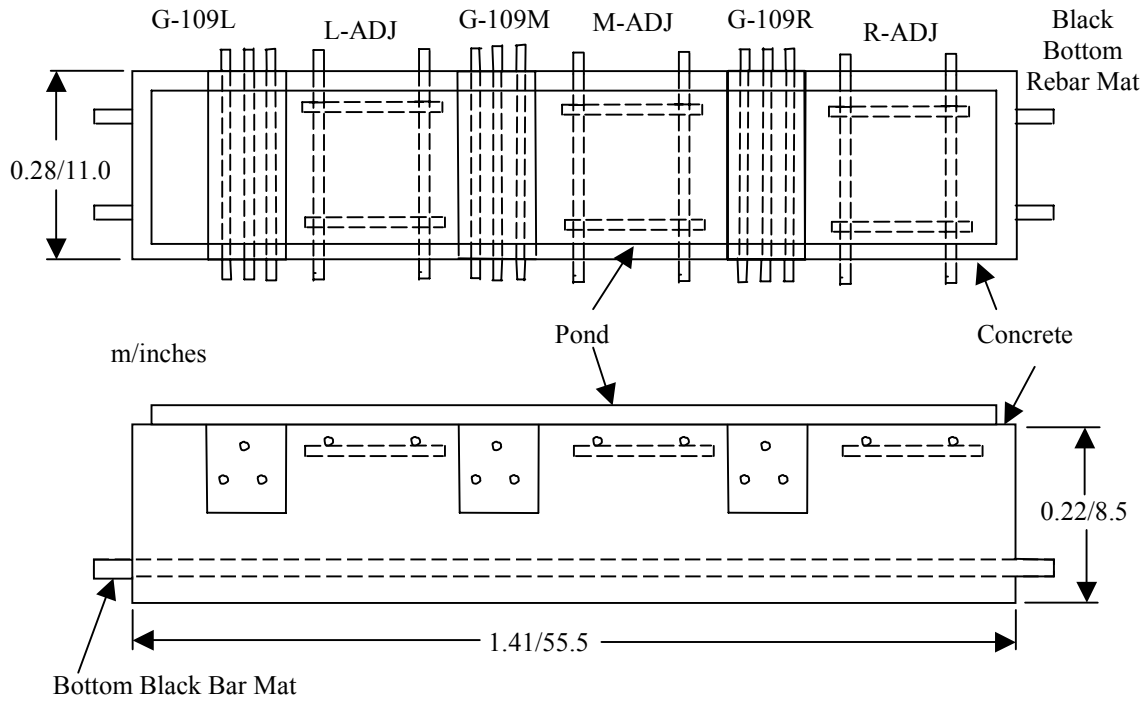

Figure C-3: Schematic illustration of a G-109 macrobeam.

Figure C-4: Photograph of three G-109 macrobeams subsequent to fabrication and demolding.

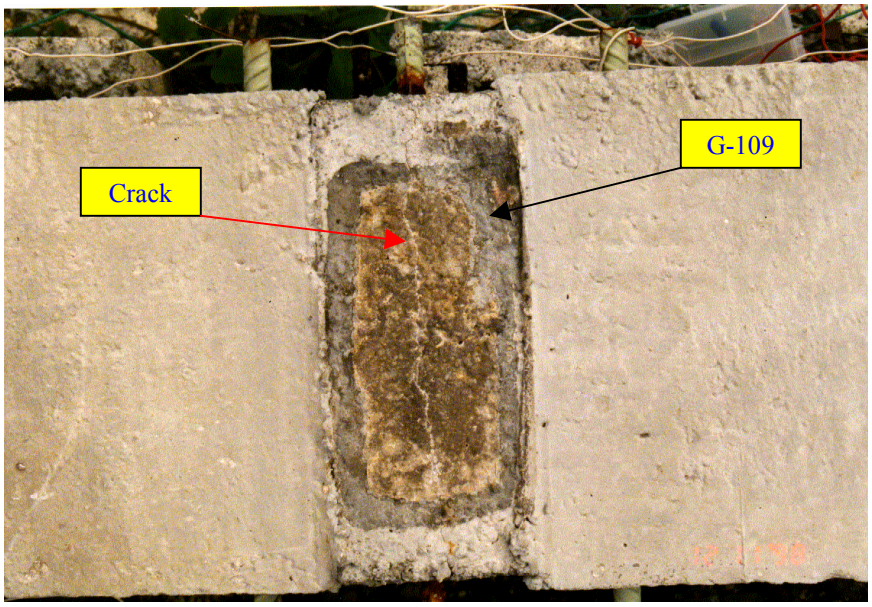

Figure C-5: Top down close-up view of a G-109 specimen embedded in a microbeam

5. Data acquisition. Figure C-6 illustrates the external circuitry with which each G-109 macrobeam was instrumented for purposes of data acquisition. This involved a direct lead wire from the ECR of each G-109 and adjacent ECR mat to a junction box, whereas the two black bars of each G-109 were connected to the bottom black bar mat. Figure C-7 shows an enlarged view of the junction box from Figure C-6 along with a designation scheme for the six pairs of connection terminals. Throughout the exposure, each terminal pair was shorted except for relatively brief periods during which both macrocell current and resistance were measured across each of the six connection pairs for each of the G-109 macrobeams.

   The former measurement (current) employed a zero resistance ammeter and the latter (resistance) a Nillson AC resistance meter and involved connecting the meter leads to the terminal pair of interest and then opening the switch that normally shorted the terminals. A distinction in these two sets of measurements (macrocell current versus resistance), however, is that the former parameter (current) was measured with all other terminal pairs (circuit legs) shorted, whereas resistance between two terminals of interest was measured with all other circuit connections open. Table C-4 provides a description then of the components between which current flow was measured in the case of each terminal pair, and Table C-5 does the same for resistance. Consequently, the measured current in the case of the L-B, M-B, and R-B terminals was that between a particular G-109 (L, M, or R) plus its adjacent ECR mat (these two components in parallel) and all other components (the other two G-109's, the other two adjacent ECR mats, and the bottom black steel).

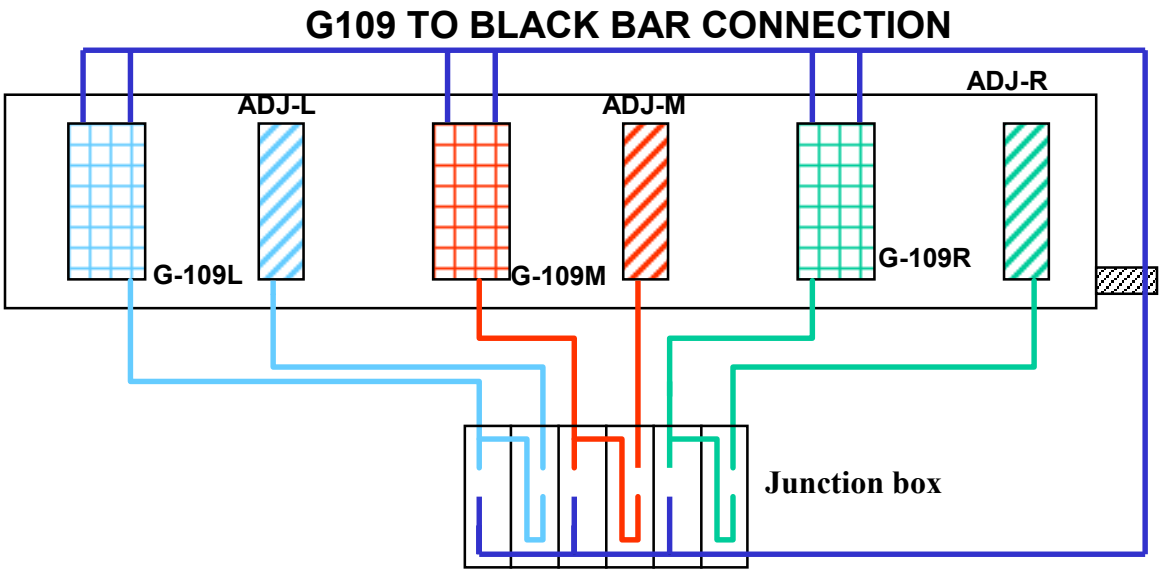

Figure C-6: Schematic illustration of a G-109 macrobeam with electrical measurement circuitry.

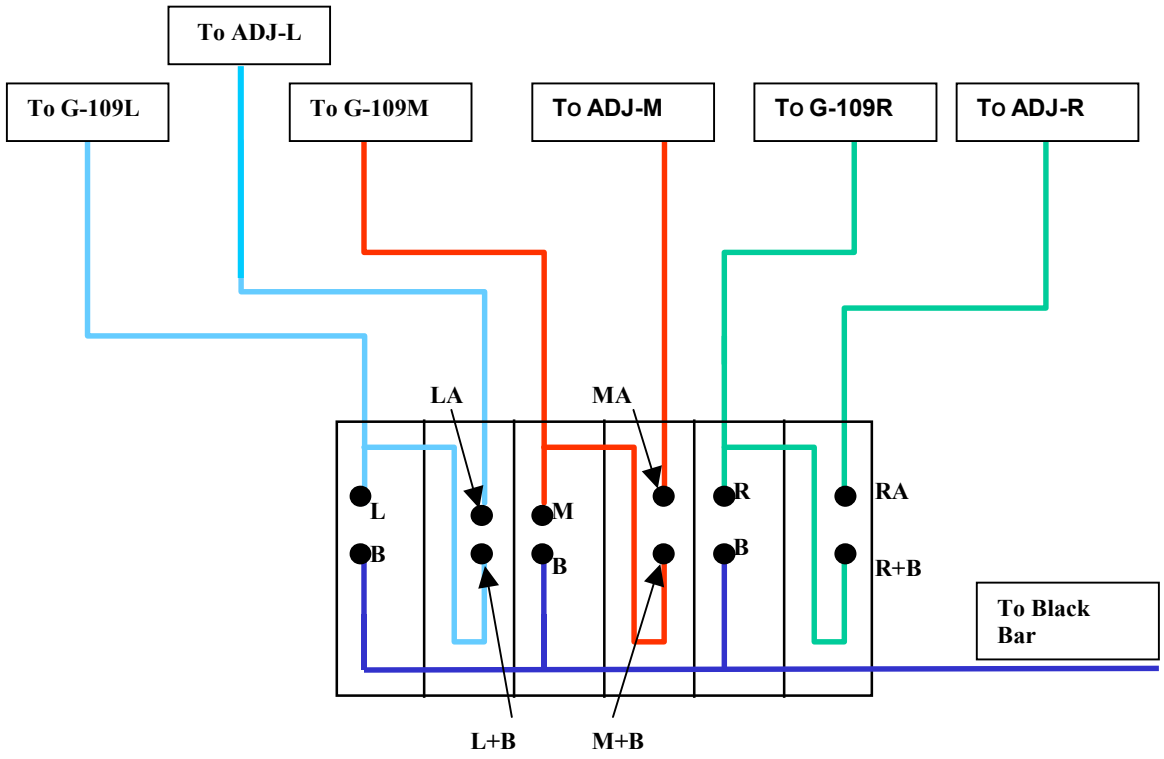

Figure C-7: Schematic illustration of the G-109 macrobeam circuit terminals for current and resistance measurements

Of course, the influence of each component upon the measured current should be a function of the resistance between it and the G-109/adjacent ECR mat pair in question. For resistance, however, the measured value was that between the two isolated components only (Table C-5). Figure C-8 shows a schematic equivalent circuit for the G-109 macrobeams with the various terminals and concrete components identified.

AC impedance (electrochemical impedance spectroscopy or EIS) scans of the G-109 ECRs were also performed with the circuit open. These utilized a MMO mesh that was placed upon a wetted sponge on the top G-109 surface. A central hole in the sponge accommodated a SCE gel electrode. The scans were performed using a Gamry system with a PC4FS1 potentiostat, a 10 mV potential amplitude for relatively poor ECRs and 50 mV for relatively good ones, and a scan range from 100 kHz to either 0.1 or 0.01 Hz. The scans were performed early in the drying cycle, and the concrete surfaces were spray wetted prior to placement of the sponge.

Table C-6 indicates the data acquisition schedule for impedance scans and Table C-7 for macrocell current and resistance.

6. Repair strategies. Table C-1 lists the repair strategy for each macrobeam. These were instituted for the new G109 macrobeams during December, 1998 and for the old ones in June, 1999.

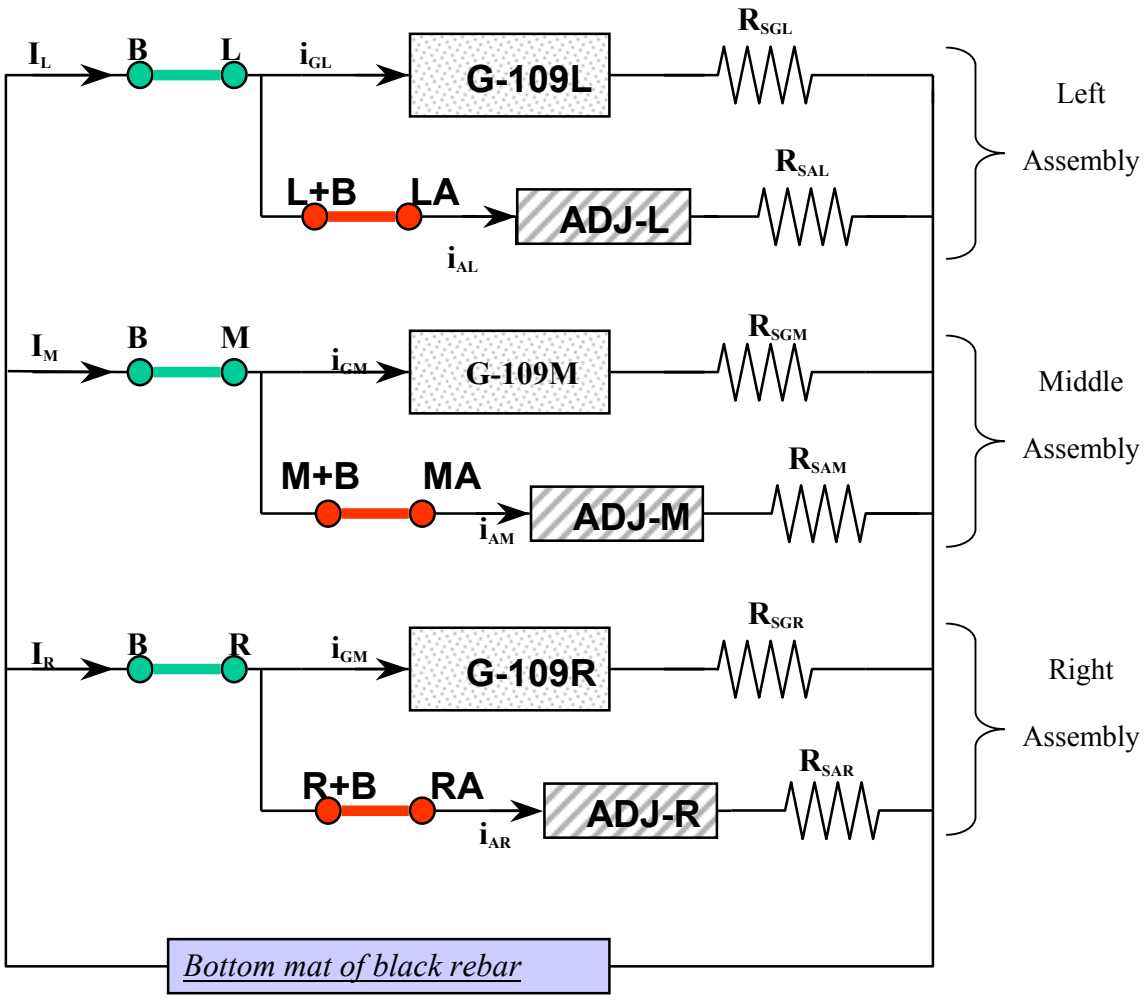

Switch

G-109X — Represents impedance of the indicated G-109

ADJ-X — Represents the total impedance of a set of parallel Circuits that comprise the indicated adjacent ECR mat.

$R_{S\#x}$ — Represents the total concrete resistance between 1) the indicated G-109 ECR or adjacent ECR mat and 2) the other two component assemblies and the bottom mat of black rebars.

Figure C-8: Representation of the G-109 macrobeam equivalent circuit.

Table C-4: Listing of the components between which current was measured for each terminal pair.

Terminals	Connection
L-B	G-109L plus ADJ-L to Adjacent Assembly Components plus Bottom Black Bar Mat.
LA-(L+B)	ADJ-L to G-109L plus Adjacent Assembly Components plus Bottom Black Bar Mat.
M-B	G-109M plus ADJ-M to Adjacent Assembly Components plus Bottom Black Bar Mat.
MA-(M+B)	ADJ-M to G-109M plus Adjacent Assembly Components plus Bottom Black Bar Mat.
R-B	G-109R plus ADJ-R to Adjacent Assembly Components plus Bottom Black Bar Mat.
RA-(R+B)	ADJ-R to G-109R plus Adjacent Assembly Components plus Bottom Black Bar Mat.

Table C-5: Listing of the components between which resistance was measured for each terminal pair.

Terminals	Connection
L-B	G-109L to Black Bar Mat.
LA-(L+B)	G-109L to ADJ-L.
M-B	G-109M to Black Bar Mat.
MA-(M+B)	G-109M to ADJ-M.
R-B	G-109R to Black Bar Mat.
RA-(R+B)	G-109R to ADJ-R.

Table C-6: Scheduling of the EIS data acquisitions.

Data Acquisition Number	Time (relative to repair)
1	Just before repair.
2	Repair plus one month.
3	Repair plus seven months.
4	Repair plus ten months.

Table C-7: Scheduling of the macrocell and resistance data acquisitions.

Data Acquisition Number	Timing
1	Baseline, Just Prior to Repair.
2	Baseline, Just After Repair.
3	Repair + One Month (wet).
4	Repair + One Month (dry).
5	Repair + Three Month (dry).
6	Repair + Four Month (wet).
7	Repair + Five Month (dry).
8	Repair + Eight Month (dry).
9	Repair + Thirteen Month (dry).
10	Repair + Twenty Month (dry).

7. Exposure testing. Subsequent to termination of the impressed current accelerated corrosion testing, the macrobeams underwent natural weathering in Southern Florida climate only. After the repairs were affected and baseline post-repair data were acquired, the top surface of each macrobeam was subjected to a two week wet, two week dry ponding cycle using a 15% NaCl solution. Subsequent data acquisitions were normally, but not always, taken during the dry portion of the cycle.

Findings & Discussion

Figure C-9 shows the G-109 ECR plus adjacent ECR, adjacent ECR mat, and estimated G-109s ECR macrocell current variations with time for each of the repair types. Figures C-11 and C-12 do the same for resistance. In these representations, each data point is an average of the parameter in question for the three identical components of a given macrobeam. For example, the "time 1" data points in Figure C-9a reflect the average macrocell current of the L-B, M-B, and R-B connections for each repair strategy. The time scale shown here is in relative units, meaning that data were not necessarily collected at equally spaced intervals. Also, because exposure of the old G-109s commenced after that of the new ones, a given data acquisition (first, second, and so on) was actually performed at different times for the two specimen groups (old versus new G-109s macrobeams). Table C-7 lists the timing of the different data acquisitions along with the slab condition (wet versus dry) at that time.

For the first eight data acquisitions, the G109 plus adjacent ECR current was positive in all cases and the adjacent ECR current was positive in most cases, meaning that the upper component, either the G-109 or adjacent mat or both, were anodic such that the bottom black steel served as a macrocathode.

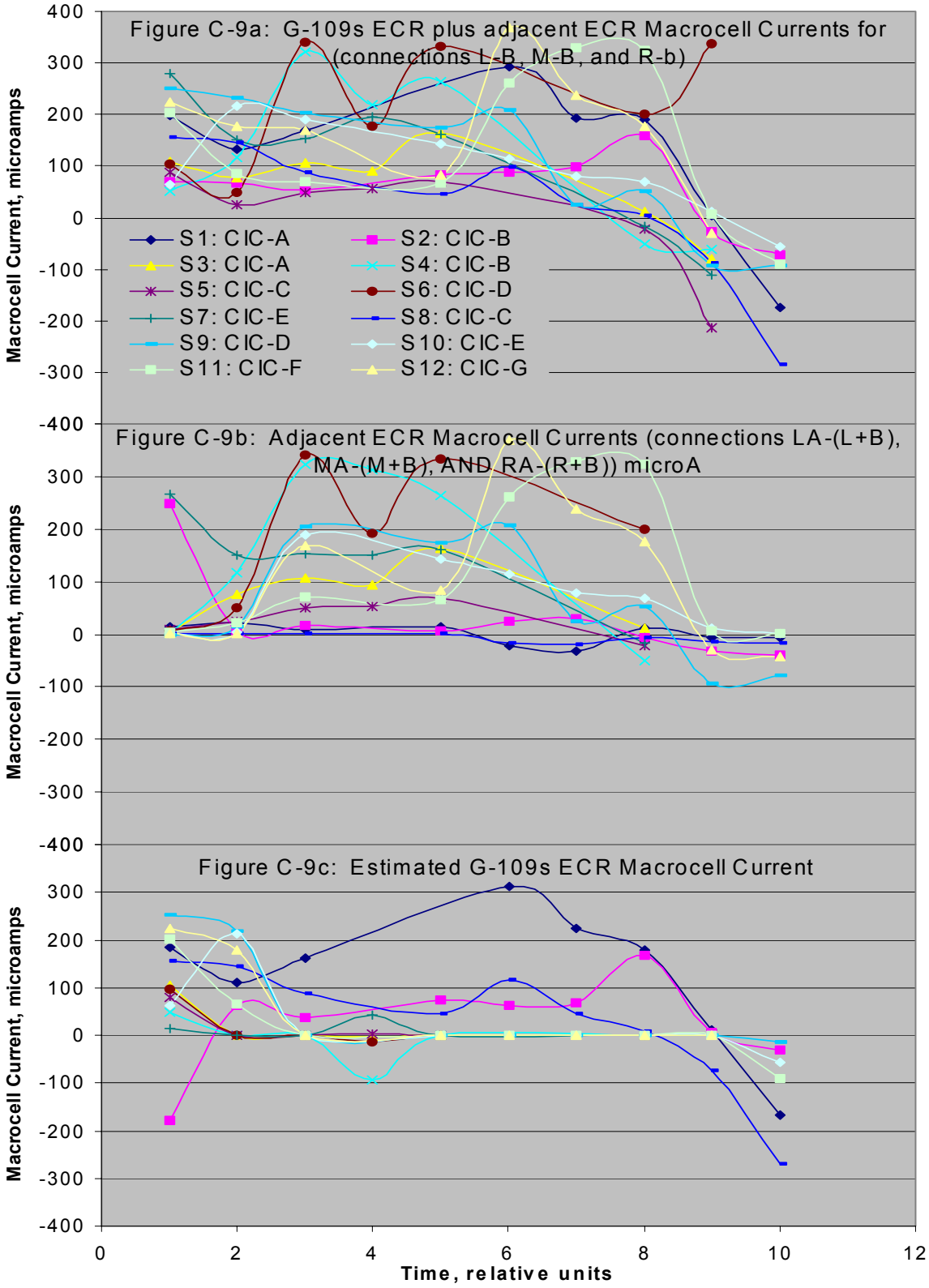

Figure C-9: Average macrocell current for each macrobeam and repair schemes as a function of time.

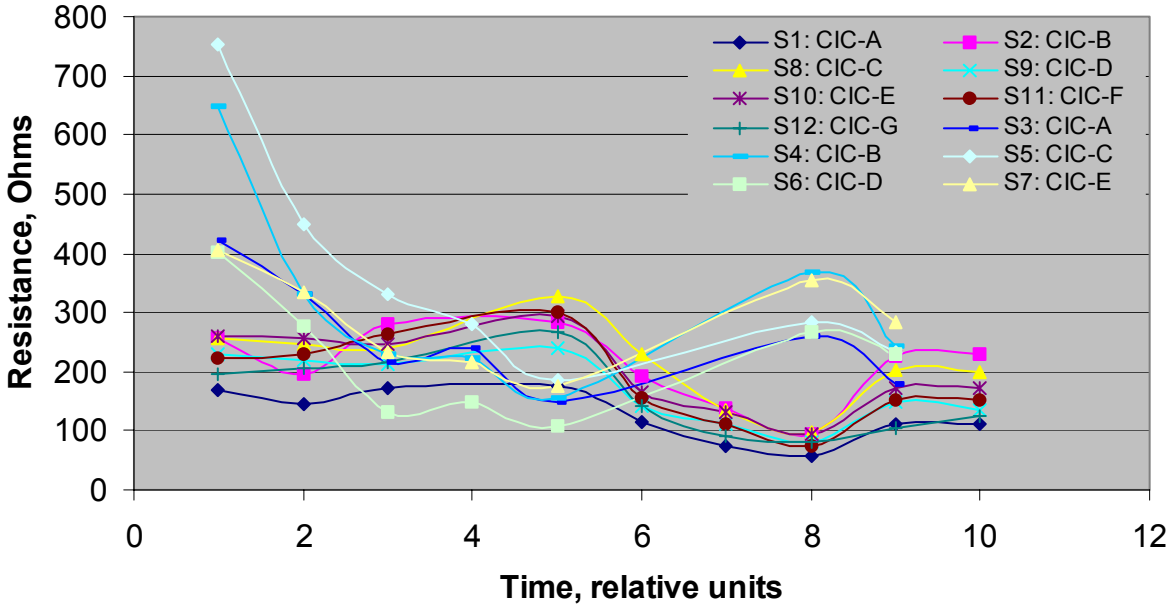

Figure C-11: Average G-109 ECR-to-black steel resistance (connections L-B, M-B, and R-B) for each macrobeam and repair schemes as a function of time.

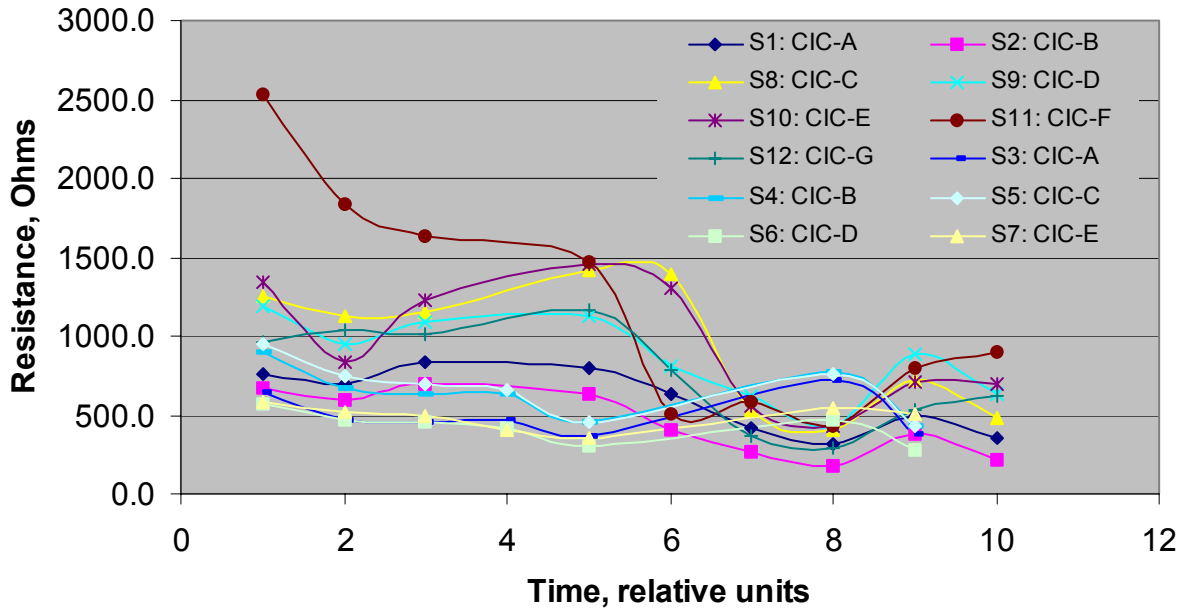

Figure C-12: Average adjacent ECR-to-black steel resistance (connections LA-(L+B), MA-(M+B), and RA-(R+B)) for each macrobeam and repair schemes as a function of time.

Figure C-9c, which was derived by subtracting the adjacent ECR macrocell current from G-109s ECR plus adjacent ECR current, suggests that with the exception of three macrobeams (S1: CIC-A, S2: CIC-B, and S8: CIC-C) all other macrobeams exhibited minimal macrocell activity for the G-109s ECR. It should be noted however that the macrocell circuit of the beams is complex, and the difference between the two measured macrocell currents is only an approximation of the G-109s ECR current.

The currents for one macrobeam compared to the next differed over about a 300 μA range and in some cases were relatively low and invariant and for others high and variable with time. The overall trend in many cases is one where current decreased with time during the final four data acquisitions and in most instances was negative at the time of the final two data acquisitions (bottom black steel was anodic to the upper G109 and adjacent ECR). Data for both the "old" and "new" specimens tend to be scattered over approximately the same range such that no distinction between these is apparent. Also, it is unclear that the macrocell current data are indicative of effectiveness versus lack of performance of a particular repair method, as opposed to simply specimen-to-specimen variations. In particular, macrocell current for the "new" baseline specimen (no repair) was intermediate to that of other specimens, while for the "old" baseline it was low (both connection types (Figures C-9a and C-9b)). Also, the G109-bottom mat macrocell current was relatively high during the monitoring period for one of the old G109 repaired macrobeams (Slab 6: CIC-D, flood with corrosion inhibitor A and epoxy injection) and intermediate-to-low for the other.

The general trend of the resistance data (Figures C-11 and C-12) was that this parameter either decreased or was relatively constant with time. As such, comparison of these data with the macrocell current results in Figure C-9 indicates that the results do not conform to the normal

trend where the magnitude of macrocell current varies inversely with resistance. In this regard, the expectation is one where corrosion activity of bars in the upper, chloride contaminated concrete should increase with time and potential should correspondingly become more negative. If potential of the bottom black steel mat remained relatively constant and positive, then an increase in potential difference and, hence, macrocell current should result. The fact that an opposite trend occurred may reflect a beneficial effect from the repairs whereby corrosion activity was reduced and potential of the G-109 elements shifted to values that were more positive than prior to repair. At the same time, either greater salt uptake by the concrete or progressive development of defects in the ECR with time (or both) should have resulted in reduced resistance between respective components. These two events may have occurred in a relatively independent manner but with the former (decrease in macrocell potential difference with time) being dominant compared to the latter (resistance decrease with time). Alternatively, the potential of the different bar components may have become more similar with time such that macrocell current decreased proportionally. This is possible if the chloride ions start to reach the bottom black steel mat of the G-109s which start to become active. The bottom mat of the G-109s is only a few inches away from the top ECR. The top layer of concrete in the G-109s has a very high level of chloride ions added to the mix, and the slabs are exposed to a biweekly ponding cycle with 15% w/o NaCl solution. With such high levels of chloride ions in the mix and the forced migration of chlorides into the specimen, it is possible for the chlorides to reach the bottom mat of the G019s and shift potential in the negative direction.

Table C-8 lists average values for these two parameters and indicates that the average macrocell current for the adjacent ECRs was approximately 4.2 times less than for the G-109s plus adjacent ECR. This is consistent with the fact that the latter bars had been pre-corroded via an impressed

current to the point where, in most cases, a concrete crack had developed and the bottom mat of the G-109s may be becoming active. That the average resistance between the adjacent mats and the other components was 2.6 times higher than for the G109s is at least qualitatively consistent with this. Differences between the new and old G109s are not considered significant.

The macrocell current for both the G-109 and adjacent mats was relatively low or negative for all macrobeams at the time of the last two data acquisitions (see Figures C-9a to 9c) but was high in some cases at earlier times. Macrobeams for which all data from the 10^{th} acquisition is available exhibit a tendency for the macrocell current for the G-109s ECRs to become more negative with time. This suggests that, although, the repair schemes were able to mitigate the development of the anodic sites, they were not successful in preventing the formation of cathodic sites in the repair area. For successful corrosion mitigation, it is necessary that the repair scheme not only mitigate corrosion in the treated area but also prevent the formation of cathodic sites that would feed anodic sites just outside of the repair area. It should be recognized that the repair schemes were tested in very aggressive corrosion environment.

Figures C-13 and C-14 present impedance data for the G109 and adjacent mat bars, respectively, where each individual data point is the average of the three identical components of a particular beam. Table C-6 shows the times at which each data acquisition was performed. The plots indicate that the range of the impedance was relatively constant initially and then was lower at the last one or two acquisition times. This suggests development of coating defects or an increase in pore water conductivity of the coating (or both). Impedance for individual specimens often increased or decreased within this band for one acquisition compared to the next, however. Although the trends here are generally similar to those of the resistance data, it must be remembered that the acquisition times were different for the two parameters (resistance versus

Table C-8: Summary of average macrocell currents and resistances.

AVERAGE G109 I, (TOTAL), µA		AVERAGE ADJ. I (TOTAL), µA		AVERAGE G109 R, (TOTAL), Ohms		AVERAGE ADJ. R (TOTAL), Ohms	
152		36		191		495	
NEW	OLD	NEW	OLD	NEW	OLD	NEW	OLD
138	107	24	52	145	234	558	406

Note: The Table C-8 averages are based upon the actual currents, whether these were anodic or cathodic. Basing the averages upon the absolute value for these currents did not change the results significantly.

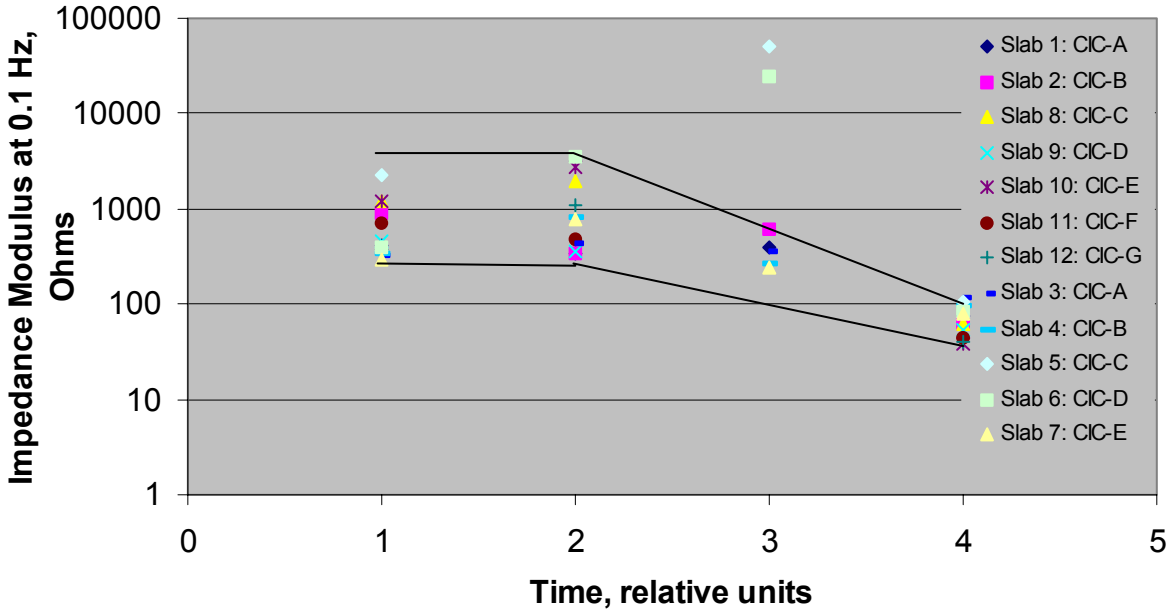

Figure C-13: Impedance data for the G109 bars.

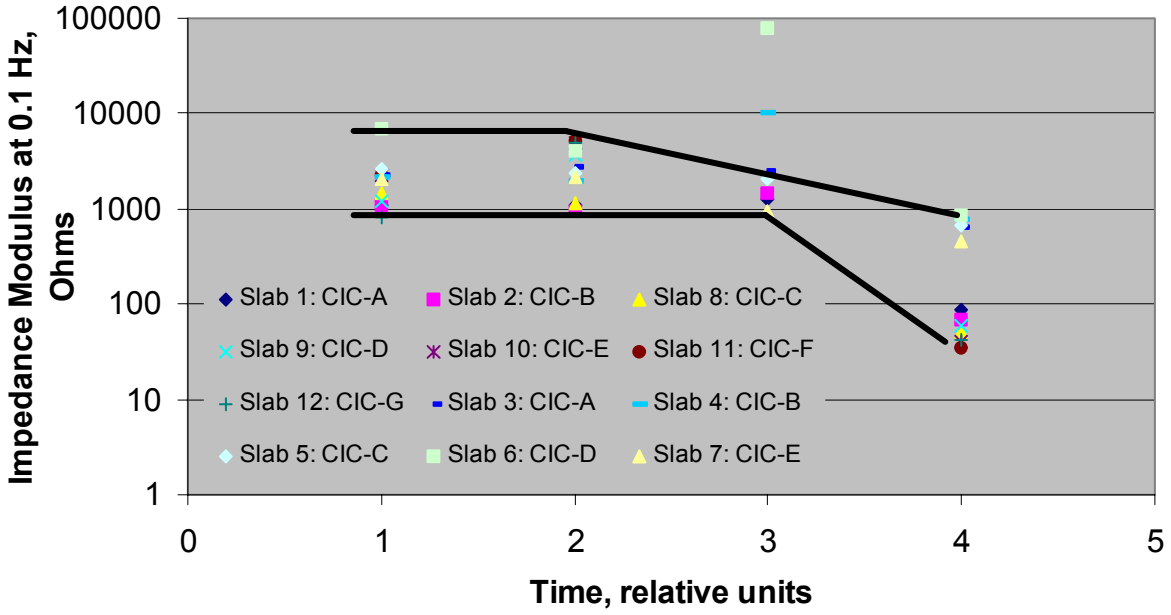

Figure C-14: Impedance data for the adjacent mat bars.

impedance). Note that impedance of the adjacent mat bars at the time of the final data acquisition is partitioned according to "new" versus "old," with the latter being about one order of magnitude greater than the former.

AGED (FHWA) SLAB STUDY

Experimental Procedure

Several extensive studies addressing the protection afforded to reinforcing steel in concrete by epoxy coatings have been performed by the Federal Highway Administration. These involved exposing slabs to a deicing salt environment where the rate of salt application and, hence, the rate of chloride uptake in the concrete was accelerated compared to what occurs for bridge decks, but all other factors were typical of actual service.

One of the studies conducted by the FHWA was initiated in 1980 and involved investigation of non-specification epoxy-coated rebars in slab-type specimens (*1*). The bars were coated with Scotchkote 213 in 1977 and were certified by the producer to meet specification with the exception of coating thickness, which was requested to be excessive by FHWA. However, the bars were stored outdoors for 3 years prior to slab fabrication and after that time were found to have holidays in excess of 83 per m (25 per foot). In the time-to-corrosion studies these bars were referred to as "non-specification," based on the excessive coating thickness, failure in the bend test in which poor coating adhesion was noted, and the holiday/bare area evaluation after outdoor exposure prior to concrete placement. However, since field bars are not normally checked for holidays and small bare areas and are not subjected to bend testing subsequent to outdoor exposure prior to concreting, these bars may not have differed greatly from many field

epoxy-coated rebars (*2*), even after additional damage of less that 1 percent of the surface area was purposely created for some of the specimens. All initial test results on the coated bars can be found in Reference 1.

A total of twelve slabs were fabricated for the 1980 study. Each slab measured 0.61 m (2 ft.) wide by 1.52 m (5 ft.) long by 0.15 m (6 in.) thick and contained two mats of reinforcing steel. The top mat of steel included four 1.3 m (51 in.) long longitudinal bars and two 0.46 m (18 in.) long transverse bars beneath them. The bottom mat of reinforcing steel consisted of seven 1.3 m (51 in.) long longitudinal bars and three 0.46 m (18 in.) long transverse bars beneath them. Details of a typical test slab are presented in Figure C.15a and the top reinforcing steel layout is shown in Figure C-15b. The clear concrete cover on the top mat was 19 mm (3/4 in.) with 35 mm (1 3/8 in.) between the top and bottom mats. The reinforcing steel in each slab was either all uncoated, all coated, or coated in the top mat only. Electrical continuity of all uncoated bottom mat steel was established by welding at each crossing point. Insulated electrical leads were attached to all epoxy-coated rebars, all top mat uncoated bars, and two of the uncoated bars in each bottom mat. All lead wires were routed outside of each slab.

The concrete used in each slab was characterized as follows: water-cement ratio of 0.53, cement content of 390 kg/m^3 (658 lbs/yd^3), air content of 7 $\pm$ 1.5 percent, and sand by volume of total aggregate of 44 percent. Other details regarding the concrete mix design can be found in Reference 1. The concrete was placed in each slab in two lifts. The mix design included 8.9 kg/m^3 (15 pcy) of chloride ions as NaCl in concrete placed around the top mat reinforcing steel, but with no intentional chlorides added to the concrete placed around the bottom mat. Exposure was at the FHWA outdoor test facility in northern Virginia and involved salt water ponding for the initial 1.5 months followed by exposure to natural weathering only.

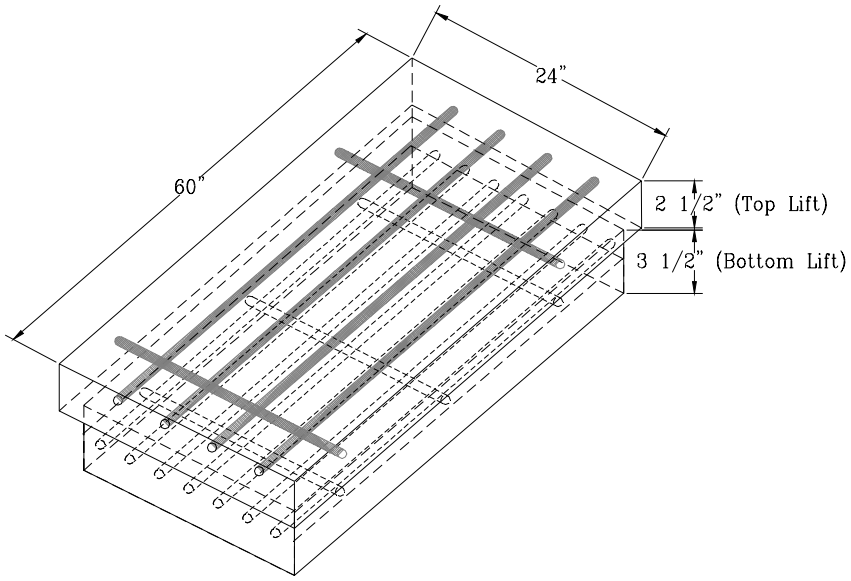

Figure C-15a. Standard test slab design.

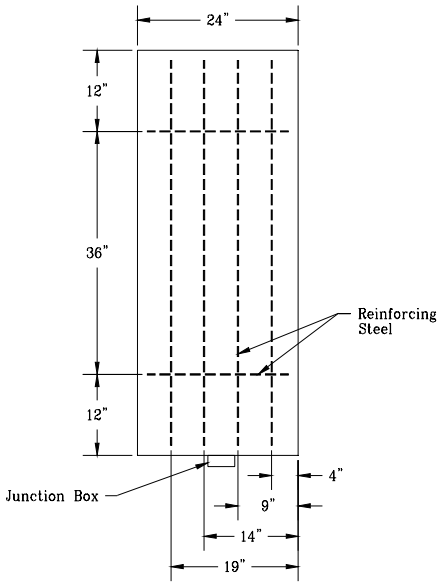

Figure C-15b. Top reinforcing steel layout.

Between 1981 and 1989, select slabs were periodically demolished to allow visual examination of the reinforcing steel. Cracking of slabs with epoxy-coated rebar was first noted in 1987 (slabs were about 7 years old), and by 1989 (about 9 years of age) all the coated rebar slabs were badly cracked as a result of corrosion(*2*). There was no significant difference in the time-to-cracking of the slabs with 1) epoxy-coated rebars in one mat compared to both or 2) intentionally damaged bars compared to ones without intentional damage.

By 1989, five slabs with ECR remained under outdoor exposure in northern Virginia. These included slabs 203, 206, 207, 208, and 210. Slab 206 had ECR in both mats of steel. The other four slabs had ECR in the top mat only. Slab 207 was found to be debonded between lifts in 1981.

As part of the NCHRP 10-37C study, it was considered that any form of accelerated damage on ECR would not sufficiently simulate real life damage. Thus, specimens that have sufficiently aged should more accurately simulate ECR damage mechanisms and the naturally observed variation in damage along ECR. Consequently, the above five slabs were included in this study as a supplement to the specimens described in section above. These slabs were not intended as a systematic study of the various physical repair/rehabilitation strategies but, instead, as an extension for specific repair strategies.

Although the history of the FHWA slabs and the variables involved in the study were considered to be ideal for this research project, a preliminary evaluation of the slabs was performed in March 1996 in order to assess their current condition. The evaluation was performed on slabs 203, 206, 207, 208, and 210 and included the following:

1. Visual survey.

2. Delamination survey.
3. Half-cell potential survey.
4. Rate of corrosion measurements.

All slabs exhibited significant corrosion induced cracking and surface rust staining. No corrosion induced delaminations were found on any of the slabs. The disbonding between lifts on slab 207 was confirmed. Half-cell potential measurements were taken at 152 mm (6 in.) intervals along bars with and without cracks. The average potential for all slabs ranged from –406 to –522 mV CSE. One rate of corrosion measurement was taken on each of the bars included in the half-cell potential survey. Test results ranged from passive conditions to high corrosion rates.

In July 1996, all slabs were transported to Concorr, Inc.'s outdoor exposure test site in northern Virginia (the slabs were about 16 years old at that time). Resistor and switch assemblies were installed between each individual top ECR and the bottom mat of steel. All other wiring was removed or disconnected. Throughout the exposure, all switches were open except when measuring instantaneous corrosion currents. Data sets before and after installing repairs included the following measurements for each ECR:

1. Voltage difference (driving volts) between the ECR and bottom steel. A high impedance voltmeter was used to measure the voltage difference between the top mat steel and the bottom mat steel with the switch in the open position.
2. Instantaneous corrosion current measured as a voltage drop across a known resistor after the switch had been closed for ten seconds.
3. AC resistance at 97 Hz between the ECR and bottom steel.

4. Half-cell potential measurements with respect to CSE at a closely spaced interval along the ECR.

Visual and delamination surveys were also performed each time data were collected.

Two sets of baseline data were collected, and then repair strategies were installed in September 1997. Ponding cycles were initiated in early October, 1997. Each cycle consisted of ponding with a 3% NaCl solution for 2 weeks (using plastic covers to minimize evaporation) followed by a 2 week dry period. During the second 2 weeks of each cycling period, an elevated cover was used on each slab to maintain a dry surface condition. Post-repair data were periodically collected for over 27 months.

At the time of repair, cracks existed above all longitudinal bars in each slab and delaminations were found along one longitudinal bar in slab 208. Slabs 203, 206, 207, and 210 also had a crack above one of the transverse bars. Crack widths ranged from hairline to 50 mils on slab 203 and from hairline to 60 mils on all other slabs. Although each slab had several cracks with widely varying widths, only one repair strategy was employed per slab.

The repairs listed in Table C-1 were installed on the subject slabs. The procedures and materials used in the repairs are discussed in more detail in Appendix A.

Findings & Discussion

About 5.2 months after repairs were installed, surface rust staining was observed on slab 210 (CIC-E). Similar observations were made on slabs 207 (CIC-B), 208 (CIC-C), and 203 (CIC-D) approximately 8.4 months after repair strategies were installed. Slab 206 (CIC-A – both mats

coated) did not exhibit any surface rust staining until about 13.9 months after repairs were installed on the other slabs.

Figures C-15 through C-17 present plots of driving volts, instantaneous corrosion current (normalized to 70F), and AC resistance (normalized to 70F) versus exposure time. In each case, the data were plotted separately for all bars, all cracked bars, and all uncracked bars. From these plots, the following observations were made:

Driving Volts

Prior to repair, all top ECR's were anodic to the bottom mat of reinforcing steel. Slab 206 (no repair – both mats coated) exhibited the least driving volts and this remained relatively constant throughout the exposure time with the top ECR's always anodic to the bottom mat. Immediately after repairs were installed, the driving volts for all other slabs shifted in the positive (or cathodic) direction although the top ECR's in slabs 203 (CIC-D) and 210 (CIC-E) remained anodic to the bottom mat. The top ECR's in slabs 207 (CIC-B) and 208 (CIC-C) became cathodic to the bottom mat. This apparent improvement (i.e. cathodic shift) was observed on these four slabs for only about one month after repairs were installed. Subsequently, the driving volts for all slabs shifted in the negative direction with the top ECR's remaining anodic to the bottom mat for the remainder of the exposure period. Slabs 203 (CIC-D) and 208 (CIC-C) exhibited comparatively larger driving volts.

Instantaneous Corrosion Current

Prior to repair, all top ECR's were anodic to the bottom mat of reinforcing steel with slab 210 (CIC-E) exhibiting the greatest corrosion current. Immediately after repairs were installed, the corrosion current decreased for all slabs and the top ECR's in slabs 207 (CIC-B) and

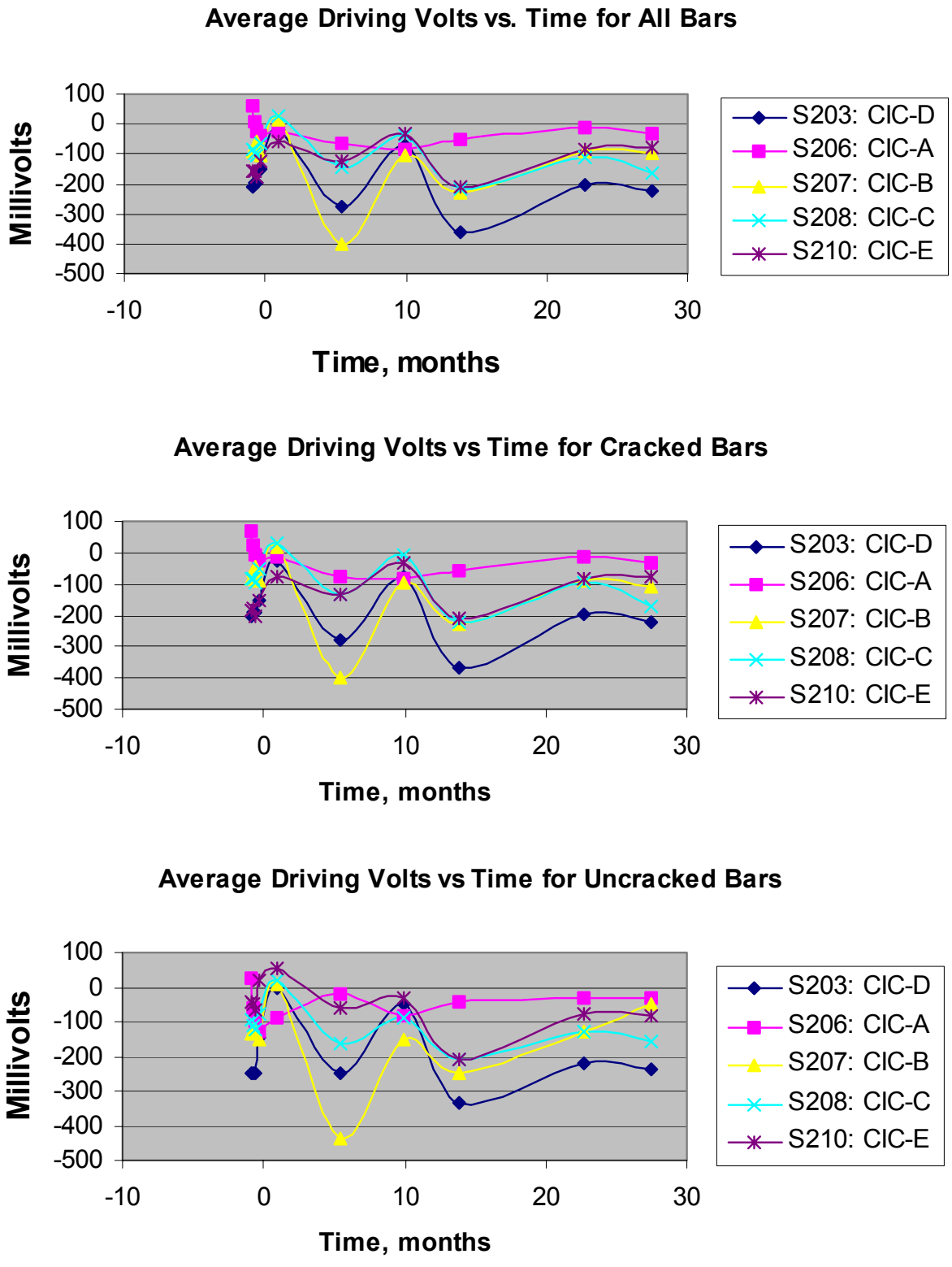

Figure C-15: Plots of driving volts vs time .

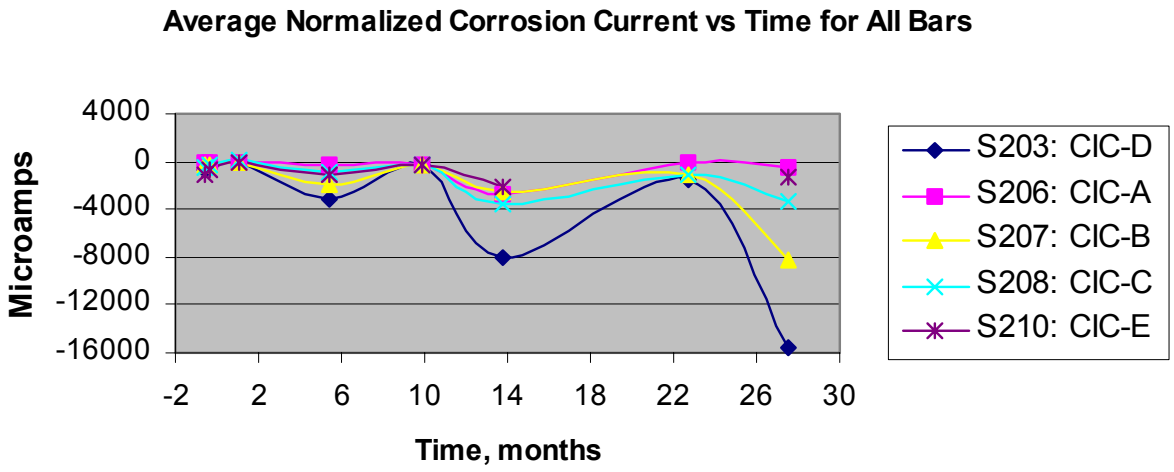

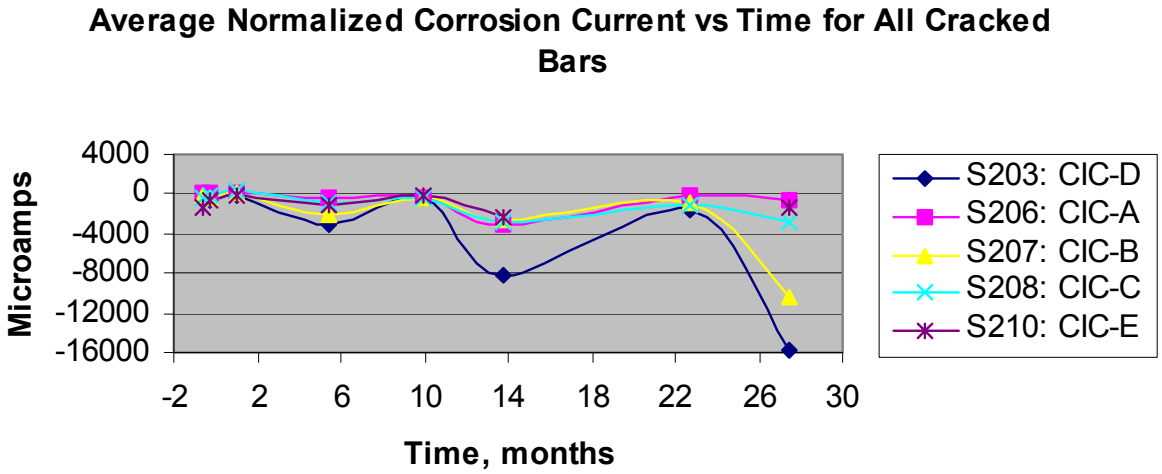

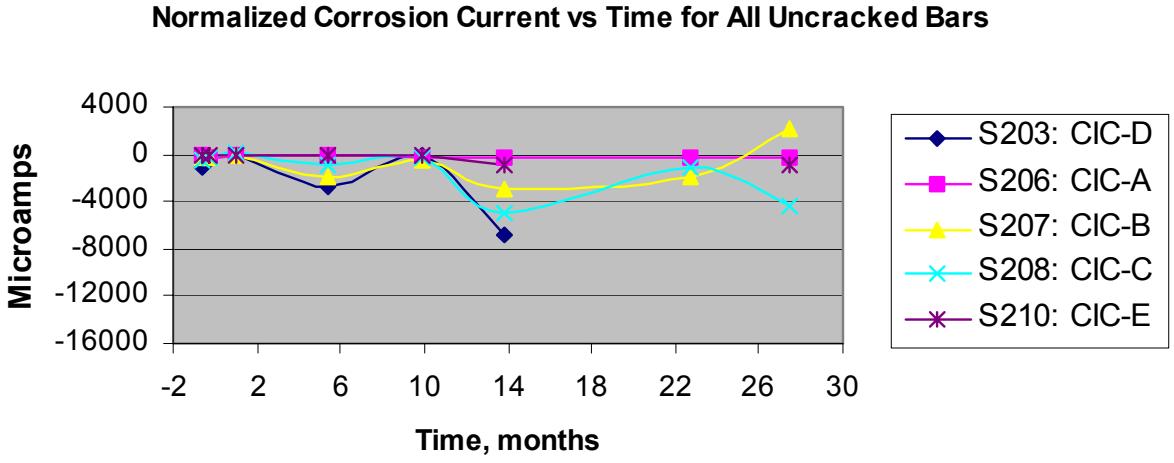

Figure C-16: Plots of corrosion current vs time for all slabs

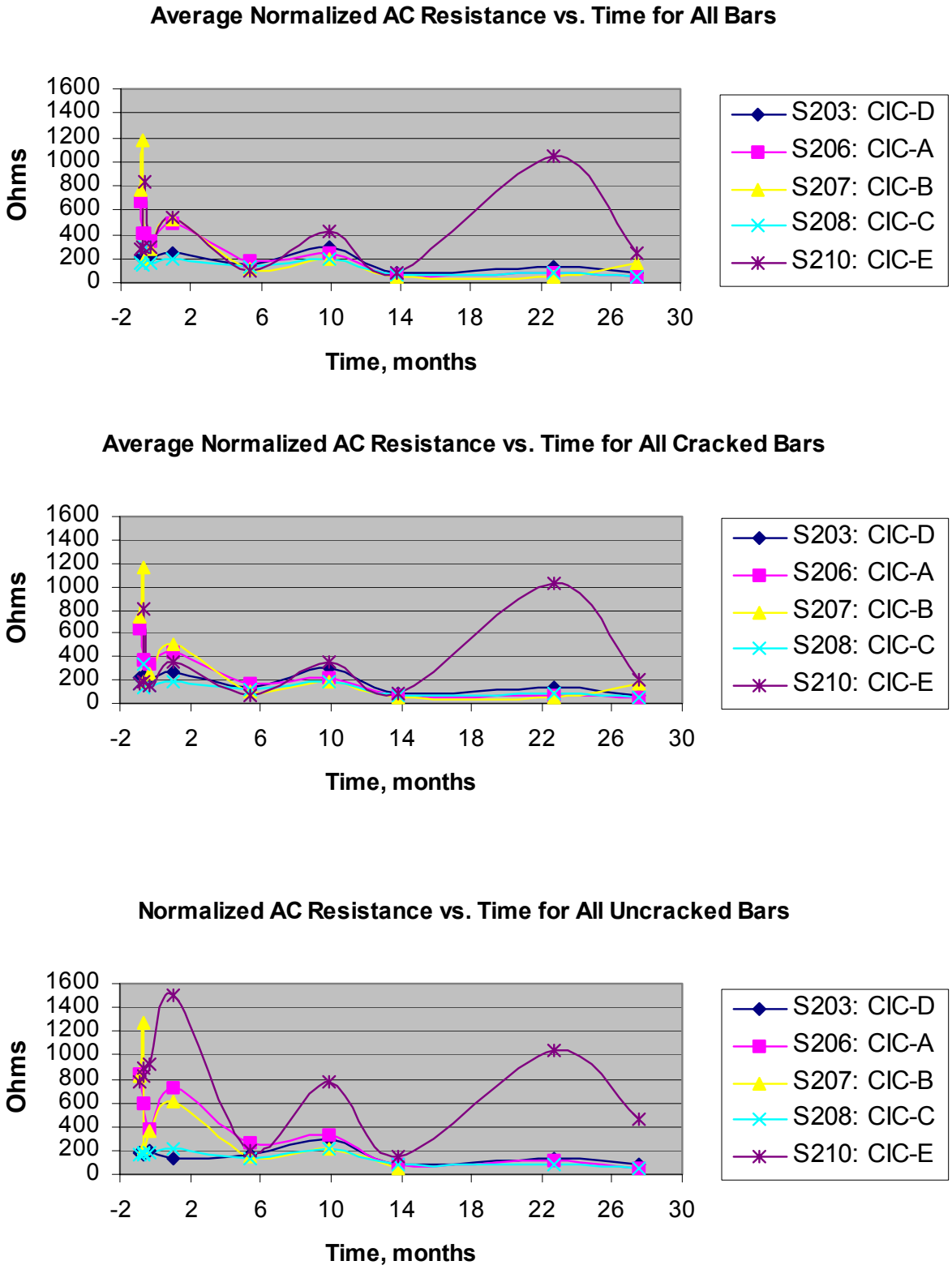

Figure C-17: Plots of AC resistance vs. time for all slabs.

208 (CIC-C) became cathodic to the bottom mat. Reduced corrosion currents were observed for only about one month after repairs were installed. Subsequently, all slabs exhibited a general trend of increasing corrosion current for the remainder of the exposure period. Overall, slabs 206 (CIC-A) and 210 (CIC-E) had the smallest corrosion currents and slab 203 (CIC-D) had the largest. However, in all cases, the magnitude of corrosion current was high.

AC Resistance

With the exception of slab 210 (CIC-E), the resistance data showed a general trend of decreasing with time. Data for slab 210 was erratic.

No significant difference was observed between ECR's with cracks and those that were not cracked. However, comparisons between cracked and uncracked bars were limited since there was only a few top ECR's that were not cracked (one transverse bar in slabs 203, 206, 207, and 210 and both transverse bars in slab 208). Also, uncracked transverse bars may have been influenced by repaired cracks over longitudinal bars.

Half-cell Potential Survey

Figures C-18 present plots of half-cell potential measurements along individual top ECR's in each slab versus exposure time. These plots show that one month after repairs the potentials of all top ECR's shifted in the positive direction (i.e. became more passive). An exception to this was observed on slab 207 (EI) where potentials before and immediately after repairs were installed were similar. About 5.5 months after repairs were installed, potential readings on all slabs became more active than the pre-repair measurements and generally remained so for the duration of the exposure period. Uncracked ECR's exhibited the same general trends as cracked and repaired ECR's.

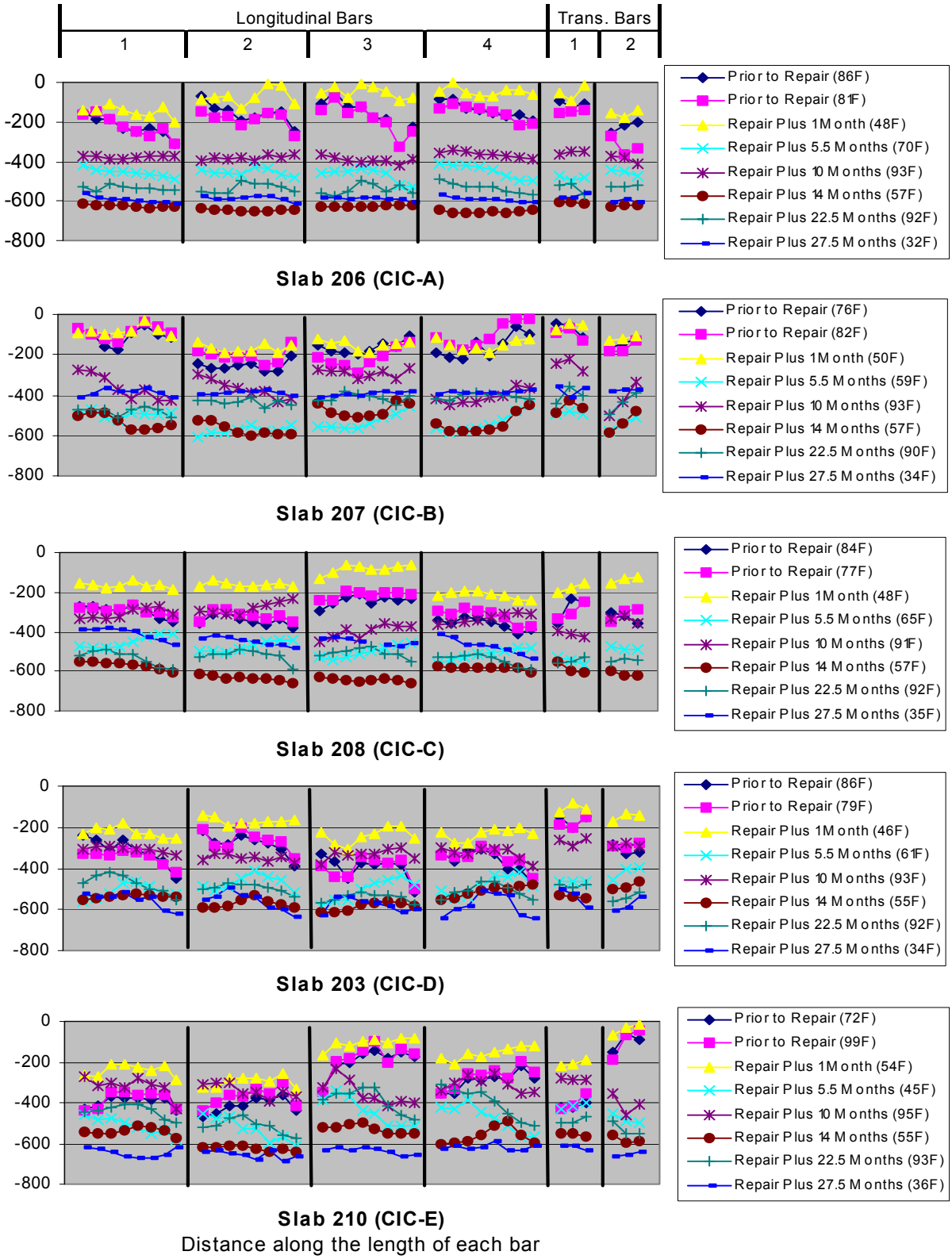

Figure C-18: Plots of Half-cell potential vs. time

AGED (BENT BAR) SLAB STUDY

Experimental Setup

There were eight ECR slabs remaining from a study (initiated in 1988) whereby the corrosion characteristics of straight and bent ECR were evaluated under accelerated southern exposure cycling as described in NCHRP Report 244 (*3,4*), however not all specimens were subjected to southern exposure cycling and some slabs were ponded with tap water following the southern exposure portion of the program. Weekly southern exposure cycling involved four days of continuous ponding of the top surface with a 15 percent (by weight) sodium chloride solution followed by draining and three days exposure to an air temperature of 100^{o}F and ultraviolet lights. Variables included seven different suppliers, bend diameter, coating thickness, coating application before and after fabrication of the bar, rate of bending, steel temperature during bending, and patching of damaged areas prior to concrete placement. All coating properties were documented prior to concrete placement (*4*). Two sizes of concrete slabs were fabricated in 1988; 0.33 m (13 in.) wide by 0.36 m (14 in.) deep by 0.18 m (7 in.) thick and 0.31 m (12 in.) wide by 0.25 m (10 in.) deep by 0.18 m (7 in.) thick. Each slab consisted of two independent specimens; one straight bar and one bent bar specimen. The former involved two bars (these were made electrically continuous external to the slab) and the latter was comprised of one bar. The bottom mat steel was uncoated in all cases. Three bottom bars were positioned beneath the bent ECR and three were placed below the two straight ECR's. In each case, the bottom bars were made electrically continuous outside of the slab concrete.

Periodic data collection included visual observations, sounding surveys, corrosion potential measurements, macrocell current measurements, rate of corrosion testing, and AC resistance

between the top ECR bars and bottom bare bars. Select slabs were also autopsied at the conclusion of the study. All other details including the concrete mix design and test data can be found in References 3 and 4.

One of the eight remaining slabs was designated N19-SE2. After completing 1.35 years of southern exposure cycling and more than 0.9 years of tap water ponding, the slab was moved to an outdoor exposure facility in northern Virginia. In April 1996 the slab exhibited surface cracking above the ECR's. The slab was approximately 8 years old at that time and was included in the NCHRP 10-37C study as a supplement to the specimens described above.

In July 1996, the slab was transported to Concorr, Inc.'s outdoor exposure test site in northern Virginia (the slab was approximately 8 years old at that time). Separate resistor and switch assemblies were still in place between the bent ECR and three of the uncoated bottom mat bars and the two straight ECR's and the other three uncoated bottom mat bars. Throughout the exposure, all switches were closed except when measuring AC resistance between ECR's and uncoated bars. Data sets before and after installing repairs included the following measurements:

1. Macrocell current (measured as a voltage drop across a resistor) between the bent ECR and bottom steel and between the straight ECR's and bottom steel.
2. AC resistance between the bent ECR and bottom steel and between the straight ECR's and bottom steel.
3. Half-cell potential measurements along the bent and straight ECR's.

Visual and delamination surveys were also performed each time data were collected.

At the start of the study, the slab had surface cracking above the bent ECR and one of the straight ECR's and no delaminations. Crack widths ranged from 330 to 508 μm (13 to 20 mils). Two

sets of baseline data were collected and Repair Option CIC-C was applied on the cracks on the slab in September 1997 . Ponding cycles were initiated in early October, 1997. Each cycle consisted of ponding with a 3% NaCl solution for 2 weeks (using plastic covers to minimize evaporation) followed by a 2 week dry period. During the second 2 weeks of each cycling period, an elevated cover was used on each slab to maintain a dry surface condition. Post-repair data were periodically collected for over 27 months.

Findings & Discussion

Although other data for this slab cover 27.5 months of post-repair exposure, visual observations and delamination survey results extend through 30.5 months. The slab did not exhibit any surface rust staining or delaminations for the entire exposure period (about 30.5 months after the cracks were repaired). However, after 30.5 months of exposure, the original cracks over one of the straight bars grew in length and additional hairline cracking developed over the same bar.

Figure C-19 presents plots of macrocell current and AC resistance (both of these parameters were normalized to 70˚F) versus exposure time. In each case, the data were plotted separately for the bent and straight ECR's. Figure C-20 presents plots of half-cell potential measurements along the bent and straight ECR's versus exposure time. Measurements for the straight bars were taken along the centerline between the two bars. Results are summarized below.

Macrocell current data show that the bent ECR was cathodic to the bottom steel before and immediately after the repair was installed while the straight ECR's were slightly anodic to the bottom steel during the same time period. Subsequently, with the exception of one data point, the bent and straight ECR's were anodic to the bottom steel for the remainder of the exposure {

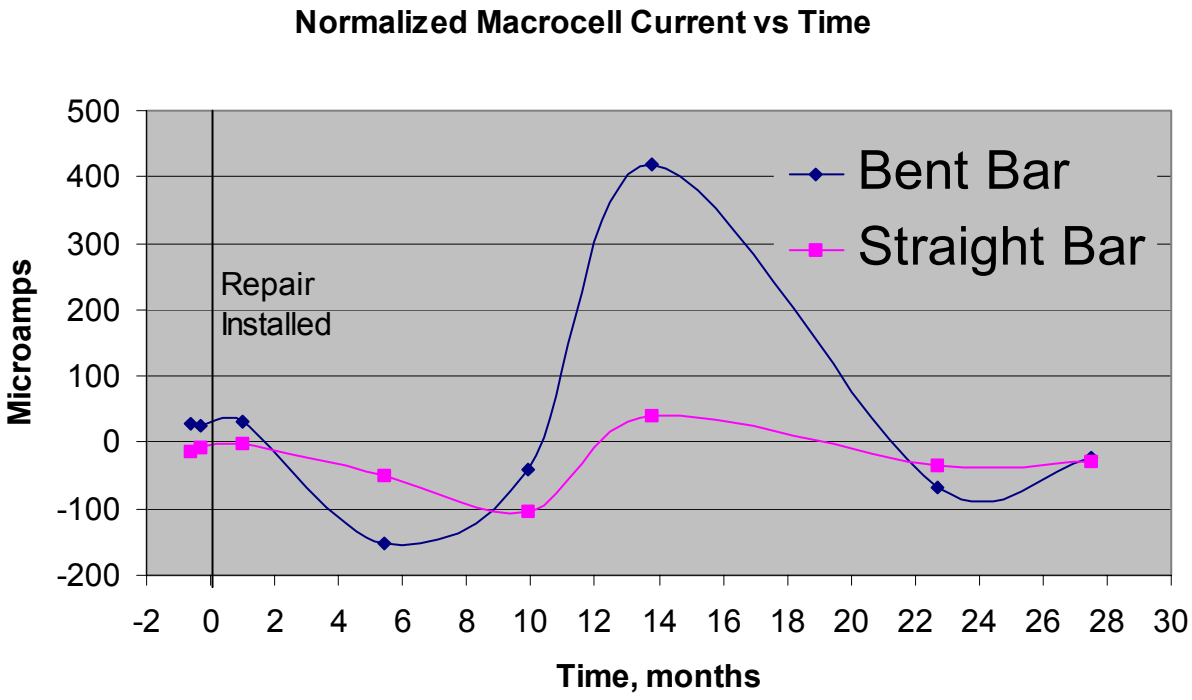

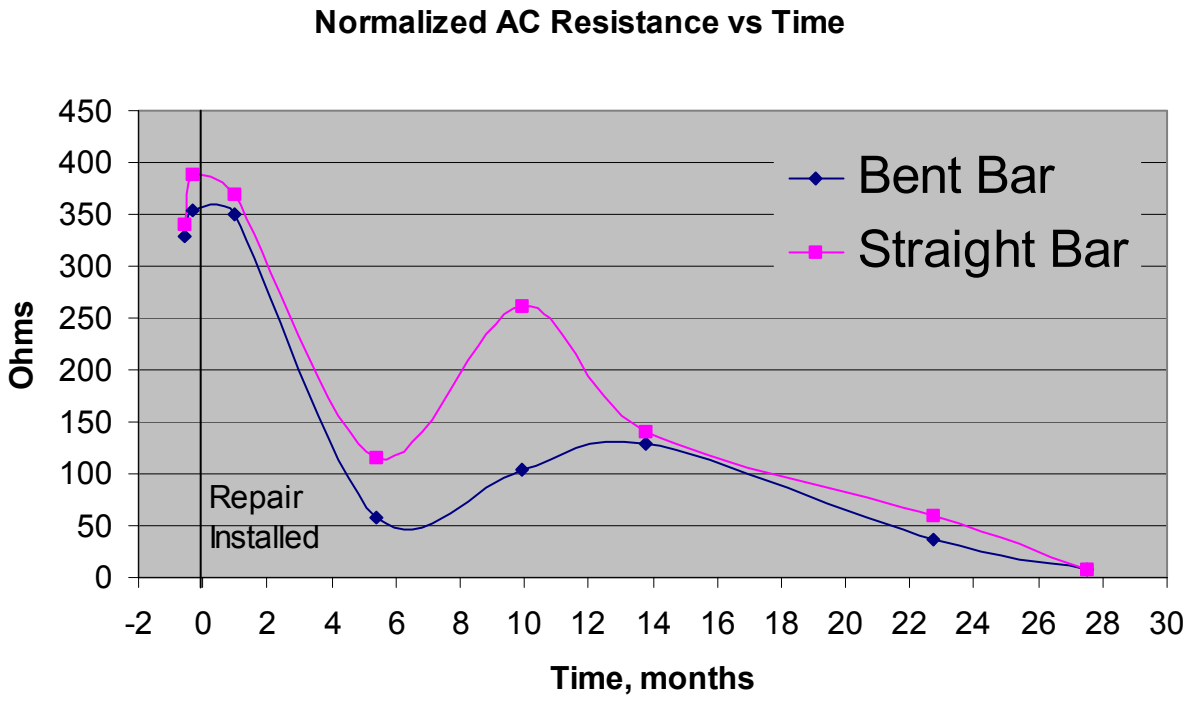

Figure C-19: Plots of macrocell current and AC resistance vs. time for slab N19-SE2

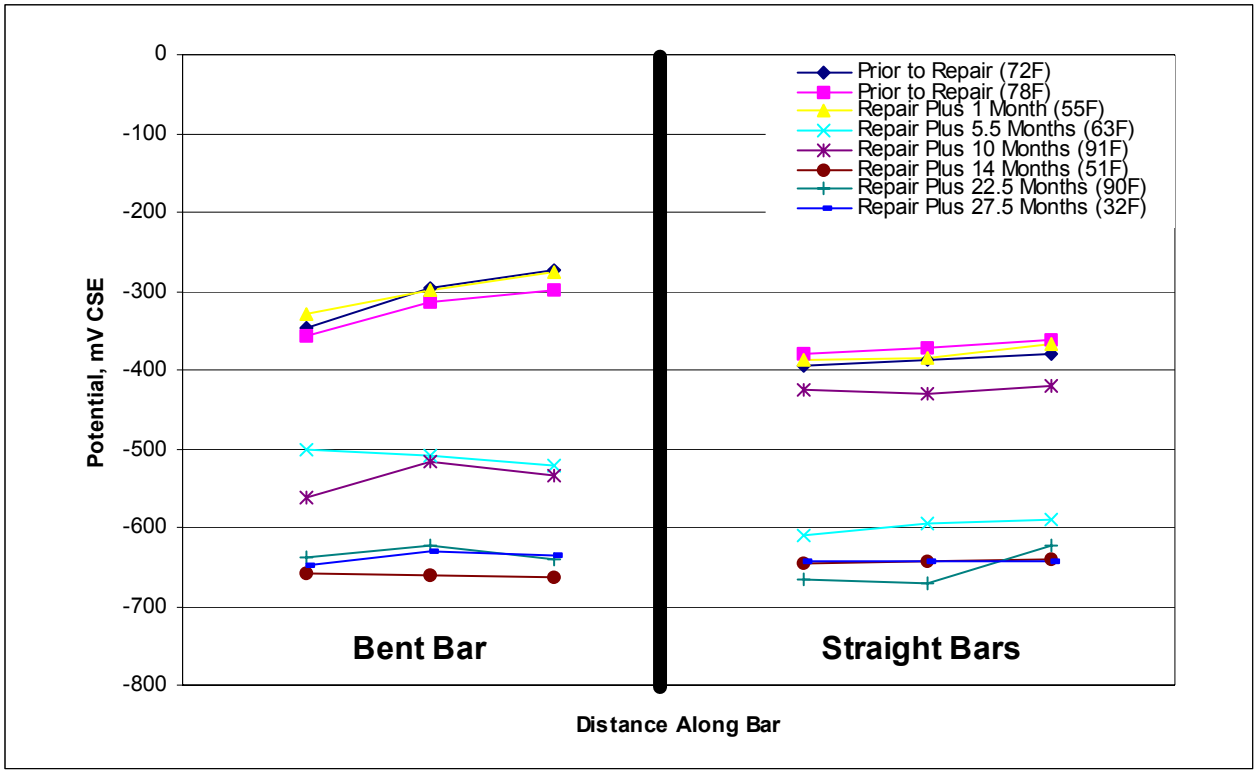

Figure C-20: Half-cell potentials for slab N19-SE2 (CIC-C)

period. Although the magnitude of the anodic current for the straight ECR's was comparatively less than that for the bent ECR, the currents were low in both cases. Resistance data for the bent and straight ECR's decreased with time throughout the exposure period. Potentials before and immediately after repairs were installed were similar for the bent and straight ECR's. After about 5.5 months of exposure following repair, all potential readings became more active and remained so for the duration of the exposure period.

BRIDGE DECK FIELD STUDY

Experimental Setup

A vital part of this project involves field validation studies of select repair and rehabilitation strategies, including crack repair and patching. One of the test sites selected for these investigations was a bridge deck in New York that had apparent corrosion induced concrete deterioration as a result of deicing salt applications. Specifically, the Schoharie Turnpike Bridge over I-88 was chosen. This bridge was built in 1981 and is located in a rural area in Duanesburg (Schenectady County). The top mat of deck reinforcing steel is epoxy-coated and the bottom mat is uncoated. The structure is subjected to deicing salt applications at the rate of 8 to 11 tons/lane kilometer per year (15-20 tons/lane mile per year). Coring by the New York State DOT confirmed that the epoxy-coating was Scotchkote 213. The bridge consists of two spans with a total length of 127.1 m (417 ft.) and two driving lanes, one eastbound and one westbound. The total deck width is 11 m (36 ft). The specified deck concrete was Class E with a 28-day compressive strength of 20.7 Mpa (3000 psi). The specified concrete cover over top reinforcing steel was 63.5 mm (2.5 in).

A standard bridge inspection was conducted on October 31, 1995. At that time, both spans exhibited transverse cracking and one span had numerous patched areas. The patch material in all cases was asphalt. The bridge has a 59 degree skew and no scuppers. As a result, ponding water was also apparent during the inspection.

As part of the NCHRP 10-37C project, an initial evaluation was conducted on a selected portion of the bridge deck in August, 1996. The objectives of this initial investigation were as follows:

1. Determine if the bridge was a suitable candidate for the project.
2. Obtain information needed to select the repair/rehabilitation strategies to install.

The following activities and tests were performed:

1. Obtain and review questionnaire/bridge inspection reports from NYSDOT.
2. Lay out a standard close interval grid over the entire test area.
3. Conduct a thorough visual and delamination survey over the entire test area.
4. Locate and measure the concrete cover over several bars.
5. Collect core samples with embedded ECR's.
6. Conduct a thorough evaluation of the ECR's extracted from the cores.
7. Obtain chloride samples and conduct depth of carbonation testing at several locations.
8. Analyze samples from Item 7 for acid soluble chloride ion content.

The selected test area was a 10 m (33 ft.) by 30.5 m (100 ft.) section on span 1 of the bridge deck. A 300 mm x 300 mm (1 ft. by 1 ft.) grid was laid out with the origin (0, 0) of the grid located at the southeast corner of the test area. All test locations are referenced as (X, Y) coordinates based on this grid layout.

A thorough visual and delamination survey of the entire test area was conducted including documentation of rust staining, spalled areas, crack locations, lengths, and widths, and patched areas. The entire survey area was either tined or saw cut. Tined surfaces were worn and exposed aggregates were visible over the majority of the deck. A large number of transverse cracks with varying widths were encountered in both lanes. The crack frequency (i.e. length of crack per sq. m of deck area) was 252 mm/square m (0.077 ft./sq. ft.) for the eastbound lane and 144 mm/square m (0.044 ft./sq. ft.) for the westbound lane. Several spalls, patches and delaminated areas were also identified in the test section. All patches consisted of asphalt and all spalls were shallow with no exposed reinforcing steel.

Based on the visual survey results, a total of 4 locations (2 in cracked concrete and 2 in sound concrete) were identified in the survey area of the west bound lane for further testing. The depth of cover in the cracked and sound areas averaged 69.9 mm (2.75 in.) A total of four (101 mm (4 inch) nominal diameter) core samples were collected, one from each of the 4 test locations. The cores were carefully preserved, brought back to the laboratory and examined in detail. Results are shown in Table C-9.

All attempts were made to retrieve both transverse (top) and longitudinal (bottom) bars with the core sample. However, only one core (Core No. 1), collected from a cracked area, had a complete set of transverse and longitudinal bars. Rust staining was observed along the crack in the core sample and significant corrosion was found on the ECR's when the core was broken open. Judging from the rebar imprint in the broken core, the crack appeared to be positioned directly above the top of the transverse bar. No bars could be retrieved with Core No. 2 as it broke at the level of the rebars (two closely spaced parallel transverse rebars). However, corrosion and coating damage was observed on the exposed rebars in the core hole. Core No. 3

had only one transverse bar while Core No. 4 had a transverse bar and part of a longitudinal bar. There were no visual signs of corrosion on the rebars in either core.

A detailed autopsy of the retrieved ECR's from the core samples was performed. This included visual observation and photographic documentation of the bars (including the condition of the bar surface beneath the coating) and bar traces (imprints), determination of coating thickness on ribs and in valleys, determination of coating adhesion in damaged and undamaged areas, determination of the number of mashed and bare areas, number of blisters and holidays, and concrete pH measurements in bar traces. A corrosion rating based on visual condition was also assigned to each bar. The ECR autopsy results are summarized in Table C-10.

Two powdered concrete samples were collected at each of the 4 test locations. In each case, sampling depths included surface chlorides (6 mm to 19 mm (0.25 to 0.75 in.)) and rebar level chlorides (concrete cover +/- 6 mm (0.25 in.)). All samples were collected in uncracked areas. In addition, powdered samples were obtained from Cores 1 and 4 at nominal depths of 95 mm and 121 mm (3.75 and 4.75 in). The powdered samples were analyzed for acid soluble chloride ion content in accordance with the AASHTO T-260 standard test method. Results are provided in Table C-11.

The chloride content at or near the bar depth at all 4 test locations is greater than the minimum threshold value (260 ppm) required to initiate corrosion of uncoated reinforcing steel. At locations 1 and 2, results were about 6 to 8 times greater than this threshold. Results at location 3 were only slightly greater than the threshold while the chloride content at the steel depth at location 4 was about 4 times greater than the threshold.

The depth of carbonation at all 4 test locations was 0 in.

Table C-9: Results of Visual Observations of Core Samples

Core No.	Core Length mm (in.)	Observations
1	140 (5.5)	Core collected from a cracked area; contains embedded transverse and longitudinal bars; rust observed on rebars.
2	89 (3.5)	Core collected from a cracked area; core broke off at rebar interface; no embedded rebars in core; rust observed on rebars left in core hole; rust staining on rebar imprint.
3	83 (3.25)	Core collected from a sound area; contains only a tranverse bar; no visible rust stains on the rebar or rebar imprint.
4	127 (5)	Core collected from a sound area; contains a tranverse bar and part of a longitudinal bar; no visible rust stains on the rebars or rebar imprints.

Table C-10: Summary of the Results of ECR Autopsies

Core No.	Coating Thickness[a]			Coating Adhesion[b]		Mashed Areas	Bare Areas	Blisters	Holidays	pH in Bar Trace[c]	Corrosion Rating[d]	Condition of Rebar Under Coating
	ECR	Ribs	Valleys	Damaged	Undamaged							
1	Top bar	13.2	12.7	5	5	1	6	0	61	10-11	4	severe corrosion
	Bottom bar	11.7	9.9	5	5	0	15	0	105	10-11	4	severe corrosion
2	No ECRs in core											
3	Top bar	13.2	11.4	5	5	1	20	0	36	10-11	2	light corrosion
	Bottom bar	No bottom bar in core										
4	Top bar	12.2	8.4	4.3	3.7	5	16	0	39	10-11	2	light corrosion
	Bottom bar	13.8	10.6	1	1	8	3	0	2	10-11	2	no corrosion

The findings showed that the concrete about the top reinforcing steel is highly chloride contaminated and ECR's in cracked areas are corroded and the results confirmed that this bridge deck was a suitable candidate for the field validation portion of the NCHRP 10-37C study.

In May 1997, a second detailed visual and delamination survey was performed and specific delaminated and cracked areas were selected for repair. During the concrete removal process for patch repairs, it was determined that the delaminations and spalls on the bridge deck were the result of poor quality concrete and concreting practices and were not corrosion induced. However, based on the findings in the initial evaluation, the structure was still considered a good candidate for crack repair.

The pre-selected crack repair strategies included CIC-A to CIC-E. Surface application of Corrosion Inhibitor A was limited to an area extending two feet on either side and at the ends of the subject crack.

Two cracks were carefully selected for each repair strategy. Pairs of cracks were selected so that the total length and width of the cracks representing each repair strategy were as similar as possible. The ten cracks so selected were labeled C1 through C10. At the time of the second survey in May 1997, a few cracks had grown in length. Table C-12 presents details associated with the cracks selected for each repair strategy.

Findings & Discussion

Repair strategies were installed in early May 1997 and visual and delamination surveys were conducted approximately 12, 25, and 34.5 months later. With the exception of crack C1 (no repair), no significant changes were found on any of the cracks throughout the 34.5 months of

Table C-11: Results of Acid Soluble Chloride Ion Content Analyses

Location Number	Rebar Depth, mm (in.)	Nominal Sample Depth, mm (in.)	Chloride Content, ppm	Grid Location, ft.
1	67 (2.63)	13 (0.5)	3870	23.2, 52.1
		70 (2.75)	2010	
		95 (3.75)	1820	
		121 (4.75)	1420	
2	73 (2.88)	13 (0.5)	3140	20.9, 89.2
		70 (2.75)	1530	
3	75 (2.94)	13 (0.5)	2260	24.2, 72.2
		70 (2.75)	350	
4	67 (2.63)	13 (0.5)	5190	24.4, 57.2
		70 (2.75)	1050	
		95 (3.75)	450	
		121 (4.75)	250	

Table C-12: Summary of Crack Details for Each Repair Stragtegy

Crack Number	Repair Strategy	Crack Length, m (ft.)	Crack Width, micrometer (mils)
C1	CIC-A	4.95 (16.5)	254-635 (10-25)
C2	CIC-A	6.69 (22.3)	330-508 (13-20)
Total		**11.64 (38.8)**	**254-635 (10-25)**
C3	CIC-B	2.22 (7.4)	406-508 (16-20)
C4	CIC-B	3.57 (11.9)	330-762 (13-30)
Total		**5.79 (19.3)**	**330-762 (13-30)**
C5	CIC-C	2.64 (8.8)	406-508 (16-20)
C6	CIC-C	2.52 (8.4)	330-406 (13-16)
Total		**5.16 (17.2)**	**330-508 (13-20)**
C7	CIC-D	2.61 (8.7)	330-508 (13-20)
C8	CIC-D	2.1 (7)	406-508 (16-20)
Total		**4.71 (15.7)**	**330-508 (13-20)**
C9	CIC-E	4.14 (13.8)	228-330 (9-13)
C10	CIC-E	3.45 (11.5)	406-635 (16-25)
Total		**7.59 (25.3)**	**228-635 (9-25)**

Exposure (see Figures C-21 and 22). During the 12 month evaluation, a 406 mm (16 inch) long rust stain was observed approximately 152 mm (6 in.) to the side of crack C1. After 34.5 months of exposure, this area became delaminated and the delamination extended over crack C1. The delamination measured 203 mm by 305 mm (8 in. by 12 in). Other observations, outside the ten subject cracks, are described below.

During the first post-repair survey (12 months after repairs were installed), one of the cracks not included in the study had grown in length by about 305 mm (1 ft.), a large rust stain developed a less than a meter to the side of crack C9, and a new shallow spall was found. No new changes were recorded during the 25 month evaluation. After 34.5 months, a large diagonal crack and a new delaminated area with several small, shallow spalls were observed. In addition, a new delamination developed along a crack that had another delamination (in a different area) since the start of the study.

Figure C-21: Overview of bridge during the final evaluation.

Figure C-22: Overview of repaired crack on the bridge.

REFERENCES

1. Virmani, Y.P., Clear, K.C., and Pasko, T.J. Jr., "Time-to-Corrosion of Reinforcing Steel in Concrete Slabs, Vol. 5: Calcium Nitrite Admixture or Epoxy-Coated Reinforcing Bars as Corrosion Protection Systems", Report No. FHWA-RD-83-012, Federal Highway Administration, Washington, D.C., September 1983.

2. Clear, K.C., Hartt, W.H., McIntyre, J.F., and Lee, S.K., "Performance of Epoxy-Coated Reinforcing Steel in Highway Bridges", NCHRP Report No. 370, National Cooperative Highway Research Program, Washington, D.C., 1995.

3. Clear, K.C., Part I “Effectiveness of Epoxy Coated Reinforcing Steel,” in “CRSI Performance Research: Epoxy Coated Reinforcing Steel,” Interim Report, Concrete Reinforcing Steel Institute, Schaumburg, IL, 1992.

4. Sohanghpurwala, A.A., and Clear, K.C., "Effectiveness of Epoxy Coatings in Preventing Corrosion of Reinforcing Steel", Transportation Research Record No. 1268, Highway Maintenance Operations and Research, 1990.

APPENDIX D

EVALUATION OF REPAIR STRATEGIES FOR CORROSION INDUCED DELAMINATION AND/OR SPALLING

EXPERIMENTAL SETUP

The objective of this part of the program was to investigate and determine the effectiveness of various options for repair of concrete delaminations and/or spalling that result from corrosion of ECR. Based on discussions presented in Appendix A, the following repair options were selected for evaluation:

a. no repair

b. repair damaged areas with cementitious patch material

c. apply protective coating on exposed steel and repair with cementitious patch material

d. apply protective coating on exposed steel and repair with cementitious patch material containing a corrosion inhibitor as an admixture

e. apply protective coating on exposed steel, repair with cementitious patch material, and apply a corrosion inhibitor on the entire surface of the element

f. apply protective coating on exposed steel, repair with cementitious patch material containing a corrosion inhibitor as an admixture, and apply a corrosion inhibitor on the entire surface of the element.

The following materials were used to implement the above repair options:

Patching Material A: pre-bagged Portland cement concrete.

Patching Material B: pre-bagged, polymer modified, silica fume concrete.

Patching Material C: Class III Portland cement concrete.

Rebar Coating A: epoxy coating.

Rebar Coating B: water based epoxy resin/Portland cement coating.

Rebar Coating C: water based alkaline coating with corrosion inhibitor.

Corrosion Inhibitor A: surface applied water based amine and an oxygenated hydrocarbon.

Corrosion Inhibitor C: water based amine and an oxygenated hydrocarbon admixture.

Corrosion Inhibitor D: calcium nitrite based inhibitor admixture.

Corrosion Inhibitor E: multi-component corrosion inhibitor and concrete densifier admixture.

These repair options were applied on 14 new specimens in which delamination and spalling was induced by forced initiation and acceleration of ECR corrosion, 4 existing specimens ("old specimens") constructed in previous studies exhibiting ECR corrosion, and on 39 columns of the Seven Mile Bridge (Florida Keys, Florida) substructure suffering corrosion induced damage. All details pertaining to the application of the repairs and materials are discussed in Appendix A.

The following specimen types were used in the laboratory evaluation:

1. **Poor Concrete Specimens (PCS):** Specimens constructed with poor quality concrete and embedded in reinforced concrete beams to simulate bridge deck environment.

2. **Bent Bar Slabs:** Existing slabs from a previous study.

All possible combinations of patch repair materials, rebar coatings, and corrosion inhibitors included in this study results in a very large matrix. Of the possible combinations, 14 were selected for evaluation. All 14 repair options were applied on the newly constructed PCS macrobeams, 13 were applied on 39 select columns of the bridge substructure, and four were installed on the old specimens. Table D-1 tabulates the repair options and the corresponding specimens utilized in this study.

Experimental procedure and tests results for each specimen type and the columns of the bridge substructure are presented below.

Table D-1: Repair Options, Materials, and Specimen Types

Repair Option/Materials	Repair Option	Specimen/Test location Identification		
		PCS Beams	Bent Bar Slabs	7 Mile Bridge Columns
No Repair	CIS-A	PCS-1		53WC 21EC 14WC
Patch Material A (Patch Material C for the 7 Mile Bridge Columns)	CIS-B	PCS-2	N8-SE1	22EC 17WC 36WC
Patch Material B	CIS-C	PCS-3		9WC 11EC 32WC
Coating A & Patch Material A	CIS-D	PCS-4	N5-SE2	24EC 10EC 10WC
Coating B & Patch Material A	CIS-E	PCS-5		9EC 18WC 56WC
Coating C & Patch Material A	CIS-F	PCS-6	N4-SE2	57EC 19WC 17EC
Coating A & Patch Material A admixed with Corrosion Inhibitor C	CIS-G	PCS-7	N12-SE2	21WC 34EC 18EC
Coating A & Patch Material A admixed with Corrosion Inhibitor D	CIS-H	PCS-8		28WC 27WC 19EC
Coating A & Patch Material A admixed with Corrosion Inhibitor E	CIS-I	PCS-9		12EC 47EC 36EC
Coating A, Patch Material A, & surface applied Corrosion Inhibitor A	CIS-J	PCS-10		13WC 26EC 26WC
Coating B, Patch Material A, & surface applied Corrosion Inhibitor A	CIS-K	PCS-11		
Coating A, Patch Material A admixed with Corrosion Inhibitor C, & surface applied Corrosion Inhibitor A	CIS-L	PCS-12		55EC 25EC 32EC
Coating A, Patch Material A admixed with Corrosion Inhibitor D, & surface applied Corrosion Inhibitor A	CIS-M	PCS-13		25WC 46EC 30EC

POOR CONCRETE SPECIMEN MACROBEAM STUDY (PCS)

Experimental Setup

The macrobeams employed in this phase of the study, which are termed "Poor Concrete Specimens" or PCS, were similar to the G-109 macrobeams (see Appendix C) except that the G-109 elements were replaced by PCS ones. Figure D-1 presents a schematic illustration of such a macrobeam and shows these to be comprised of three generalized components, as listed below:

1. Three PCS elements. These consisted of an electrically continuous ECR mat that was embedded at the upper macrobeam surface. These were designated as "L", "M", and "R" according to the relative location of each (left, middle, or right). A total of 42 such specimens were fabricated.

2. Three separate ECR mats at the same level as and adjacent to the PCS elements. As with the PCS elements, the bars in each of these were electrically continuous. Within each macrobeam, these mats were designated as "LA," "MA," and "RA" according to the relative position of each.

3. A bottom mat of black steel. This was similar to the bottom mat of the G-109 macrobeams except that it consisted of four longitudinal bars.

Fabrication and testing of the PCS macrobeams involved the following steps and procedures:

1. Preparation of the PCS specimens. A six station PCS mold was used to construct a PCS specimen consisting of a 5 x 5 ECR array for which the final dimensions were 0.36 x 0.36 x 0.10 m (14.0 x 14.0 x 4.0 inches). Electrical continuity was achieved by a common lead wire

to each of the longitudinally aligned bars and by external wiring of the transversely aligned bars subsequent to concrete pouring and removing the forms. The concrete for these was the same as for the Cl^- admixed G-109 specimens as described in Appendix C (see Table C-2). A series of 14 intentional coating defects of 3.2 mm (0.125 in) diameter was introduced to the top surface of bars of the ECR mat in an approximately circular pattern. These specimens were fabricated in January, 1997.

2. Accelerated corrosion of the PCS specimens. Subsequent to curing the PCS specimens, corrosion of the ECRs was induced by application of a 0.5 mA impressed anodic current similar to what was described in Appendix C for the G-109 specimens. To expedite the experimental program in view of the fact that corrosion induced cracking did not occur in the anticipated time, macrobeams were fabricated in July, 1997.

3. Casting of PCS macrobeams. The configuration of these was similar to the G-109 macrobeams, as noted in Appendix C (see Figure C-3), except that the G-109 elements were replaced by PCS ones. Two concrete lifts were involved, where the bottom one was Cl- free and the top contained 11.88 kg/m^3 (20 pcy) of Cl^- as NaCl. The mix designs were the same and the same concretes were employed as for the G-109 macrobeams (see Table C-1). Clear cover for all outer bars was 25 mm (1.0 in). A total of 14 PCS macrobeams were prepared. Figure D-2 presents a photograph of a typical beam.

4. Continued impressed current accelerated corrosion of the PCS specimens. Accelerated corrosion of the embedded PCS specimens continued subsequent to fabrication of the macrobeams. To accelerate the cracking, the current was increased to 4 - 9 mA in March, 1998; and cracking of some specimens was detected the following month (April, 1998).

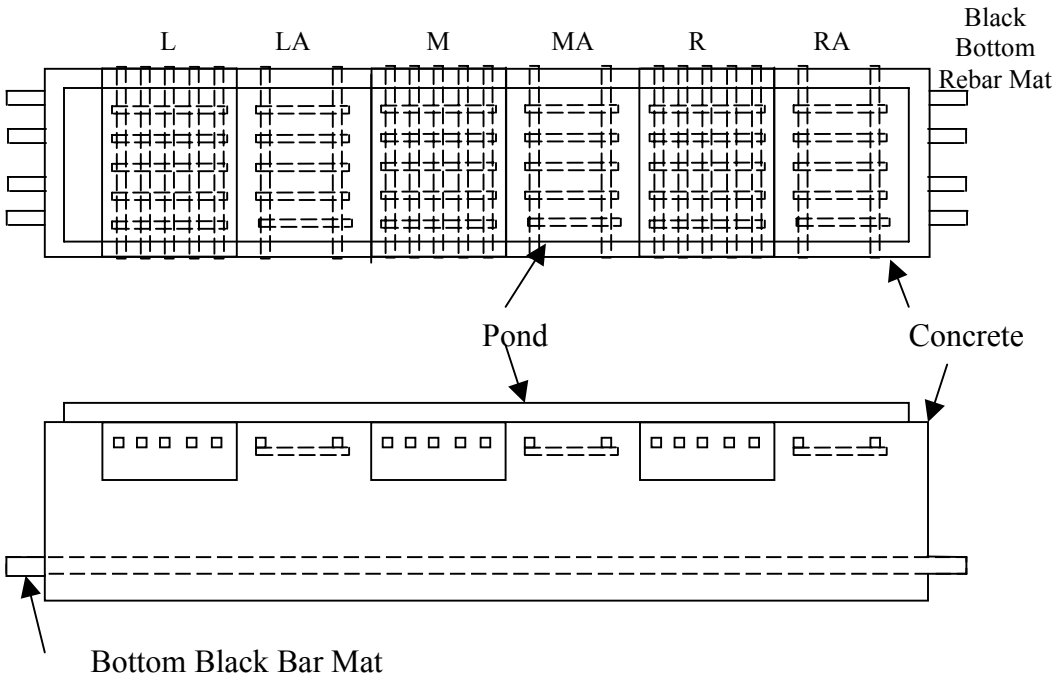

Figure D-1: Schematic illustration of a PCS macrobeam.

Figure D-2: Photograph of a PCS macrobeam.

Once cracking of individual PCS specimens reached an appropriate level, the impressed current was terminated; and exposure continued as natural weathering only. By September, 1998, all PCS specimens contained significant cracking.

5. Data acquisition. Figure D-3 illustrates the external circuitry with which each PCS macrobeam was instrumented for purposes of data acquisition. This involved a direct lead wire from 1) each PCS element, 2) each adjacent ECR mat, and 3) the bottom black bar mat to a junction box. Figure D-4 shows an enlarged schematic view of the junction box from Figure D-3 along with a designation scheme for the six pairs of connection terminals. The same testing and measurement protocol that was described in Appendix C for the G-109 macrobeams was employed also for the PCS ones. Table D-2 provides a description of the components between which current was measured in the case of each terminal pair, and Table D-3 does the same for resistance. Consequently, the measured current in the case of the L-B, M-B, and R-B terminals was that between a particular PCS (L, M, or R) plus the adjacent ECR mat (these two components were in parallel) and all other components (the other two PCSs, the other two adjacent ECR mats, and the bottom black steel). Of course, the influence of each component upon the measured current should be a function of the resistance between it and the PCS/adjacent ECR mat pair in question. For resistance, however, the measured value was that between the two isolated components only (Table D-3). The same data acquisition schedule was employed for the PCS macrobeams as for the new G-109 ones (see Table D-4).

6. Repair strategies. Table D-1 lists the repair strategy that was used for each macrobeam. The repairs were instituted in December, 1998 at the same time as for the new G-109

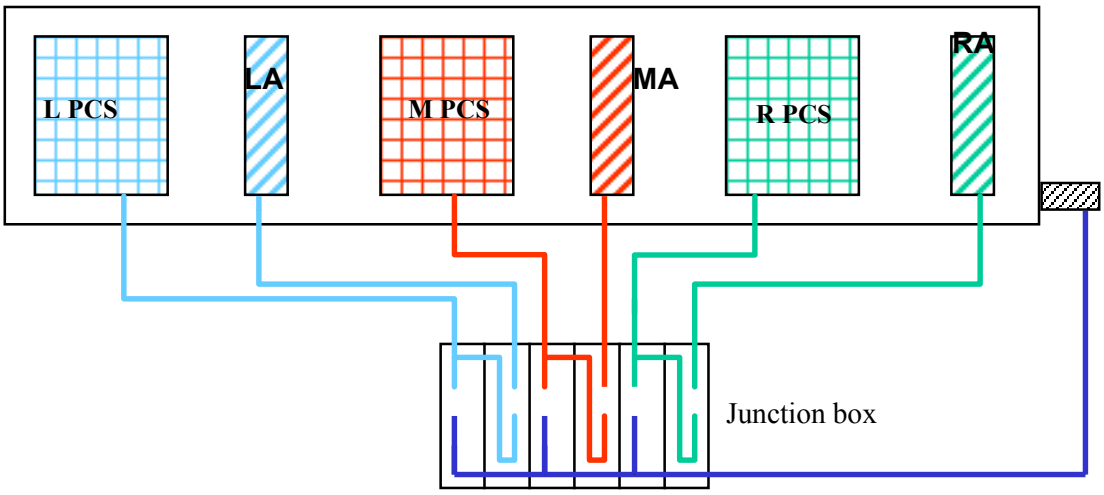

Figure D-3: Schematic illustration of a PCS macrobeam with electrical measurement circuitry.

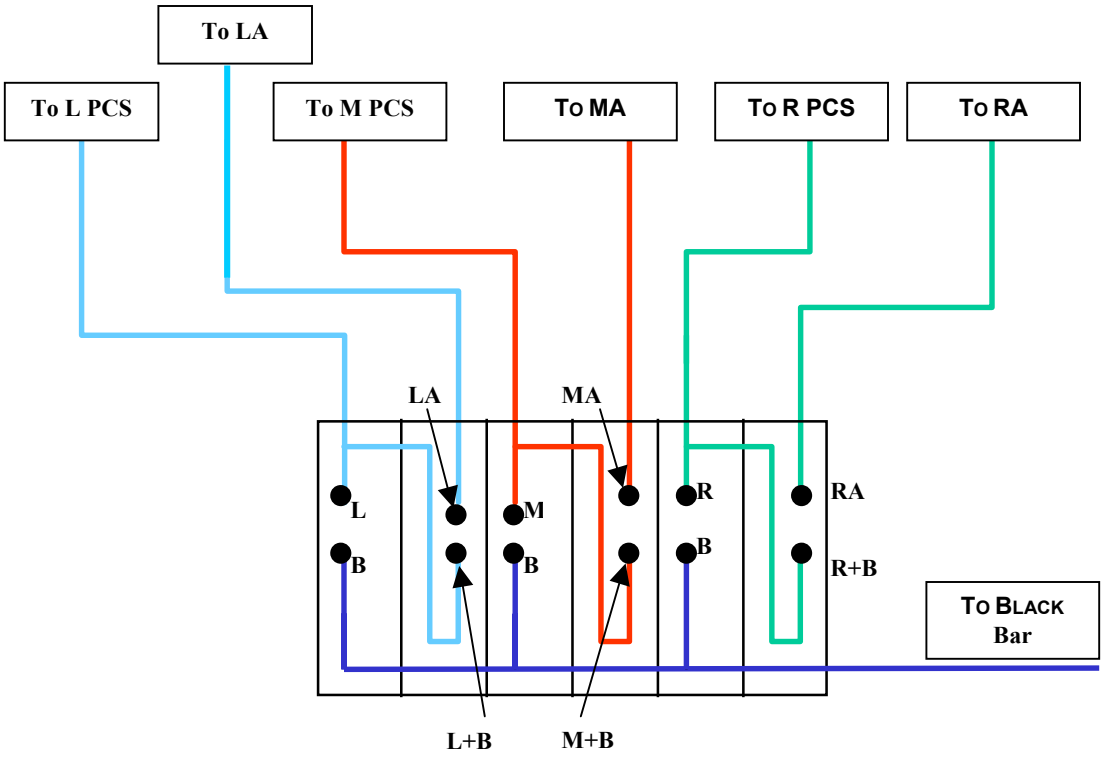

Figure D-4: Schematic illustration of the PCS macrobeam circuit terminals for current and resistance measurements.

Table D-2: Listing of the components between which current was measured for each terminal pair.

Terminals	Connection
L-B	L PCS plus LA mat to Adjacent Assembly Components plus Bottom Black Bar Mat
LA-(L+B)	LA to L PCS plus Adjacent Assembly Components plus Bottom Black Bar Mat
M-B	M PCS plus MA to Adjacent Assembly Components plus Bottom Black Bar Mat
MA-(M+B)	MA to M PCS plus Adjacent Assembly Components plus Bottom Black Bar Mat
R-B	R PCS plus RA to Adjacent Assembly Components plus Bottom Black Bar Mat
RA-(R+B)	R PCS to RA plus Adjacent Assembly Components plus Bottom Black Bar Mat

Table D-3: Listing of the components between which resistance was measured for each terminal pair.

Terminals	Connection
L-B	L PCS to Black Bar Mat
LA-(L+B)	LA to L PCS plus Black Bar Mat
M-B	M PCS to Black Bar Mat
MA-(M+B)	MA to M PCS plus Black Bar Mat
R-B	R PCS to Black Bar Mat
RA-(R+B)	RA to R PCS plus Black Bar Mat

Table D-4: Scheduling of the different data acquisitions.

Data Acquisition Number	Data Acquisition Date	Description
1	12/6-10/98	Baseline data obtained just prior to repair.
2	12/10-18/98	Baseline data obtained just after repair.
3	1/21-23/99	First Post Repair data acquisition.
4	3/23-4/1/99	Second Post Repair data acquisition.
5	4/29-5/2/99	Third Post Repair data acquisition.
6	6/8-10/99	Fourth Post Repair data acquisition.
7	9/21-28/99	Fifth Post Repair data acquisition.
8	1/15-17/00	Sixth Post Repair data acquisition.
9	11/11-12/00	Seventh Post Repair data acquisition.

macrobeams. Figure D-5 shows the typical appearance of a PCS mat after the cracked and spalled concrete was removed and in preparation to affect the repair.

7. Exposure testing. Procedures here were identical to those for the G-109 macrobeams described in Appendix C.

Findings & Discussion

Figure D-6 presents plots of the average macrocell current between the ECR elements and the bottom black steel for each repair strategy (alternatively, for each specimen) at the time of the successive data acquisitions. The left column of plots presents current flow data for the PCS specimens and the- bottom black steel mat connections (this was derived by subtracting the current flow between terminals LA-(L+B) from L-B) and the right column plots presents flow between the adjacent ECR mat and the bottom black steel mat (current measured between terminals LA-(L+B)). Note, however, that the time scale is in arbitrary units where the indicated number refers to a data acquisition number from Table D-4. In all cases, a positive current is anodic (that is, positive current flows from the element, either the PCS or adjacent mat, into the concrete) and negative cathodic. This shows the trend in Figure D-6 to be one where current for the no repair macrobeam was relatively high and positive; but current was either much less positive or was negative for most of the others. For the adjacent mat case, however, most currents were relatively low at the initial data acquisitions but increased for some subsequently. Here also, however, current for the no repair macrobeam was one of the highest.

Analysis of these macrocell currents suggests that patching alone with Materials A and B resulted in the formation of cathodic sites in the repaired area. Use of Coatings A and C significantly reduced macrocell current between the PCS specimens and the bottom black steel,

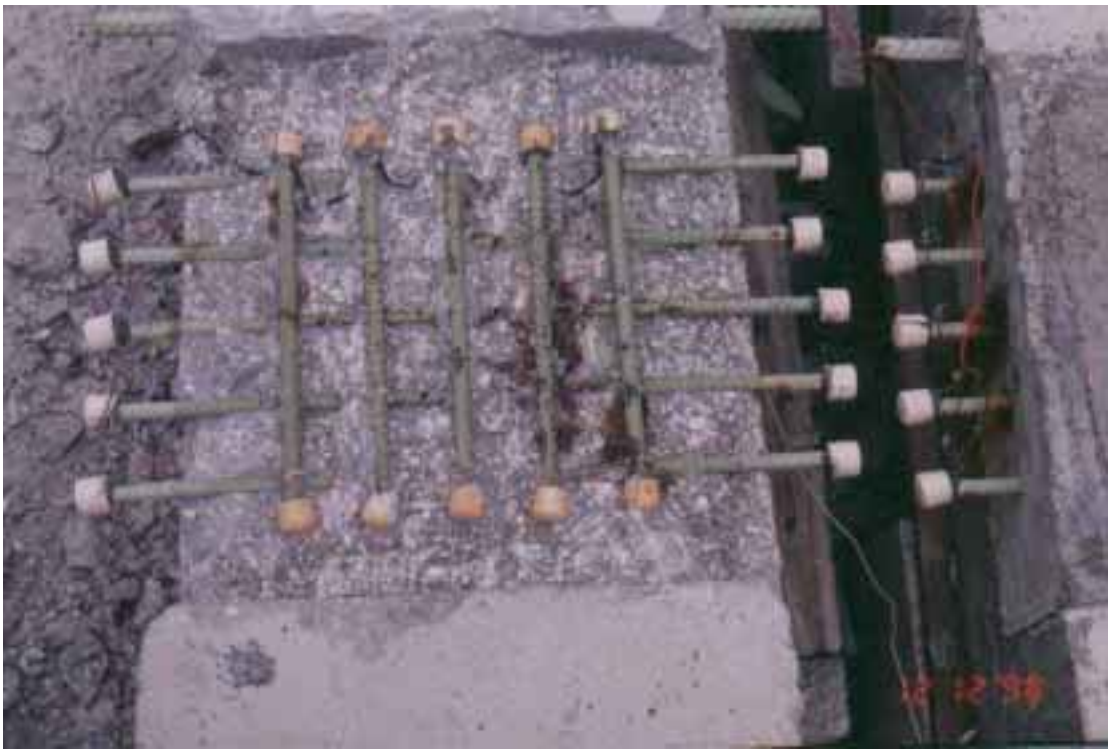

Figure D-5: Photograph of the ECR mat from a PCS specimen after removing the cracked and spalled concrete.

Average macrocell current between PCS and black steel.

Average macrocell current between Adjacent ECR and black steel.

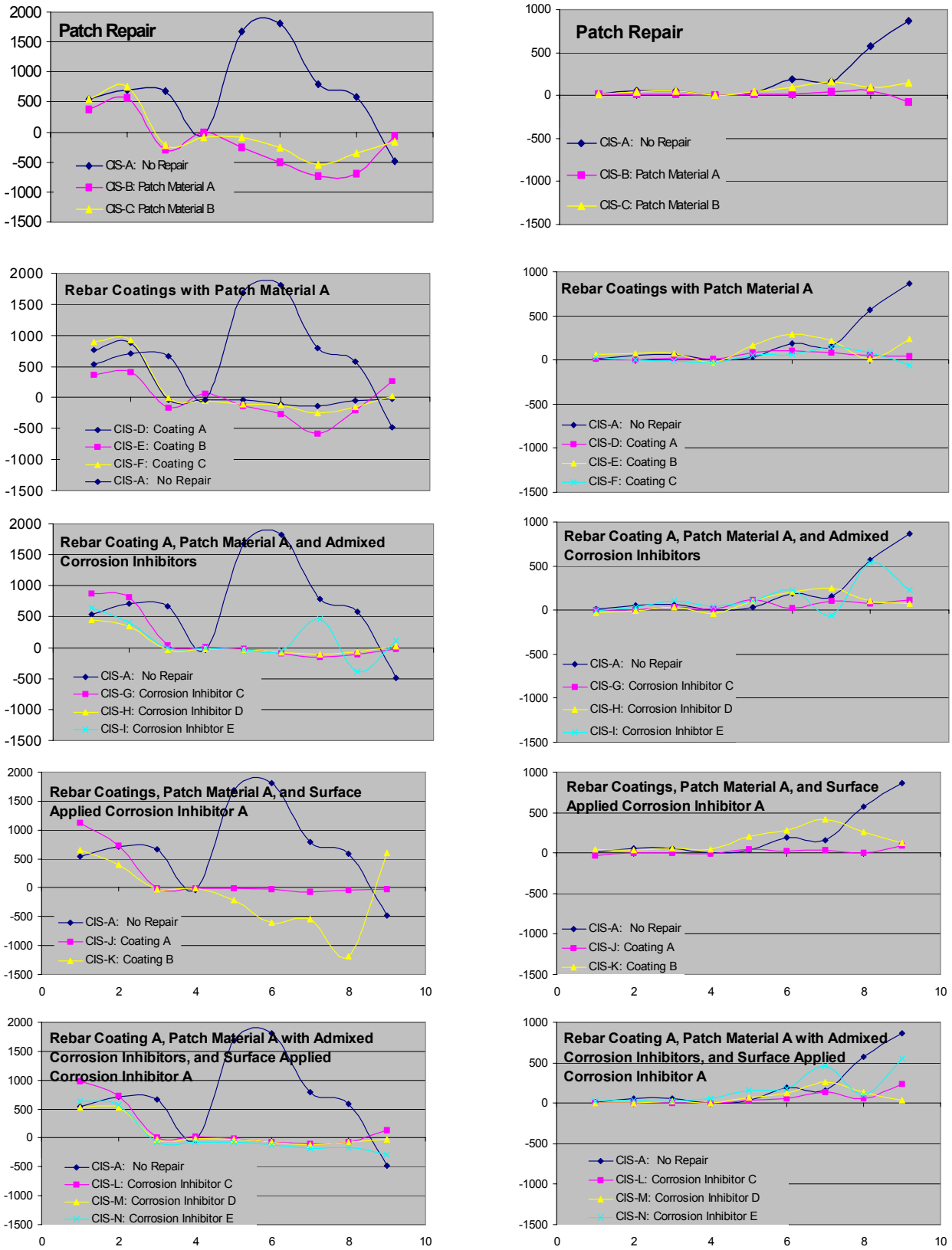

Figure D-6: Average macrocell current (µA) versus time.

and a small reduction in the adjacent ECR-to-bottom black steel current was also noted. No further reduction in macrocell current is apparent from the use of admixed and surface applied corrosion inhibitors. The lack of improvement from the use of corrosion inhibitors can be attributed to either a) the inhibitors are not effective or b) there was no room for further improvement. No improvement was also realized from the use of surface applied corrosion inhibitor when used in conjunction with Coating B. Thus, based on macrocell currents, it may be concluded that the use of corrosion inhibitors do not provide any beneficial effects when used in conjunction with rebar coatings.

Figures D-7 and D-8 plot resistance versus time for the PCS-to-black steel and adjacent mat-to-PCS plus black steel, respectively. Figure D-9 illustrates that there was, in general, an inverse relationship between the absolute value for macrocell current and resistance.

Table D-5 lists results of a visual survey performed on the PCS macrobeams in November, 2000. Thus, the control specimen (PCS macrobeam number 1, no repair) showed the most damage; and Figure D-6 indicates that macrocell current for this specimen was greater than for the other macrobeams. With this exception, however, no correlation was apparent between visual condition and macrocell current. To illustrate this, Table D-6 lists the sum of absolute values for the average PCS-B and AJD-(PCS+B) macrocell currents from the last three data acquisitions for each beam compared to a condition rating. This correlation was attempted using the absolute value of current since it was reasoned that any electrochemical activity should have a negative impact in that a cathodic current upon one element indicates an anodic current elsewhere. The ranking was normalized such that Specimen PCS-1 (no repair) was a 1 and uncracked beams a 10. Figure D-10 presents a graphical representation of the Table D-6 results and indicates that

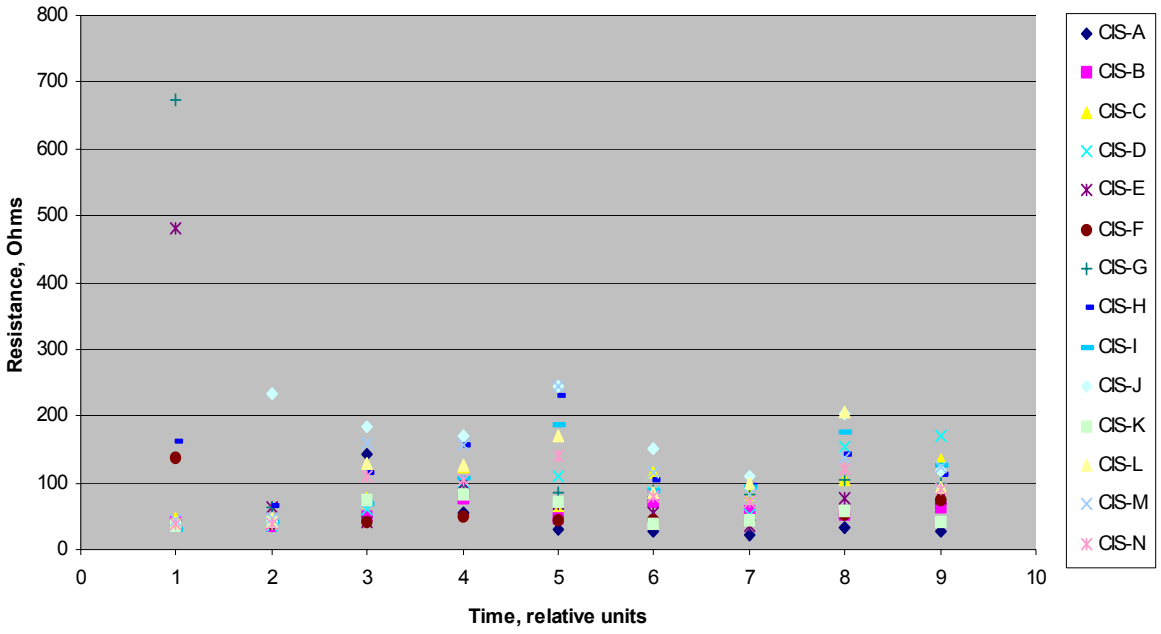

Figure D-7: Plot of the average PCS-to-black steel resistance for each specimen (repair strategy) versus time.

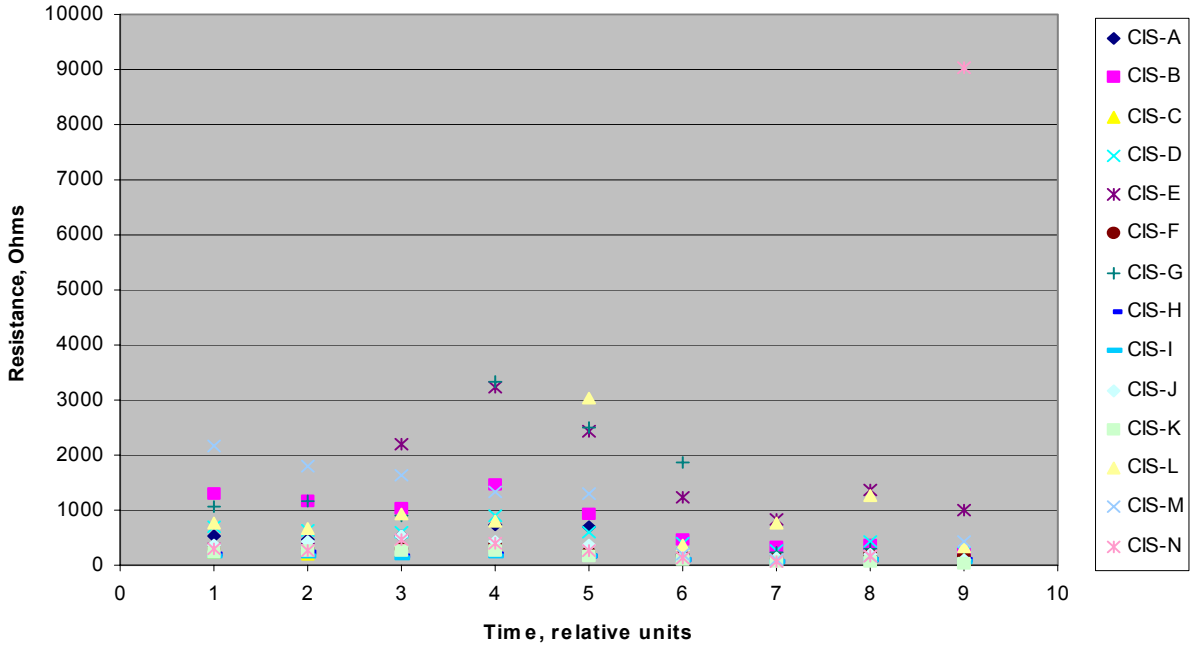

Figure D-8: Plot of the average adjacent mat-to-PCS plus black steel resistance for each specimen (repair strategy) versus time.

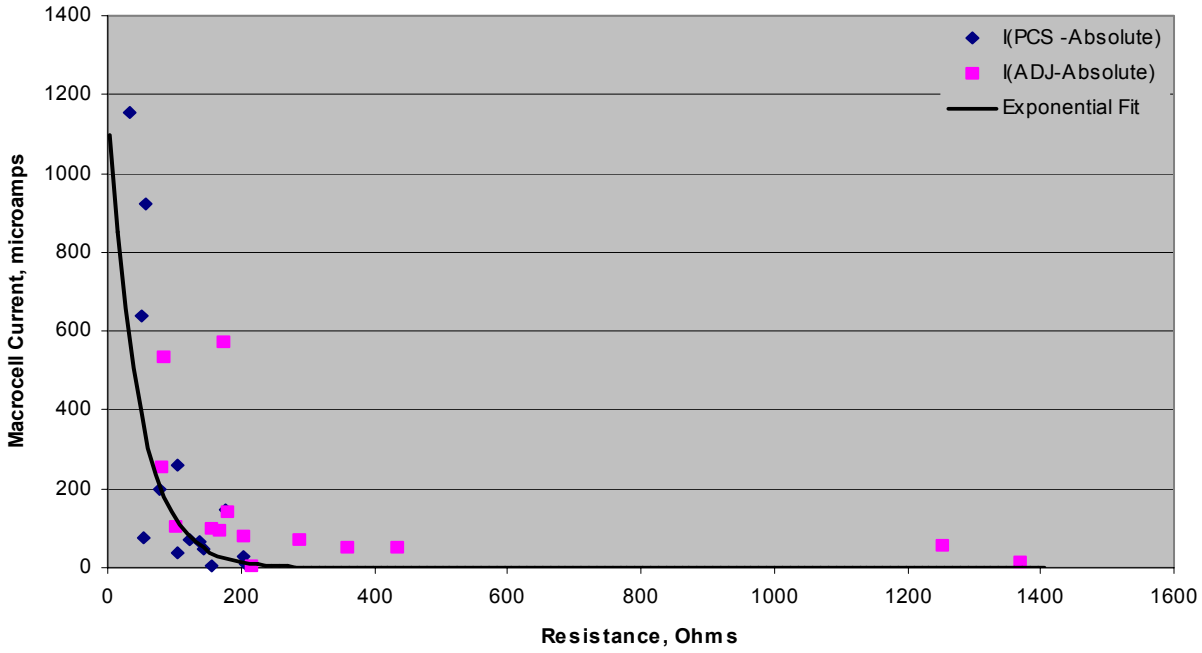

Figure D-9: Plot of the PCS-B and ADJ-PCS plus B macrocell current.

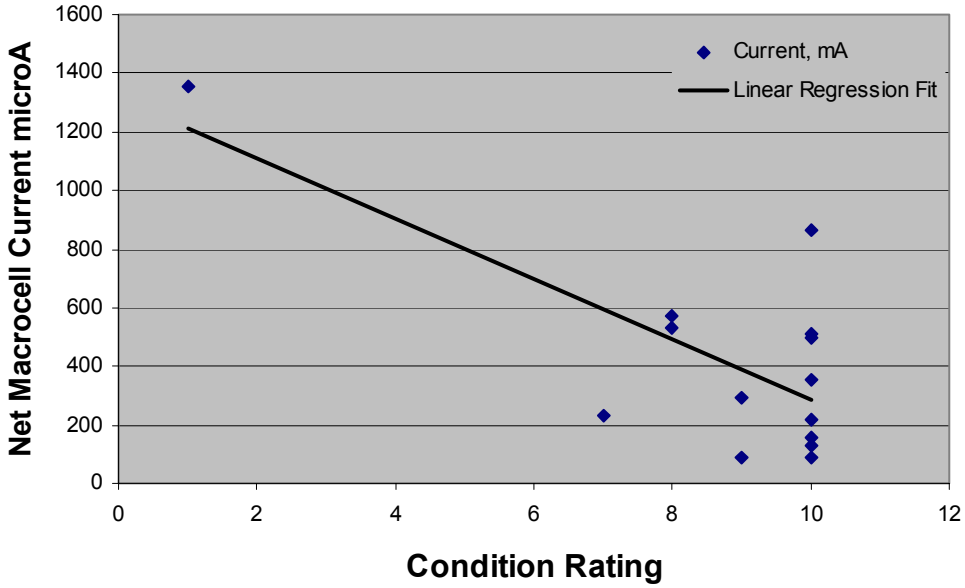

Figure D-10: Plot of net macrocell current versus condition rating.

Table D-5: Results of a visual condition assessment of the PCS macrobeams performed in November, 2000

Beam No.	Repair Treatment	Visual Condition Assessment
1	CIS-A	All PCS elements show shrinkage crack network. One major corrosion induced crack above an adjacent mat bar. 23 of 30 PCS bars and 1 of 12 adjacent mat bars show rust at ends.
2	CIS-B	No cracks. All PCS bars and 2 of 12 adjacent mat bars show rust at ends.
3	CIS-C	No cracks. 25 of 30 PCS bars and 2 of 12 adjacent mat bars show rust at ends.
4	CIS-D	Short, hairline crack at edge of one adjacent mat bar. 12 of 30 PCS and 4 of 12 adjacent mat bars show rust at ends.
5	CIS-E	No cracks. 7 of 30 PCS bars and 5 of 12 adjacent mat bars show rust at ends.
6	CIS-F	No cracks. 11 of 30 PCS bars and 2 of 12 adjacent mat bars show rust at ends.
7	CIS-G	No cracks. 9 of 30 PCS bars and 3 of 12 adjacent mat bars show rust at ends.
8	CIS-H	One hairline crack above bar in two PCS elements. One hairline crack above one adjacent mat bar. 9 of 30 PCS bars and 3 of 12 adjacent mat bars show rust at ends.
9	CIS-I	One hairline crack above bar in two PCS elements. 10 of 30 PCS bars and 5 of 12 adjacent mat bars show rust at ends.
10	CIS-J	No cracks. 3 of 30 PCS bars and 4 of 12 adjacent mat bars show rust at ends.
11	CIS-K	No cracks. 12 of 30 PCS bars and 6 of 12 adjacent mat bars show rust at ends.
12	CIS-L	Short, hairline crack at edge of one adjacent mat bar. 7 of 30 PCS and 6 of 12 adjacent mat bars show rust at ends.
13	CIS-M	No cracks. 2 of 30 PCS bars and 3 of 12 adjacent mat bars show rust at ends.
14	CIS-N	One major corrosion induced crack and rust above one adjacent mat bar. 15 of 30 PCS bars and 9 of 12 adjacent mat bars show rust at ends.

Table D-6: Attempted correlation between macrocell current and visual appearance of PCS macrobeams.

Specimen No.	Current, mA	Condition Rating
1	1674	1
2	638	10
3	389	10
4	103	9
5	367	10
6	177	10
7	121	10
8	291	7
9	516	8
10	45	10
11	779	10
12	108	9
13	259	10
14	385	8

the data scatter exceeds any tendency for these parameters (macrocell current and condition) to correlate. Other attempts resulted in no improvement in the correlation. As noted earlier, macrocell current generally varied inversely with resistance. This same trend was apparent also for the G-109 macrobeam data, as discussed elsewhere; and the same rationale for explaining this can be applied to both situations (G-109 and PCS macrobeams). Thus, a relatively low resistance is ascribed to either a high chloride uptake of the concrete or to development of coating defects upon the ECR (or both), whereas high macrocell currents presumably resulted from either these same causes or from the potential difference between the respective elements becoming relatively large. The observation that the average PCS-bottom black steel macrocell current for the individual specimens tended to be cathodic for a number of specimens at the time of the latter data acquisitions tends to support this. Further, the macrocell current data for the adjacent mat elements were normally positive, indicating that these ECRs were probably anodic to both the PCS ones and the bottom black steel. This indicates that, in many cases, it is corrosion activity stemming from the adjacent mats that should be of greatest concern. Of course, the adjacent mats were not repaired; but in some cases they were flooded with a corrosion inhibitor. However, the magnitude of current from adjacent mat elements of macrobeams in this latter category (flooded with a corrosion inhibitor) were about the same as for the non-flooded ones, as can be seen from Figure D-6 by comparing the current for treatments CIS-A through CIS-I (no inhibitor flooding) with that for CIS-J through CIS-N (inhibitor flooded).

Figures D-11 and D-12 present impedance modulus data at different times for the PCS and adjacent mat elements, respectively. The general trend here is one where elements of the no repair macrobeam exhibited the lowest impedance. For the repaired beams, impedance

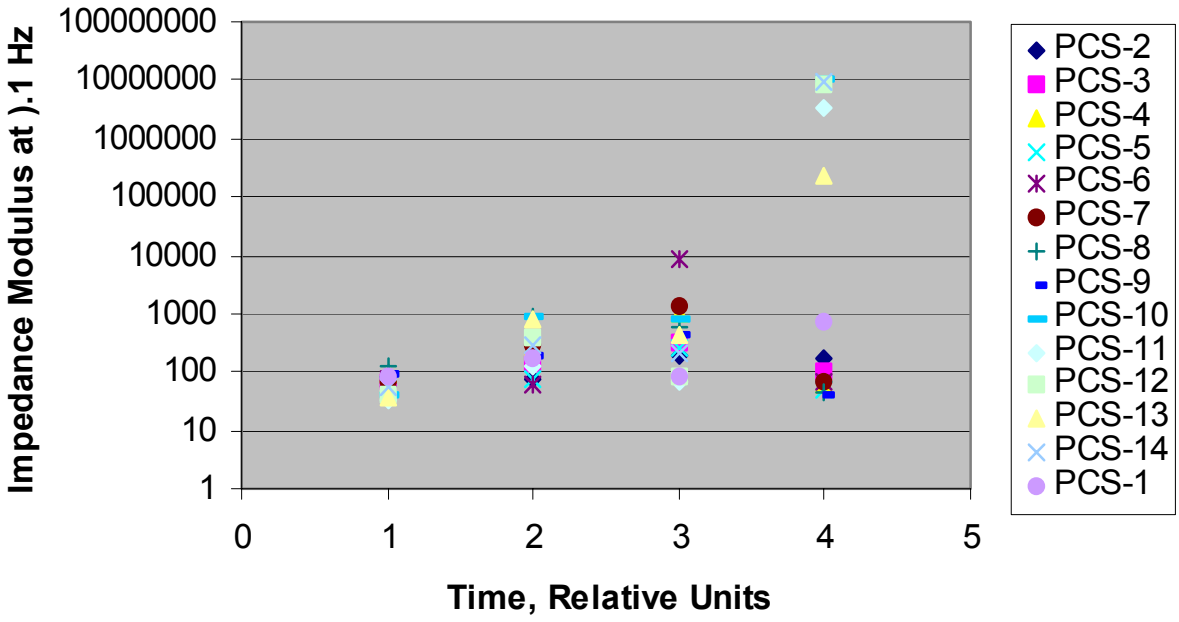

Figure D-11: Impedance modulus as a function of time for the PCS units.

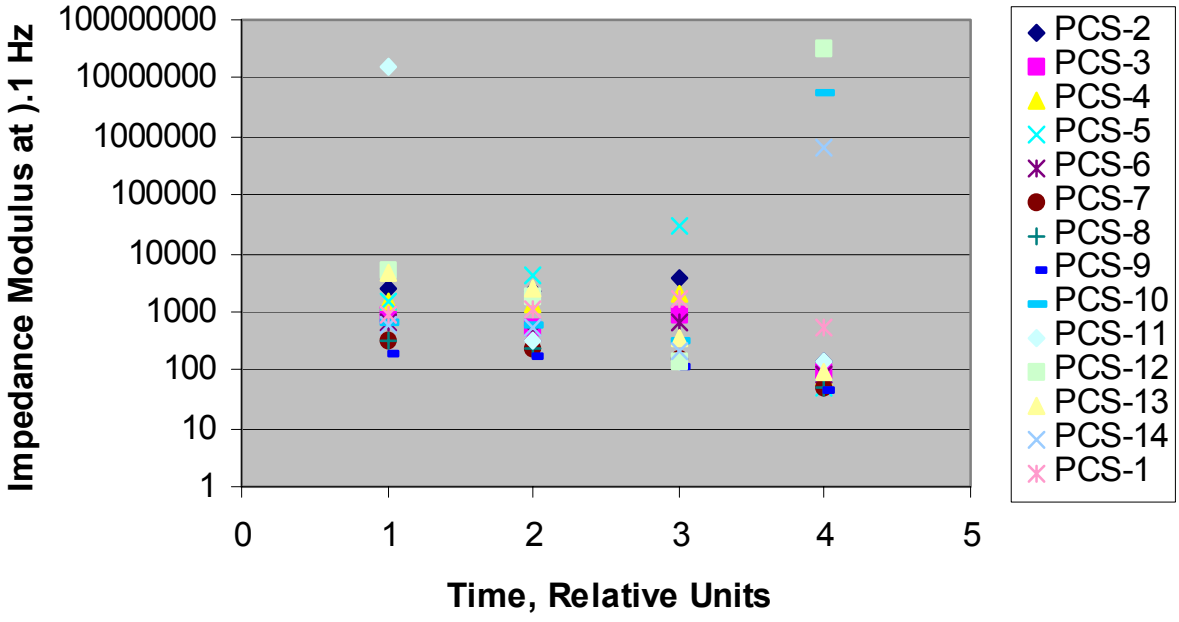

Figure D-12: Impedance modulus as a function of time for the adjacent elements.

increased, typically by an order of magnitude or more, once the repair was made. Subsequently, impedance increased with time and either remained constant or decreased at the time of the last data acquisition. This presumably reflects changes in the number and size of bare areas, as affected by the repairs, or changes in the coating capillary pore structure and resistivity. The fact that the final impedances for the repaired specimens were typically an order of magnitude or more greater than prior to repair indicates that the coating effectiveness was improved and that at least some of this improvement was retained at the time of the final data acquisition. The very high impedance exhibited by several specimens at certain times probably was a consequence of a low resistance connection not being made.

Based upon the data developed within the time frame at hand, the following conclusions are reached:

1. Corrosion resistance seems to have been restored to the repaired areas per se in all cases.

2. The repairs apparently have accelerated corrosion within the adjacent mat areas (compared baseline data with post-repair data). While this corrosion activity is low in some cases, no correlation could be established between the magnitude of corrosion and the type of repair that had been affected upon the PCS.

3. No benefit of using admixed corrosion inhibitors or corrosion inhibitor flooding on the surface as a component of a repair was apparent.

BENT BAR STUDY

Experimental Setup

There were eight ECR slabs remaining from a study (initiated in 1988) whereby the corrosion characteristics of straight and bent ECR were evaluated under accelerated southern exposure cycling as described in NCHRP Report 244 (*1, 2*), however not all specimens were subjected to southern exposure cycling and some slabs were ponded with tap water following the southern exposure portion of the program. Weekly southern exposure cycling involved four days of continuous ponding of the top surface with a 15 percent (by weight) sodium chloride solution followed by draining and three days of exposure to an air temperature of 100^{o}F and ultraviolet lights. Variables included seven different suppliers, bend diameter, coating thickness, coating application before and after fabrication of the bar, rate of bending, steel temperature during bending, and patching of damaged areas prior to concrete placement. All coating properties were documented prior to concrete placement (*2*). Two sizes of concrete slabs were fabricated in 1988; 330 mm (13 in.) wide by 356 mm (14 in.) deep by 178 mm (7 in.) thick and 305 mm (12 in.) wide by 254 mm (10 in.) deep by 178 mm (7 in.) thick. Each slab consisted of two independent specimens; one straight bar and one bent bar specimen. The former involved two bars (these were made electrically continuous external to the slab) and the latter was comprised of one bar. The bottom mat steel was uncoated in all cases. Three bottom bars were positioned beneath the bent ECR and three were placed below the two straight ECR's. In each case, the bottom bars were made electrically continuous outside of the slab concrete.

Periodic data collection included visual observations, sounding surveys, corrosion potential measurements, macrocell current measurements, rate of corrosion testing, and AC resistance

between the top ECR bars and bottom bare bars. Select slabs were also autopsied at the conclusion of the study. All other details including the concrete mix design and test data can be found in References 1 and 2.

Four of the eight remaining slabs were designated N4-SE2, N5-SE2, N8-SE1, and N12-SE1. After completing 1.35 years of southern exposure cycling and a minimum of 0.9 years of tap water ponding, these slab were moved to an outdoor exposure facility in northern Virginia. In April 1996, slabs N4-SE2 and N12-SE1 exhibited surface cracking, partial delamination, and rust staining on bent and straight bars, slab N8-SE1 had surface cracking and partial delamination on the bent bar, and slab N5-SE2 had surface cracking only. The slabs were approximately 8 years old at that time.

The above described slabs were included in this study as a supplement to the laboratory specimens described above. These slabs were not intended as a systematic study of the various physical repair/rehabilitation strategies but, instead, as an extension for specific repair strategies.

In July 1996, the slabs were transported to a outdoor exposure test site in Northern Virginia (the slabs were approximately 8 years old at that time). Separate resistor and switch assemblies were still in place between the bent ECR and three of the uncoated bottom mat bars and the two straight ECR's and the other three uncoated bottom mat bars on each slab. Throughout the exposure, all switches were closed except when measuring AC resistance between ECR's and uncoated bars. Data sets before and after installing repairs included the following measurements:

1. Macrocell current (measured as a voltage drop across a resistor) between the bent ECR and bottom steel and between the straight ECR's and bottom steel.

2. AC resistance between the bent ECR and bottom steel and between the straight ECR's and bottom steel.

3. Half-cell potential measurements along the bent and straight ECR's.

Visual and delamination surveys were also performed each time data were collected.

The condition of the slabs at the start of the study is described in Table D-7.

In September 1997, two sets of baseline data were collected and then the slabs were repaired as indicated in Table D-1.

In all cases the bent bar was repaired (approximately 152 mm (6 in.) or less of the bent bar in slabs N8-SE1, N5-SE2, and N12-SE1 was not repaired and only about 127 mm (5 in.) of the bent bar in slab N4-SE2 was repaired). The straight bars in slab N8-SE1 were not repaired and the straight bars in slab N5-SE2 were removed from the slab. The later was necessary due to the severe damage around these bars and the fact that they completely dislodged from the slab during the concrete removal process. A minimum of half the length of the rightmost straight bar in slabs N4-SE2 and N12-SE1 was repaired. The concrete removal process did not include undercutting of the exposed portion of bars.

Ponding cycles were initiated in early October 1997. Each cycle consisted of ponding with a 3% NaCl solution for 2 weeks (using plastic covers to minimize evaporation) followed by a 2 week dry period. During the second 2 weeks of each cycling period, an elevated cover was used on each slab to maintain a dry surface condition. Post-repair data were periodically collected for over 30.5 months.

Findings & Discussion

Visual observations throughout the exposure period are presented in Table D-8. No delaminations developed on any of the slabs through 30.5 months of exposure.

Figures D-13 and D-14 present plots of macrocell current and AC resistance (both of these parameters were normalized to 70°F) versus exposure time for all slabs. In each case, the data were plotted separately for the bent and straight ECR's. Additionally, Figure D-15 present plots of half-cell potential measurements along the bent and straight ECR's versus exposure time for slabs N8-SE1 (CIS-B), N5-SE2 (CIS-D), N4-SE2 (CIS-F), and N12-SE1 (CIS-G) respectively. Measurements for straight bars were taken along the centerline between the two bars in each slab. Results are summarized below.

Bent Bars

After repair, the macrocell current for slabs N8-SE1 (CIS-B) and N5-SE2 (CIS-D) remained relatively constant and near zero through about 14 months of exposure. Subsequently, the macrocell current markedly increased (such that the ECR was anodic to the uncoated bottom steel) through 30.5 months of exposure. The AC resistance between ECR's and uncoated steel in these slabs remained relatively constant through about 22 months of exposure at which time there was a significant decrease in resistance for both slabs. Potentials were either more passive or similar to the pre-repair measurements through about 22.5 and 14 months of exposure for slabs N8-SE1 and N5-SE2 respectively. After 27.5 months of exposure for slab N8-SE1, potentials were significantly more active than the pre-repair data. For slab N5-SE2, potentials became increasingly active after 22.5 months of exposure.

Table D-7: Condition of Slabs Prior to Repair

Slab	Bent Bar	Straight Bars	Bottom Bars
N8-SE1	Surface and side cracks and partially delaminated.	No cracking or delaminations.	Crack on left side and along all bars at the back and partially delaminated.
N5-SE2	Surface cracking.	Surface and side cracks and partially delaminated.	No cracking or delaminations.
N4-SE2	Surface and side cracks and partially delaminated.	Crack on side and partially delaminated.	No cracking or delaminations.
N12-SE1	Surface cracking.	Crack on side and partially delaminated.	Crack on right side and partially delaminated.

Table D-8: Condition of Slabs During Post-Repair Exposure.

Slab	Repair Option	Bent Bar	Straight Bar
N8-SE1	CIS-B	Bar was repaired and no visual damage was observed through 30.5 months.	These bars were not repaired. Two small cracks formed between the bars after 27.5 months. At 30.5 months these cracks had grown together and extended over the rightmost bar.
N5-SE2	CIS-D	Bar was repaired and no visual damage was observed through 30.5 months.	Bars were removed during the repair process.
N4-SE2	CIS-F	Bar was repaired. Surface ruststaining developed at a crack near the edge of the patch after 14 months. The crack was not originally repaired since there was no delamination. The condition of this area worsened with time. Additional cracks formed inside and outside the patch after 30.5 months.	Only the rightmost bar was repaired and no visual damage was observed on either bar through 30.5 months.
N12-SE1	CIS-G	Bar was repaired. Surface rust staining developed outside the patch after 14 months. The condition of this area worsened with time and a crack formed after 27.5 months. Two additional cracks also developed after27.5 months and these continued togrow through 30.5 months.	Only the right most bar was repaired.No visual damage associated with this bar was observed through 30.5 months. One small crack formed alongthe leftmost bar after 30.5 months.

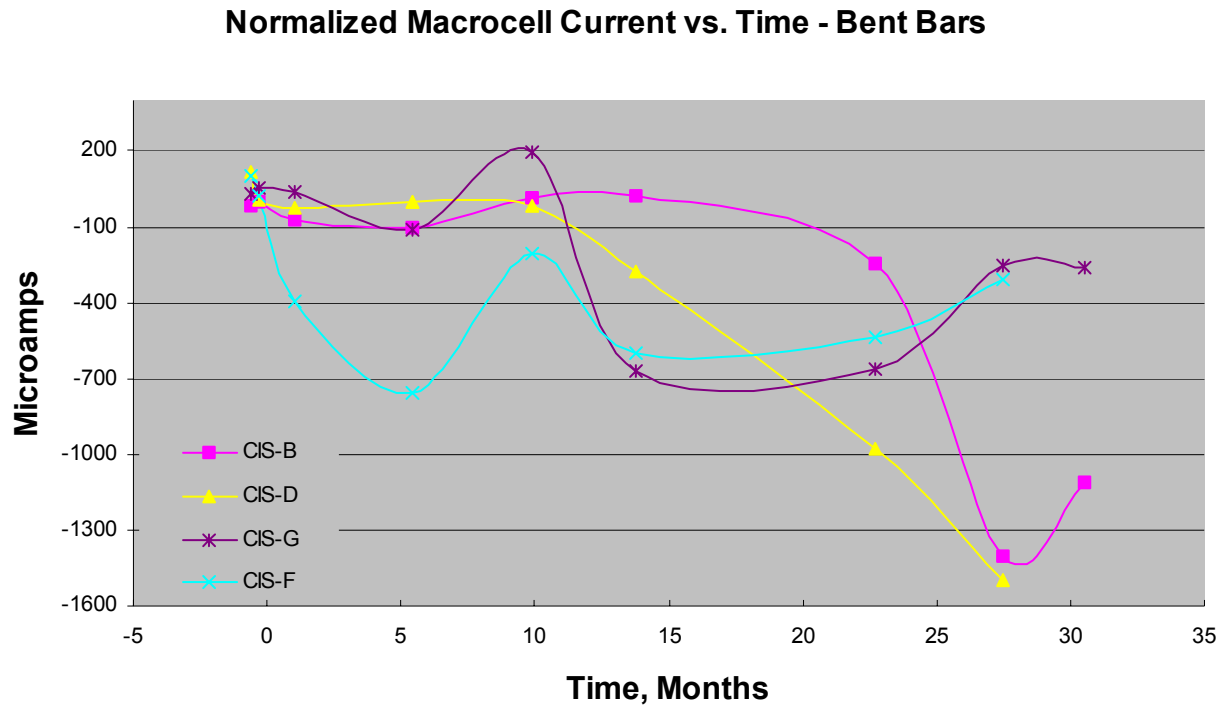

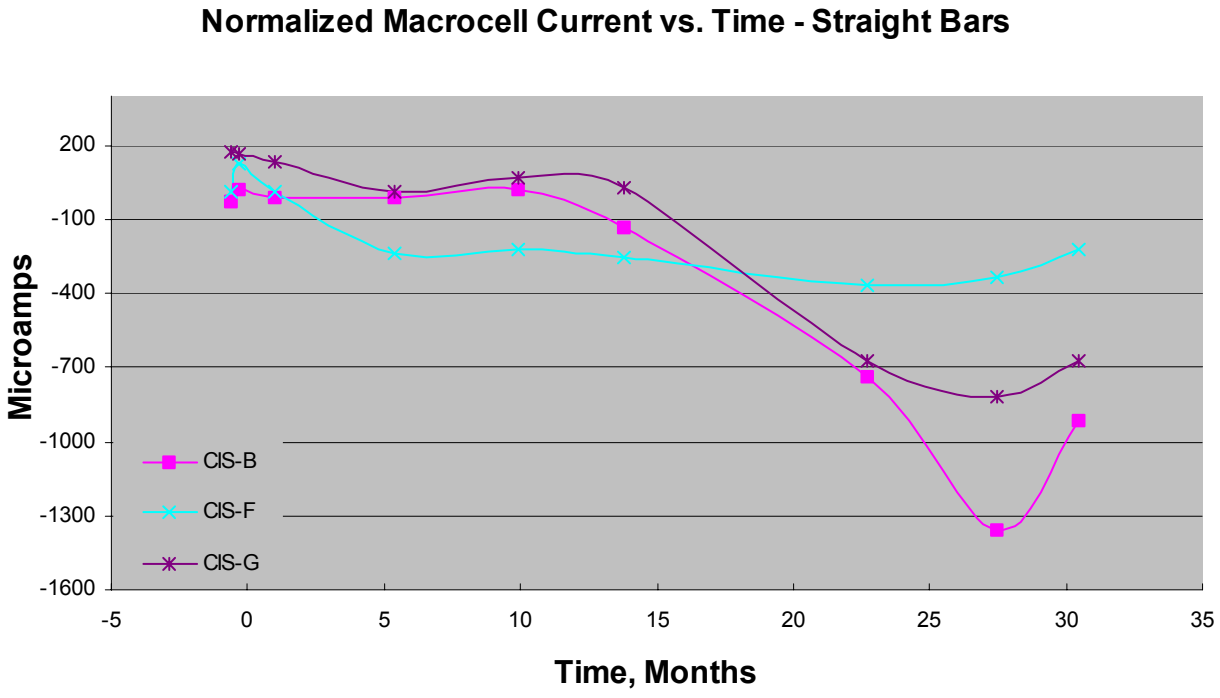

Figure D-13: Plot of Macrocell vs. Time for all Slabs.

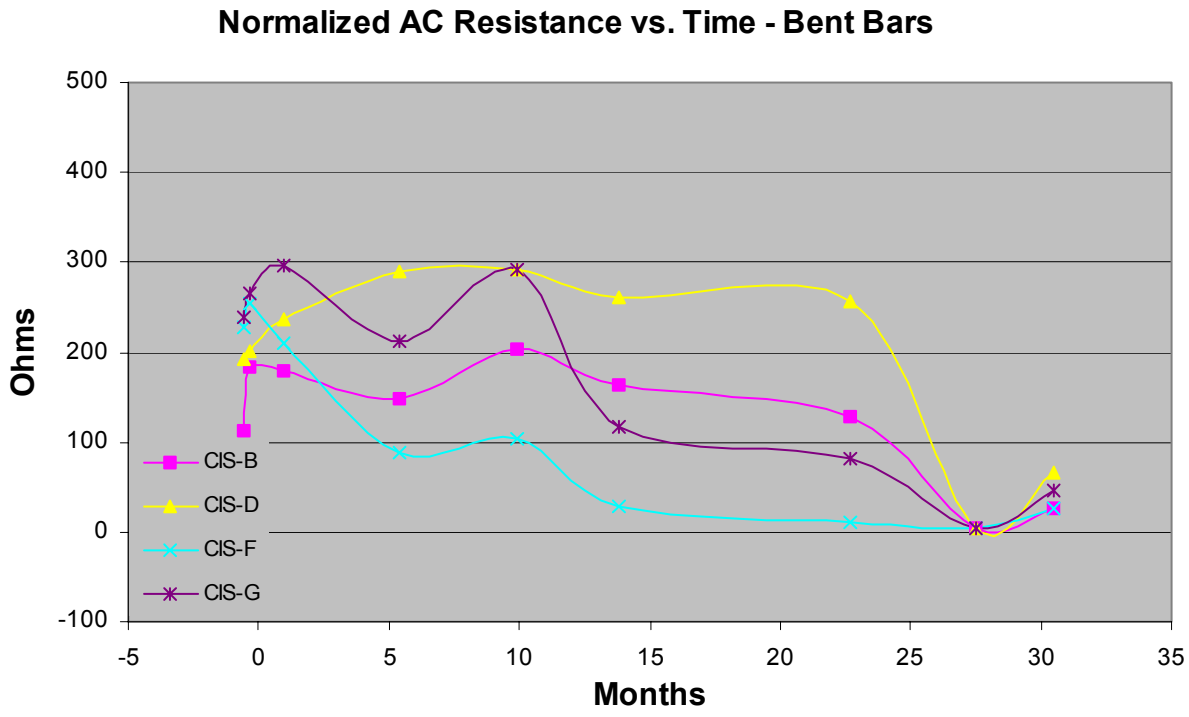

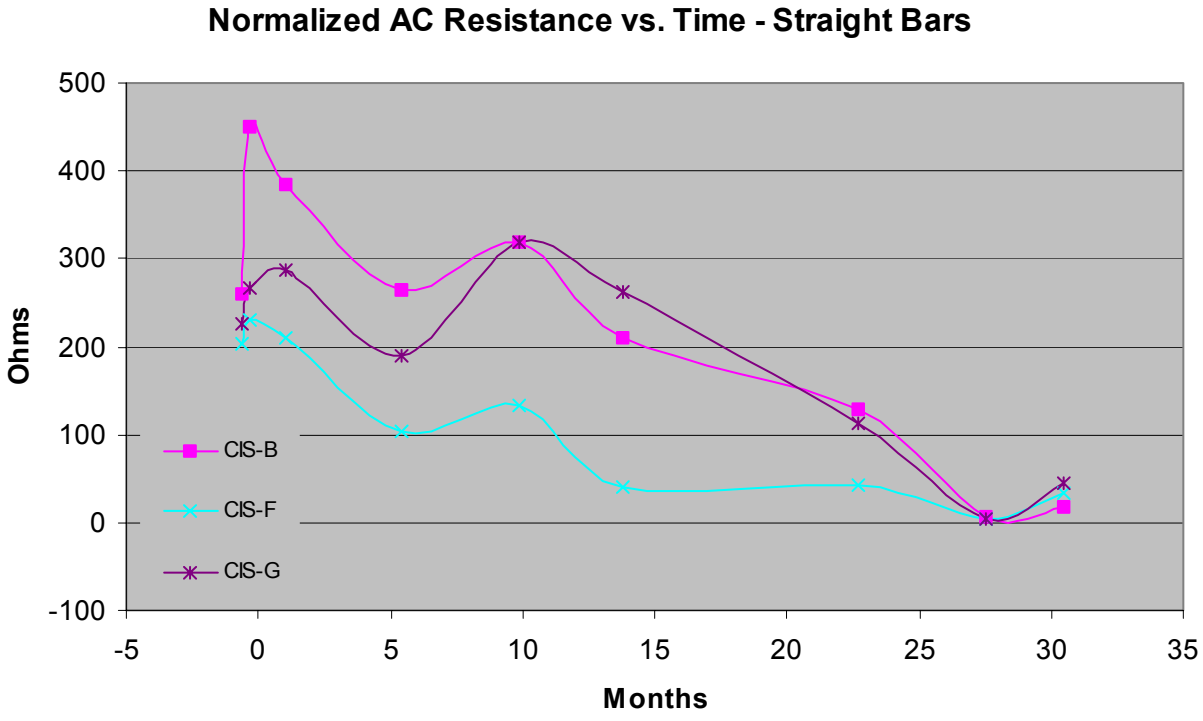

Figure D-14: Plot of AC Resistance vs. Time for all Slabs

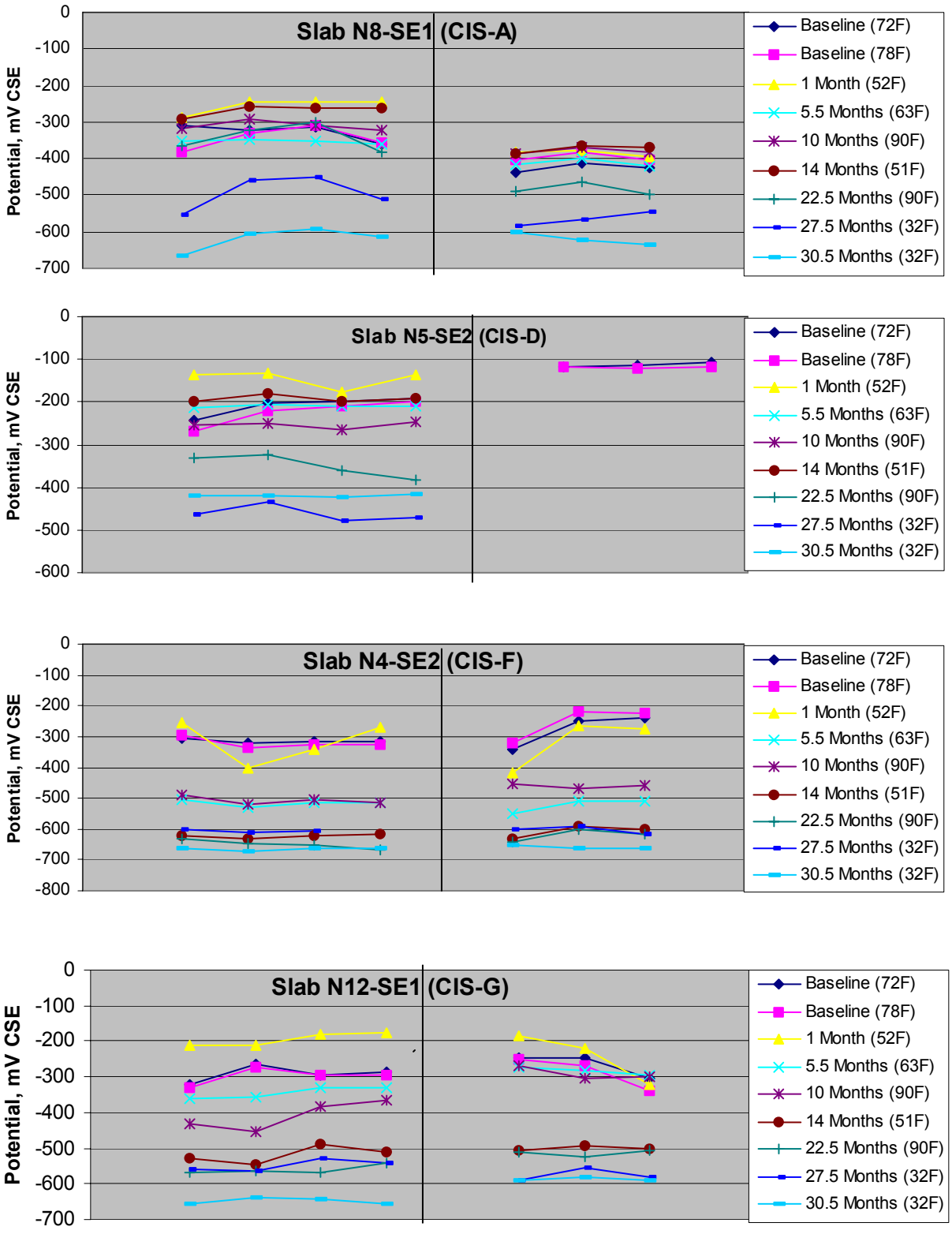

Figure D-15: Half-cell Potentials for all Slabs vs. Time.

About one month after repair, the macrocell current for slabs N4-SE2 (CIS-F) and N12-SE1 (CIS-G) generally increased (such that the ECR's were anodic to the uncoated bottom steel) with exposure time. Over the same period, the AC resistance between ECR's and uncoated steel in these slabs continually decreased. One month after repairs were installed, potentials measurements on slab N4-SE2 were generally similar to the pre-repair measurements, whereas on slab N12-SE1 potentials were more passive immediately after repair. Subsequently, for slab N4-SE2, potentials became more active and remained so for the duration of the exposure period and for slab N12-SE1, potentials became increasingly active through 30.5 months of exposure.

Straight Bars

After repair, the macrocell current for slabs N8-SE1 (CIS-B) and N12-SE1 (CIS-G) remained relatively constant and either near zero (in the case of slab N8-SE1) or cathodic to the uncoated bottom steel (for slab N12-SE1) through approximately 14 months of exposure. Subsequently, there was a marked increased in the macrocell current (such that the ECR's were anodic to the uncoated bottom steel) through 30.5 months of exposure. Potentials for slab N8-SE1 remained relatively constant and active through 14 months of exposure. Subsequently, these became increasingly active for the duration of the exposure period. The straight bars in this slab were not repaired. For slab N12-SE1, potentials were generally similar to the pre-repair measurements through about 10 months of exposure. After 14 months of exposure, potentials became more active and remained so for the duration of the exposure period.

Between about 1 and 5.5 months after repair, the macrocell current for slab N4-SE2 (CIS-F) increased from approximately 0 to 300 microamps (i.e. the ECR became anodic to the uncoated bottom steel) and then remained relatively constant for the duration of the exposure period.

Potentials one month after repairs were slightly more active than the pre-repair measurements. Thereafter, the potentials became more active and remained so for the duration of the exposure period.

The AC resistance between ECR's and uncoated steel in all three slabs continuously decreased throughout the exposure period.

None of the repair options installed on the existing specimens exhibited sufficient level of protection. It should be noted that the bars were not completely exposed on all sides and that is expected to significantly impact the performance of the repair options.

BRIDGE SUBSTRUCTURE COMPONENT FIELD STUDY

Experimental Setup

A vital part of this project involved field validation studies of select repair and rehabilitation strategies, including crack repair and patching. One of the test sites selected for these investigations involved corrosion damaged substructure components on the Seven Mile Bridge in Florida. This bridge, which is part of US-1 in the Florida Keys, was selected to represent corrosion induced concrete deterioration as a result of marine exposure. The bridge has a total of 266 bents, an overall length of 10.93 km (35,863 ft), and a deck width of 10.97 m (36 ft) that consists of two travel lanes. Construction of the bridge was completed in 1980. The substructure consists of 910 mm (36-in.) diameter columns that terminate in drilled shafts with one strut beam between each column pair (see Figure D-16). There are two columns per bent and these are designated east (EC) and west (WC) in each case. Vertical and horizontal

reinforcement in the columns consists of 31.75 mm (#10) and 15.88 mm (#5) epoxy-coated bars, respectively.

Corrosion of the epoxy-coated rebars was first noted in 1988 when spalling was encountered on 8 bents. The damage progressively increased and, as of 1995, the total number of corrosion damaged bents was 264. A metallized zinc cathodic protection system was used as a corrosion control measure on several columns. Based on information provided by the Florida Department of Transportation (FDOT), a total of 56 spalled columns were metallized as of early 1995. The most recent repair contract, which was completed in 1998, involved re-application of the zinc anode as well as new applications on other columns. Depending on the extent of corrosion-induced deterioration on each column, zinc was either applied directly onto exposed and cleaned reinforcing steel and surrounding concrete without patching or on the surface of patched areas.

Based on information provided by FDOT regarding the extent of concrete damage on the columns and the availability of specific columns for the NCHRP 10-37C project, a total of 39 columns were identified for inclusion in the patch repair portion of the study. It was decided that 13 different repair strategies would be investigated with three columns devoted to each. Detailed visual and delamination surveys were conducted on these columns in August and September 1996 for the purpose of selecting specific columns for each repair strategy. The grouping of columns was defined such that the cumulative delaminated area for each repair strategy was as similar as possible. A test area, encompassing the entire circumference of the column to a height 1.83 m (6 feet) measured from the drilled shaft was defined on each column.

Comprehensive technical special provisions were developed covering all aspects related to the installation of the various repair strategies and embedded instrumentation (reference cells and

rebar probes) for monitoring purposes. In May 1998, a second detailed visual and delamination survey was performed and the findings resulted in a few changes in the columns that had been chosen for each repair strategy. Table D-1 shows the final group of three columns designated for each repair strategy. This table also describes the various experimental repair approaches employed. Several combinations of patch repair materials, reinforcing steel coatings, and corrosion inhibitors were included. Repair strategy CIS-A corresponds to the "do-nothing" approach and was considered a control for the study.

Installation of Repair Strategies

Installation of repair strategies was funded by FDOT under a separate bridge rehabilitation project involving the Seven Mile Bridge. The NCHRP 10-37C project team assisted FDOT project inspectors with inspections related to the experimental repair strategies. The installation was completed between June and September 1998.

A silver-silver chloride (Ag-AgCl) reference electrode was installed in one of the patch areas on each of the 39 columns. A total of three rebar probes (two in patch areas and one in sound original concrete just outside the boundary of a patch) were also installed in most columns (see Figure 17). The installation specification provided requirements for electrical continuity related to installation of the rebar probes. In cases where these requirements were not met, rebar probes were not installed. Only two columns were instrumented for repair options CIS-B, CIS-C, CIS-F, and CIS-L and only one column was instrumented for repair options CIS-A, CIS-G, and CIS-J. All three columns were instrumented for the remaining six repair options. Each rebar probe consisted of a 38 mm (1.5 in.) long segment of a 13 mm (#4) rebar and a lead wire connection. Each end of the probe was coated with epoxy prior to installation.

Figure D-16: Photograph of a typical bent of the Seven Mile Bridge.

Figure D-17: Photographs showing installation of the probes and junction box for data collection.

Significant congestion of vertical reinforcement was encountered during construction. Consequently, the specified undercutting requirement was eliminated for vertical bars with a concrete cover exceeding 64 mm (2.5 in.) unless more than 25% of the circumference of the bar was exposed.

In certain instances, the specifications also required chlorides to be added to patch material. Situations where this was required included patching of all rebar probes where these were installed outside repair areas, patching of reference cells on the control columns, and patching of areas on control columns where delaminated concrete was unintentionally removed during the reference cell and rebar probe installation procedures. In all cases, reagent grade NaCl was used at a rate of 8.78 kg/m^3 (14.8 pcy) of concrete. This equates to about 5.34 kg/m^3 (9 pcy) of chloride ions per unit volume of concrete.

The specifications permitted patch material to be placed by troweling or forming; the latter was actually used. The actual area of concrete removal on each column is shown in Table D-9.

Post-Installation Monitoring

Visual and delamination surveys were conducted immediately after repairs were installed. Hurricane Georges, which hit the Florida Keys in September 1998, delayed data collection on embedded instrumentation until December 1998. However, all rebar probes had been connected to their respective grounds since August 1998.

Two other complete evaluations were performed in September 1999 (approximately one year after repair) and January 2001 (approximately 2 ¼ years after repair). These included physical condition evaluations on each column and data collection on embedded instrumentation.

Findings & Discussion

Physical condition evaluations involved visual inspections and delamination surveys of the repaired areas (or damaged areas in the case of the control columns) as well as adjacent areas around the circumference of the columns within the test area.

A hairline crack was observed in a repaired area on column 25EC (CIS-L) during the first visual inspection. A vertical crack developed outside patched areas on column 17EC (CIS-F) about one year after repairs were installed.

Results of the delamination surveys are also presented in Table D-9. With the exceptions discussed below, none of the patched areas exhibited delaminations during the study. A delamination in a patched area was observed on column 17WC (CIS-B) immediately after the installation of the repair and was located at the edge of a patch and had an area less than .093 m^2 (1 sq.ft.). The size of this delamination remained unchanged throughout the study, and therefore, is not attributed to ongoing corrosion. Approximately 2 ¼ years after the installation of the repairs, a delamination developed in a patch located on column 28WC (CIS-H).

Of the 39 columns included in the evaluation, 11 exhibited delaminations in original concrete within the test area which grew in size with time. These 11 columns were distributed in 7 of the 13 repairs options evaluated. Three of these columns belonged to the no-repair options (CIS-A), two each to repair options CIS-C and CIS-D, and one each to repair options CIS-B, CIS-F, CIS-J, and CIS-L. All delaminations found outside patched areas were located some distance away from any patch (i.e. the delaminations were not at the boundary of patches).

Corrosion potential measurements obtained from Ag-AgCl reference cells (embedded in patched areas) are presented in Figure D-18. In each case, the average potential is shown for each repair strategy. The average potential for all repair options become more passive with time.

Rebar probe lead wires were shorted with their respective ground wires except when data were collected. At the time of measurement, an appropriately sized resistor was temporarily placed in the circuit and the millivolt drop across the resistor was recorded. In each case, the resistor used had a value less than 10% of the AC resistance measured between each set of rebar probe and ground lead wires. Resistors were installed and measurements were taken without interrupting the circuit (i.e. the shorted connection between each set of lead wires was not removed until the resistor and another set of lead wires had been temporarily installed). Polarity was such that a negative reading indicated that the probe was anodic to the ECR it was connected to. However, with respect to probes installed in patched areas (these probes were treated with the same repair strategy as the ECR's in the same patch area), current flowing to or from the probe would indicate that the repair strategy failed (either the repair of the ECR in the patch or the repair applied to the probe). Consequently, the magnitude of the current density through these probes is considered more relevant than the polarity of the readings. The situation is different for probes installed outside of patched areas. In this case, the polarity and magnitude of the readings are considered to be important. However, it is not be possible to determine where the corrosion cell is located and to what steel the probe is anodic or cathodic to.

Figure D-19 shows the average rebar probe current density for probes installed in patched and unpatched areas for the various classes of repair options. Repair options CIS-C (Patch Material B) and CIS-D (Coating A and Patch Material C) exhibited probe currents closest to an ideal for

Table D-9: Percent Area Repaired & Results of Delamination Surveys.

Repair Options	% Area Patched	Delamination Survey Results, % of Total Area Under Study					
		Within Repaired Areas			Outside Repaired Areas		
		1998	1999	2001	1998	1999	2001
CIS-A	18.25%	18.25%	18.25%	18.25%		2.26%	22.46%
CIS-B	16.81%	0.39%	0.39%	0.39%		6.47%	6.47%
CIS-C	18.54%				4.63%	4.63%	5.78%
CIS-D	16.73%					0.72%	1.43%
CIS-E	23.84%						
CIS-F	29.08%					1.67%	2.36%
CIS-G	20.55%						
CIS-H	18.53%			0.59%			
CIS-I	21.47%						
CIS-J	23.52%					0.29%	1.05%
CIS-L	20.44%					0.54%	1.84%
CIS-M	17.72%						
CIS-N	19.22%						

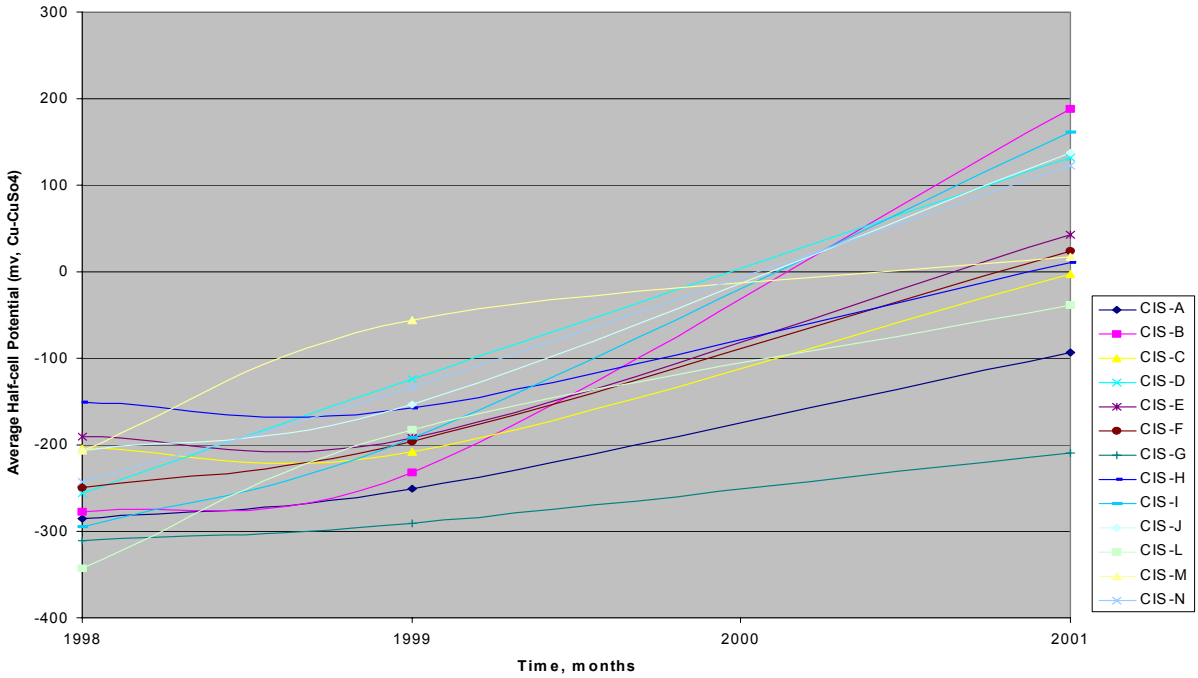

Figure D-18: Average Half-cell Potentials of Repair Options vs. Time.

Probes located in repairs.

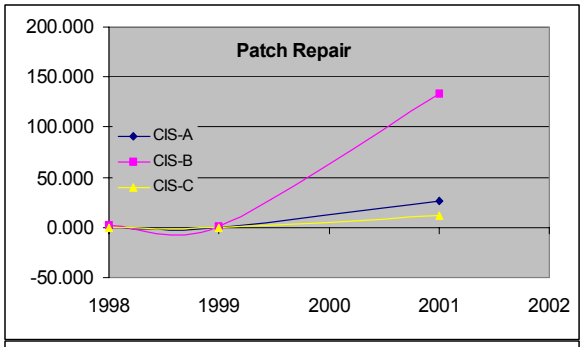

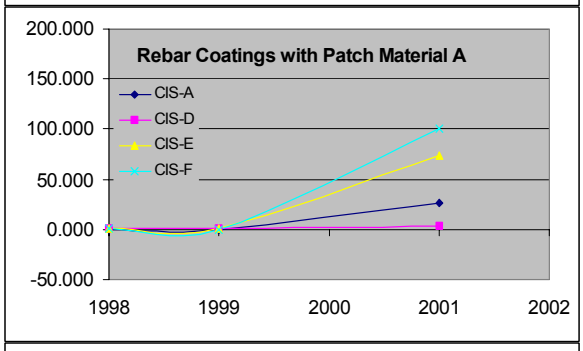

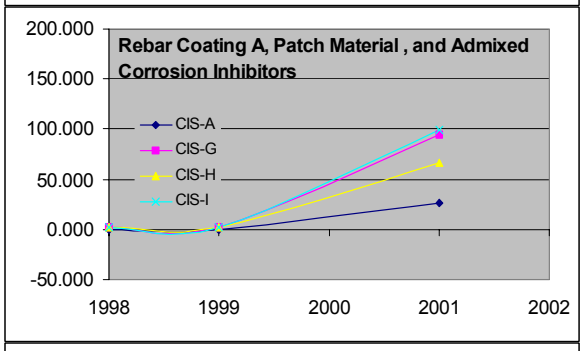

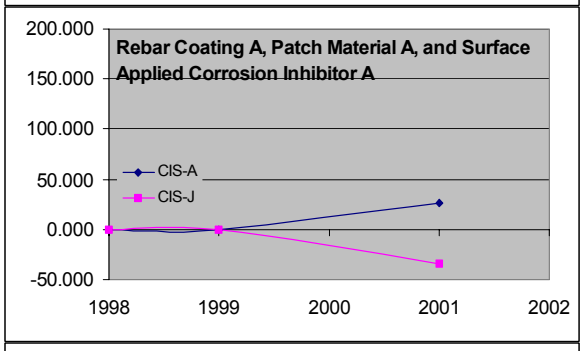

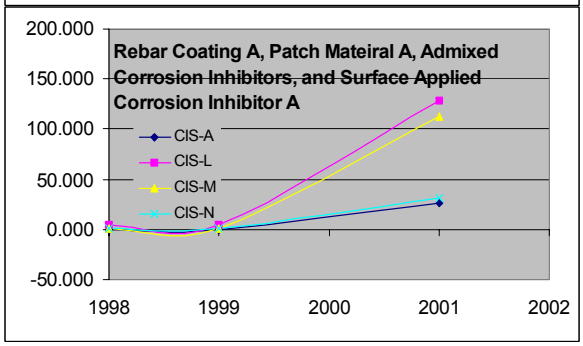

Probes located outside of repair areas.

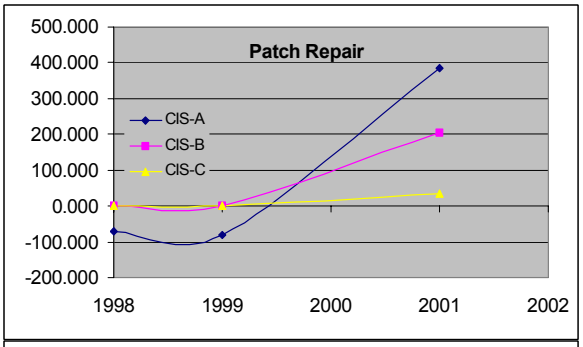

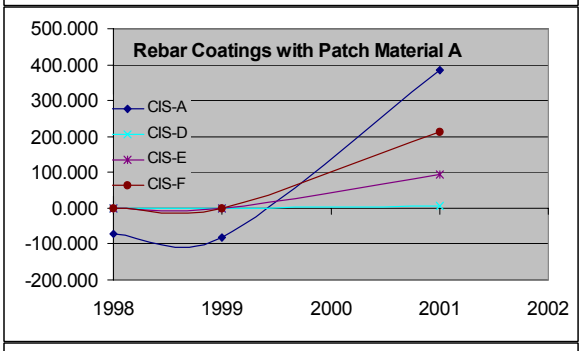

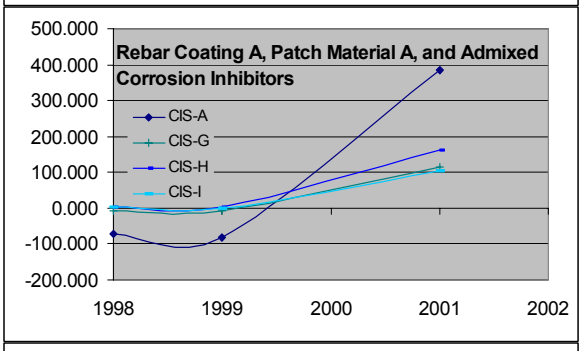

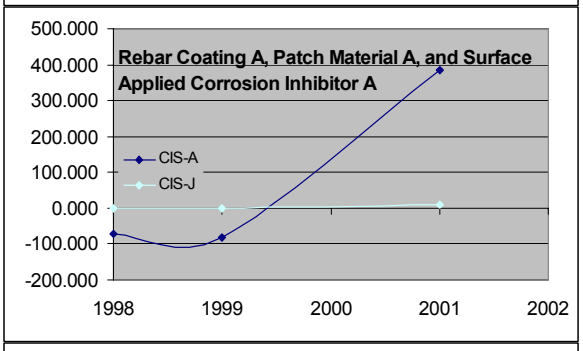

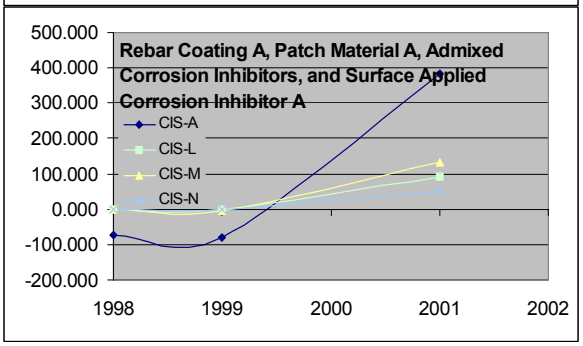

Figure D-19: Probe Current (µA) vs Time.

probes located inside repaired areas. Whereas, CIS-C, CIS-D, and CIS-J (Coating A, Patch Material C, and Corrosion Inhibitor A) exhibited very low average current for probes located outside the repair area. It should be noted that repair options CIS-G to CIS-N included the use of Coating A and Patch Material C in conjunction with admixed and/or surface applied corrosion inhibitor and these exhibited average probe currents much larger than that exhibited by CIS-D. This suggests that the use of corrosion inhibitors reduced the efficacy of Coating A when used in conjunction with Patch Material C.

AC resistance measured between each probe and its ground is presented in Table D-10. In general the probe resistances remained constant (i.e. within the same order of magnitude) with time with the exception of CIS-H and CIS-N. The large increase or decrease in average resistance for these repair options resulted from variation in one probe.

Table D-10: AC Resistance between Probes and Probe Grounds.

Repair Options	AC Resistance between Probe and Probe Ground Connection					
	Average of Probes 1 and 2			Average of Probe 3		
	1998	1999	2001	1998	1999	2001
CIS-A	585	695	645	35	25	34
CIS-B	470	552	738	415	500	2,155
CIS-C	2,225	2,225	5,075	165,000	210,000	150,000
CIS-D	3,233	3,350	2,255	3,133	2,933	1,583
CIS-E	512	622	2,075	9,833	10,600	16,383
CIS-F	1,060	1,630	5,575	7,425	6,440	2,050
CIS-G	360	570	5,350	350	300	5,700
CIS-H	357	488	13,168	917	990	887
CIS-I	1,041	1,015	2,143	720	787	2,697
CIS-J	2,350	2,300	3,500	1,700	1,900	1,800
CIS-L	1,925	1,923	1,068	910	940	1,445
CIS-M	9,365	9,422	4,578	1,467	1,560	1,470
CIS-N	1,455	1,490	790	15,750	15,377	1,083

REFERENCES

1. Clear, K.C., Part I “Effectiveness of Epoxy Coated Reinforcing Steel,” in “CRSI Performance Research: Epoxy Coated Reinforcing Steel,” Interim Report, Concrete Reinforcing Steel Institute, Schaumburg, IL, 1992.

2. Sohanghpurwala, A.A., and Clear, K.C., "Effectiveness of Epoxy Coatings in Preventing Corrosion of Reinforcing Steel", Transportation Research Record No. 1268, Transportation Research Board, Washington, D.C., January 1990.

APPENDIX E

EVALUATION OF THE EFFECTIVENESS OF IMPRESSED CURRENT CATHODIC PROTECTION

INTRODUCTION

Cathodic protection (cp) is the only documented method for which long-term service experience is available for controlling corrosion of black reinforcement in concrete. Application of this approach to ECR, however, requires that two possible limitations be overcome. The first pertains to the fact that electrical continuity throughout the ECR network is likely to be limited, in which case both a lack of protection and stray current corrosion may result. This difficulty can be overcome by conducting a continuity determination and establishing such continuity to the extent that this is determined to be necessary. However, such an undertaking may be costly and render alternative approaches more appropriate. The second limitation addresses the possibility that protective current may not be adequately distributed to steel at locations where the coating has become disbonded. Thus, the confined geometry beneath the coating combined with the fact that the electrolyte here may be of relatively high resistivity can give rise to attenuation of the otherwise protective current and under-protection beyond a certain distance. Such corrosion has been shown to be significant in the case of cathodically protected coated buried pipelines. For the purpose of addressing this, a series of experiments was performed where ECR specimens with various levels of coating quality and defects were polarized in accelerated experiments that employed salty sand.

In anticipation of the future need to use cp on existing ECR structures, Taylor, et.al.[1] conducted a laboratory study involving concrete samples reinforced with ECR containing intentional coating defects. The objectives of this investigation were to determine if cp can effectively mitigate

corrosion of ECR without adversely affecting the rebar/concrete interface and to examine the effect of cp on the disbonding characteristics of the coating/rebar interface in the concrete environment. The concrete specimens were designed to allow for cathodic polarization, electrochemical interrogation, and mechanical testing of rebar pullout characteristics. Cathodic polarization was conducted at four current levels (0X, 1X, 5X and 10X of 1.08 $\mu A/cm^2$, scaled to a 1% coating defect area) and three time intervals. Five replicate samples were employed for each condition. Open-circuit potential measurements, electrochemical impedance spectroscopy, and linear polarization were performed on each sample prior to, during, and after the application of cp. After each cp exposure, the load versus strain behavior of the rebar was quantified in an MTS load frame using LVDT for strain determination. All electrochemical tests indicated that the cp current levels and application times used were effective in preventing corrosion of the embedded ECR. The tests also revealed that the cp levels and times had no effect on the splitting failure characteristics, at a 95% confidence level. However, EIS tests indicated that the coating was delaminating at the periphery of defects, which was verified by post mortem SEM analysis. Although the levels of delamination in this study did not affect mechanical performance, it was recommended that the use of a protective level that does not induce film disbonding be explored.

In another study, three bridge structures (the Long Key Bridge, Niles Channel Bridge, and Seven Mile Bridge; all located on U.S. Highway 1 in the Florida Keys) were selected for application and evaluation of sprayed zinc anodes on substructure components containing ECR.[2] All three structures had experienced severe corrosion damage. The Niles Channel Bridge had previously been metallized in November 1988, thus providing an opportunity to acquire long-term performance information. The behavior of the metallized structures was found to be encouraging. The zinc coatings remained in place and retained reasonable physical integrity

after up to 4.5 years of service in the subtropical marine environment. Adhesion between the zinc coating and the concrete remained high. While some signs of anode wastage were evident on the oldest installation (Niles Channel Bridge), most of the metallizing was still providing protective current. Test results indicated that current delivery was maintained for over 4.5 years at about 0.5 mA/ft^2 (0.5 $\mu A/cm^2$) of concrete in structures containing corroded ECR. While there was little evidence with regard to the current density levels necessary to protect ECR, design values for corrosion protection of buried pipeline steel with a coating in poor condition are typically one tenth or less of those specified for bare steel. Results from the subject bridges amply met this criterion. Progressing damage was reported on piers that had not been cathodically protected. In contrast, no new cracking or other corrosion related damage was observed on piers that had been cathodically protected for 4.5 years.

As part of the NCHRP 10-37C project, limited experiments were performed to verify the effectiveness of cp in combating corrosion of ECR using 1) salty sand specimens and 2) six aged concrete slabs from previous ECR studies. These are discussed separately below.

SALTY SAND EXPERIMENTS

A series of experiments was performed where ECR specimens with various levels of coating quality and defects were polarized in accelerated experiments that employed salty sand. The purpose of these was to determine the extent to which protection is achieved beneath disbonded coatings, as discussed above.

Experimental Procedure

Two sets of experiments were performed, where the first was largely for screening purposes and the second for determination of cp feasibility in the case of ECR. These involved number five ECRs that were obtained from three sources, **A, D** and **F**, as so designated in the initial NCHRP 10-37 study (3). Source **A** and **F** ECRs were judged previously as "intermediate" performers, whereas **D** bars were "good." The ECRs were 30.5 cm (12 in.) long, and some specimens from source **A** contained holidays due to insufficient availability of defect-free stock. Individual holidays were located and counted using a M-1 holiday detector and marked with a permanent marker. Specimens were prepared such that the test areas contained no bare areas but pin-holes only, as indicated by the holiday detector. Five artificial circular defects (diameter = 3.2 mm or 1/8 in.) were introduced per specimen; and if the specimen had holidays, as some **A** source bars did, then the intentional holidays were overlaid upon these to minimize the total number of defects.

Two test cells, each consisting of an ECR working electrode (WE), a 3.8 cm (1.5 in.) mixed metal oxide titanium ribbon reference electrode (Ti RE) located 2.5 cm away from the WE, and a surrounding Elgard mixed metal oxide titanium mesh counter electrode (CE) ring, were placed in individual 18.9 liter (5-gallon) polyethylene containers. Figure E-1 provides a schematic illustration of the test setup. Five batches of wet sand were prepared by mixing commercially available sand with a simulated pore water solution, where the latter consisted of 0.20 w/o calcium hydroxide, 1.00 w/o potassium hydroxide, 92.45 w/o sodium hydroxide, 3.20 w/o potassium chloride, and distilled water (93.15 w/o). Target resistivity of the conditioned sand in a standard soil box, as measured by a Nilsson soil resistance meter, was 10 KΩ-cm Once resistivity of each batch was within 5 percent of the target value, the wet sand was transferred to

a test bucket and the in-box resistance was measured using the Nilsson meter. These initial readings ranged from 340 to 500 Ω and increased with exposure time. Upon termination of testing, it was found that condensation, as evidenced by water droplets under the lid of each container, had occurred, indicating that evaporation of moisture from the wet sand may have been responsible for the increased resistance. Table E-1 summaries these resistances and lists the number and density of coating defects for each specimen as well as the polarization history.

During the 12 weeks of testing, three potential readings were made for each Ti RE with respect to an external saturated calomel electrode (SCE) (see the last two columns of Table E-1 for the initial and final values). The general trend was that the initial potential readings were negative but they became more positive within a relatively brief time. Potential change of the Ti RE throughout the tests was such that a predetermined polarization level could not be maintained, since the potentiostats were operated in conjunction with the embedded Ti RE. However, these variations were small compared to the magnitude of polarization, which was a minimum of 500 mV, thus rendering the procedure at least qualitatively valid.

Seven different combinations of polarization were employed, as listed in Table E-1. Thus, ECR #7 was polarized at +1.0 V vs. Ti RE (V_{Ti}) for 12 weeks and three other specimens (ECRs #8-10) were initially polarized at the same potential for four weeks. This was to simulate ECRs with actively corroding bare areas. Cathodic protection was then simulated by polarizing at three different levels. A control (no polarization) specimen was also employed. For comparison, cathodic polarization at these same three levels was applied to six other specimens (ECRs #11-16) without prior anodic polarization. This was intended to provide information regarding ECR behavior when bars are subjected to cp at locations where corrosion has not yet initiated.

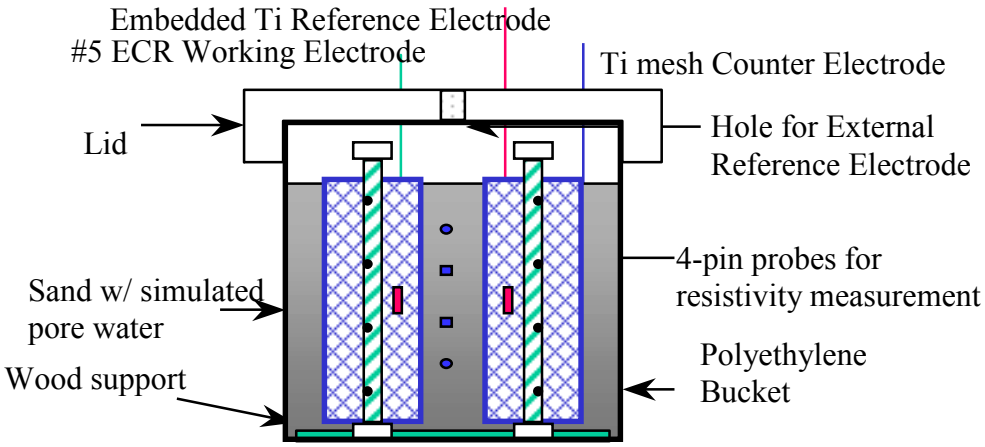

Figure E-1: Schematic of the Salty Sand Experimental Setup.

Table E-1: Test Variables for the Salty Sand Experiments

Specimen ID (Source)	Polarization and Duration	Number of Initial Defects* A.D. (Beep) ? Total	In-box Resistance (?)		Potential Ti RE vs. SCE (mV)	
			Initial	Final	Initial	Final
ECR #7 (D)	"+"1.0 V_{Ti} for 12 weeks	4 (1) ? 4	450	780	-100	84
ECR #8 (D)	"+"1.0 V_{Ti} for 4 weeks followed by free corroding for 8 weeks	0 (6) ? 6	450	780	-63	7
ECR #9 (A)	"+"1.0 V_{Ti} for 4 weeks followed by -1.0 V_{Ti} for 8 weeks	4 (5) ? 7	400	680	-361	-147
ECR #10 (A)	"+"1.0 V_{Ti} for 4 weeks followed by -1.5 V_{Ti} for 8 weeks	4 (5) ? 8	400	680	-155	86
ECR #11 (A)	"-"1.0 V_{Ti} for 12 weeks	4 (4) ? 7	460	820	-130	82
ECR #12 (A)	"-"1.5 V_{Ti} for 12 weeks	4 (5) ? 5	460	820	-155	46
ECR #13 (A)	"-"0.5 V_{Ti} for 12 weeks	4 (1) ? 4	340	565	-160	47
ECR #14 (A)	"-"1.0 V_{Ti} for 12 weeks	4 (2) ? 4	340	565	-133	69
ECR #15 (F)	"-"1.5 V_{Ti} for 12 weeks	4 (0) ? 4	500	640	N/A	N/A
ECR #16 (F)	"-"1.0 V_{Ti} for 12 weeks	4 (0) ? 4	500	640	N/A	N/A

- Defect nomenclature key:
  First digit (A.D.) – Number of artificial defects.
  Second digit () – Number of holiday detector beeps.
  Third digit – Total defects.
  Note: The total number of defects is not necessarily the sum of the two component types because the two types sometimes superimposed.

Physical condition of the ECRs in response to polarization testing in salty sand was characterized subsequent to the exposures. This involved removing the disbonded coating and estimating the degree of coating delamination. As many as six knife adhesion tests were performed per specimen at sites where the coating remained intact after exposure.

A potentiodynamic (pd) polarization scan was performed upon ECRs #15 and 16 just before and approximately 20 hours after polarization testing in an attempt to characterize the electrochemical behavior of the specimens. All scans began after steady-state had been reached, as indicated by a stable open-circuit potential. Each scan started at –1.5 V relative to the open circuit potential (ocp) and proceeded in the noble direction at a rate of 1 mV/s with a constant scan increment of 5 mV. Potential sweeps were terminated at +1.5 V relative to the ocp. EG&G M352 software with automatic IR compensation was used for the data acquisition. Resistance between the ECR and embedded Ti RE (separation distance 2.5 cm) was also measured using the Nilsson meter.

Findings and Discussion

Coating Delamination

The coating delamination results are listed in Table E-2. These indicate that the most negative cathodic polarization (-1.5 V_{Ti} for ECRs #10, 12 and 15) produced the most extensive coating delamination regardless of prior anodic polarization. On the other hand, the least delamination occurred for ECR #8 which was subjected to four weeks of anodic polarization at +1.0 V_{Ti} followed by eight weeks of free corrosion. However, the coating on this ECR (#8) contained six holidays in lieu of the intentional defects (see Table E-1). ECR #7 with four artificial defects

Table E-2: Test Results for Salty Sand Experiments.

Specimen ID (Source)	Polarization and Duration	Coating Delamination, Percent	Ranking
ECR #7 (D)	"+"1.0 V_{Ti} for 12 weeks	< 5	2
ECR #8 (D)	"+"1.0 V_{Ti} for 4 weeks followed by free corroding for 8 weeks	<1	1-Best
ECR #9 (A)	"+"1.0 V_{Ti} for 4 weeks followed by -1.0 V_{Ti} for 8 weeks	50	4
ECR #10 (A)	"+"1.0 V_{Ti} for 4 weeks followed by -1.5 V_{Ti} for 8 weeks	96	7
ECR #11 (A)	"-"1.0 V_{Ti} for 12 weeks	65	6
ECR #12 (A)	"-"1.5 V_{Ti} for 12 weeks	98	8
ECR #13 (A)	"-"0.5 V_{Ti} for 12 weeks	30	3
ECR #14 (A)	"-"1.0 V_{Ti} for 12 weeks	60	5
ECR #15 (F)	"-"1.5 V_{Ti} for 12 weeks	100	9-Worst
ECR #16 (F)	"-"1.0 V_{Ti} for 12 weeks	100	9-Worst

exhibited the second least delamination after anodic polarization at +1.0 V_{Ti} for 12 weeks. Thus, for the level of cathodic polarization involved here (-1.5 V_{Ti}), anodic polarization alone did not induce noticeable delamination, thereby indicating that cathodic processes were the primary, if not sole, mechanism of coating disbondment.

The ECRs that underwent lesser amounts of cathodic polarization exhibited various degrees of delamination depending upon polarization history. ECR #13 exhibited approximately 30 percent delamination after 12 weeks at –0.5 V_{Ti} and ECRs #9, 11 and 14, each of which were polarized to –1.0 V_{Ti}, showed about 50-65 percent delamination over the same period. However, ECR #16, which was polarized to –1.0 V_{Ti} for 12 weeks, exhibited 100% delamination. Results from the NCHRP 10-37 study[3] indicated that ECRs from source **F**, as ECR #16 was, exhibited relatively weak adhesion in hot water tests.

For the same level of cathodic polarization, ECRs that had been subjected to prior anodic polarization exhibited less disbondment than those without anodic polarization. Apparently, the cathodic reaction rate at corroded bare areas was slower than at clean bare area defect sites of non-anodically polarized specimens.

Potentiodynamic Scan Data

The baseline and final polarization curves for ECRs #15 and 16 are shown in Figures E-2 and E-3, respectively. The baseline curves exhibit almost identical shapes, including some indications of passive behavior. Within the potential sweep range, the apparent passive zone extended more than 700 mV with a passive current (I_{pass}) of approximately 3 μA. This indicates the formation of a passive film on bare areas exposed to the alkaline, chloride environment. A transpassive or pitting region occurred roughly over the current range from 10 μA to 1 mA for both ECRs. The

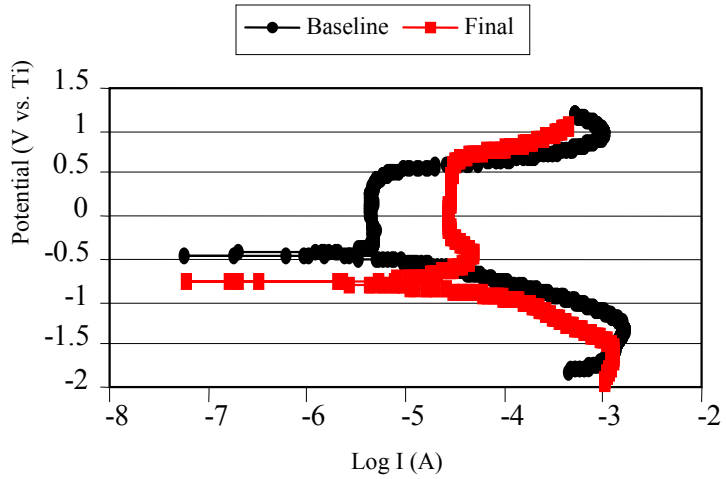

Figure E-2: Potentiodynamic Polarization Scans before and after Salty Sand Experiments for ECR #16 (-1.5 V_{Ti} for 12 Weeks).

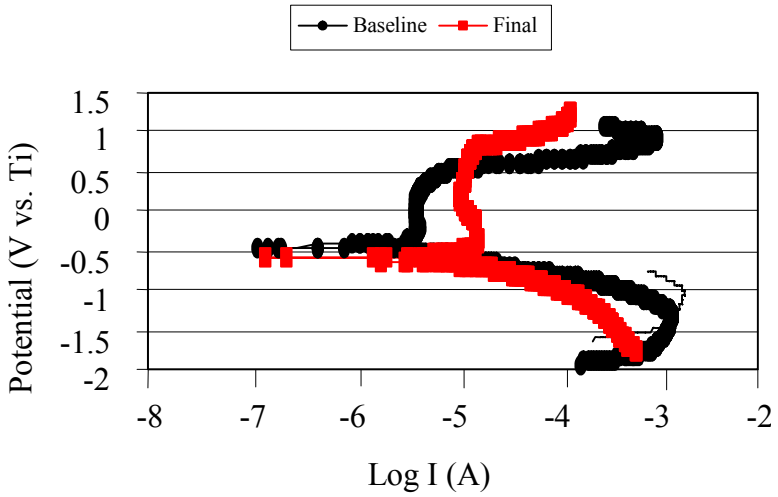

Figure E-3: Potentiodynamic Polarization Scans before and after Salty Sand Experiment for ECR #16 (-1.5 V_{Ti} for 12 Weeks).

anodic portion of the curves near +1.0 V_{Ti} exhibited fluctuations that may have been due to secondary passivity.

The baseline cathodic polarization curves exhibit a tail in the potential range near –2.0 V_{Ti}. This is thought to have resulted from increased bare areas (indicated by increasing current) from cathodic delamination of the coating around the artificial defects at this range of excessively negative potential. This effect decreased as potential became more positive, and a limiting current (I_L) was approached in the neighborhood of log I (A) = –3. The finding that no such curvature was apparent in the final cathodic polarization curves is consistent with this explanation.

Three distinctions between the initial and final pd curves, in addition to the one mentioned above (cathodic tail), are apparent. The first is an active shift of the ocp for the final curves to near –0.5 V_{Ti} with specimens that experienced greater cathodic polarization exhibiting a larger shift. Second, the applied cathodic current ($I_{app/c} = I_c – I_a$) for the final scans was less at any polarized potential at the end of the test compared to initially, indicating less current demand. Lastly, the final anodic curves show increased I_{pass} and a widen passive zone compared to the baseline curves. It is thought that the former was due to increased passivated bare areas beneath the disbonded coating adjacent to coating defects and the latter to increased pH from production of hydroxyl ions through the cathodic reduction reaction. Presence of chloride ions in wet sand did not appear to compromise integrity of the passive film for cathodically polarized ECR. This may have been a consequence of electromigration of this species away from the steel.

No information about degree of disbondment could be obtained from the experimental pd scan data. However, this technique can be employed to characterize the electrochemical response

change that transpires at defects in conjunction with polarization. Here it was found that cp can induce extensive coating disbondment, although the rate and extent of this are unknown. Also, this rate was apparently greater the more negative the potential; but at the same time, cp did effectively mitigate corrosion beneath the delaminated coating. Experimental results indicate that a corrosion-free condition can be maintained for almost 100 percent delaminated ECRs for up to 12 weeks. Longer-term study is necessary to investigate the effectiveness of cp for control of ECR corrosion where different physical conditions are involved; for example, different coating thicknesses, percentages of bare area, and extents of delamination. Also potentially important are environmental variables, including degree of water saturation, chloride concentration, resistivity, and pH. However, based upon the information available and despite the fact that cp can cause coating disbondment, no indications that this method could not be relied upon to provide adequate corrosion control of ECR were apparent.

AGED SPECIMENS FROM PREVIOUS STUDIES

History of Aged Slabs

ECR has been extensively used historically in bridge decks with uncoated bottom mat reinforcing steel while other structures have utilized coated steel in the bottom mat. A study was initiated in 1991 to investigate these situations with regard to providing corrosion protection to the top ECR's using cp. Concrete slabs with two mats of reinforcing steel were employed and cp was initially applied to four of these in late 1991[4]. All slabs were highly chloride contaminated to the level of the top reinforcing steel and had been involved in extensive research studies on ECR (without cp). The slabs and their condition at the time the cp study was initiated are briefly discussed below[4].

Slab 1 had ECR in both mats with the top mat undergoing the early stages of deterioration. Slab 2 had the same ECR, but with an uncoated bottom mat. Both slabs were 30 cm (1 ft.) wide by 60 cm (2 ft.) deep, long-term outdoor exposure slabs[4]. Slabs 3 and 4 were from a bent bar slab (with bent and straight ECR in the top mat) which was cut in half [5,6]. Thus, slab 3 had a severely corroded bent ECR in the top mat while slab 4 had severely corroded straight ECR's in the top mat. Both slabs had straight bare rebar in the bottom mat. Slabs 3 and 4 exhibited corrosion induced cracking at the time the cp study was initiated.

In addition to these four slabs, there were two control slabs that were not cathodically protected[4,5]. One slab had ECR in both mats (slab 5 in this report) and the other employed ECR in the top mat only (slab 6 in this report).

Details of the cp study (through December 1992) are provided in Reference 3 and a summary through 2 years of cp is available in Reference 5. In all cases, the cathodic protection anode was installed on the top slab surface, and the top and bottom reinforcing steel remained interconnected throughout the study. Initially, the cp system voltages required to maintain a constant total rebar current density of 1 $\mu A/cm^2$ (1 mA/ft^2) ranged from 1.5 to 3.5 volts. After 2 years of cp, the system voltages ranged from 3.5 to 4.8 volts. Half-cell potentials were monitored at three to five locations per slab, including via wells drilled close to the top mat bars. Initial and 2 year polarization/depolarization exceeded 100 mV at all sites monitored. It was found that the polarization was greatest for the slab with ECR in both mats and least for the slab exhibiting the highest corrosion rate before cp was applied. It was also reported that more current was received by the uncoated bottom mat steel in three of the slabs than the bottom ECR in the other slab. However, no related problems were found with regard to providing adequate protection of the top steel in any of the slabs.

During the 2 year test period, the control slabs exhibited progressive rust staining, cracking, and delamination. In contrast, no additional cracking, rust staining or delaminations occurred on the cathodically protected ECR slabs.

The slabs remained under cp with data being collected periodically through July 1996. By July 1996, the slabs had been cathodically protected for over 4.5 years at a constant total rebar current density of 1 $\mu A/cm^2$ (1 mA/ft^2). All historical information including specimen fabrication, ECR details, exposure history, and corrosion evaluation data can be found in References 5 through 7.

As part of the NCHRP 10-37C project, the above six slabs were transported to Concorr, Inc.'s outdoor exposure test site in northern Virginia in July 1996. The scope of work for these slabs involved maintaining cathodic protection for an additional 2.5 years at the same level used previously, periodically collecting standard cp data during this time and regularly performing visual and delamination surveys. ECR autopsies were to be conducted at the conclusion of the study.

Experimental Procedure

Initial data were collected and the cp systems were re-activated in September 1996. The slabs remained under cp through March 1999. During that time, cp system voltages and current outputs were monitored daily and standard depolarization tests were performed twice; after the slabs had been cathodically protected for a total of 6.2 and 7.2 years. At the conclusion of the study (after the slabs had been under cp for a total of 7.2 years), autopsies were performed on many of the ECR's.

Findings and Discussion

Figure E-4 shows plots of cp current output and system voltage for all slabs for the 2.5 year monitoring period and Table E-3 presents a statistical summary of these data. The current output for each slab was maintained at a relatively constant level of 1 $\mu A/cm^2$ (1 mA/ft^2) of total rebar. System voltages for all four slabs averaged from 3.4 to 4.5 volts (ranged from 1.5 to 9.5 volts) during the same period. The average system voltages (after 7.2 years of cp) were similar to the data collected after 2 years of cp. Figure E-5 presents the average percent of the total cp current that was received by the top ECR's in each slab. As found in the earlier study, more current was received by the uncoated bottom mat steel in three of the slabs than the bottom ECR in the other slab. However, as shown in Table E-3, the average current density on the top ECR's in all the slabs ranged from 2.5 to 3.4 $\mu A/cm^2$ (2.5 to 3.4 mA/ft^2).

Average 4-hour depolarization values (see Figure E-6) after a total of 6.2 and 7.2 years of cp exceeded 100 mV for slabs 1, 2, and 3. Four hour depolarization values for slab 4 exceeded 100 mV after 6.2 years of cp, but averaged less than 100 mV after 7.2 years of cp. However, the average 24-hour depolarization value for this slab after 7.2 years of cp was 237 mV.

Based on conventional criteria for effective cp of bare reinforcing steel, all top ECR's were adequately cathodically protected for a total of 7.2 years. At the conclusion of the study, visual and delamination surveys did not reveal any new corrosion induced concrete damage on the cp slabs. The reinforcing steel mats in the control slabs were inadvertently uncoupled for the last 17 months of exposure. In spite of this, these slabs exhibited progressive cracking, rust staining, and delaminations with slab 6 (ECR in the top mat only) showing comparatively more damage than slab 5 (ECR in both mats). Slab 6 had delaminations associated with both mats of rebar.

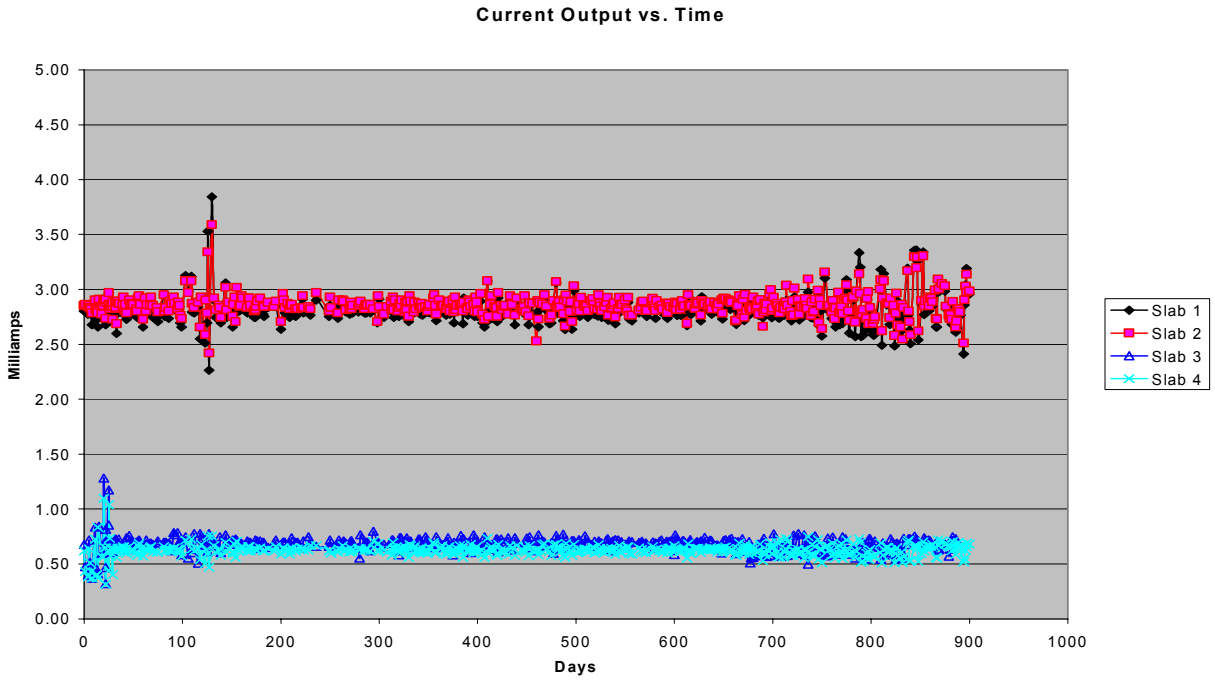

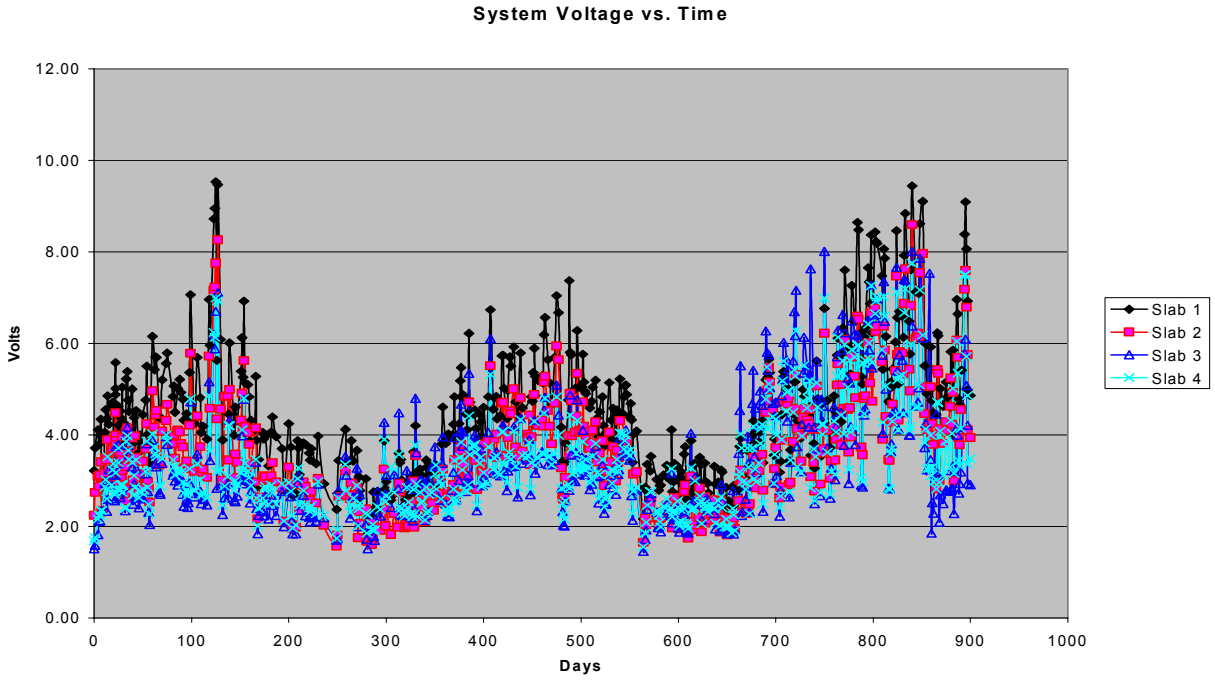

Figure E-4: CP Current Output and System Voltage for al Slabs vs. Time.

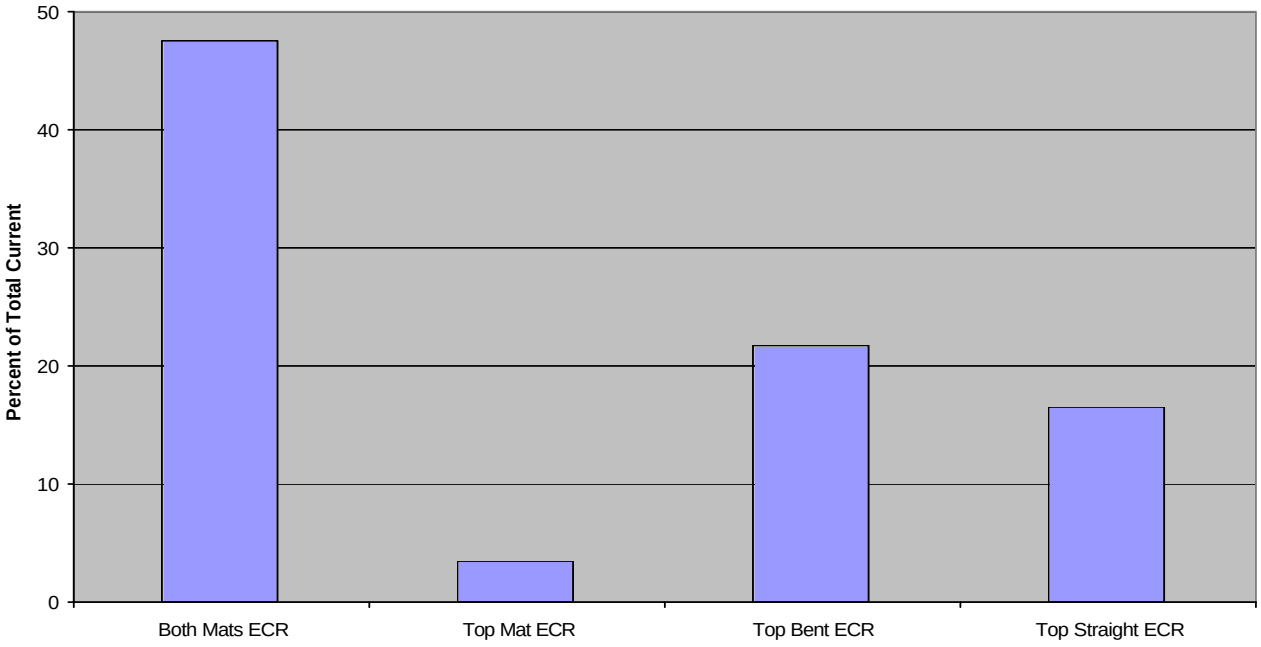

Figure E-5: Average Percentage of Total Current Received by Top ECR.

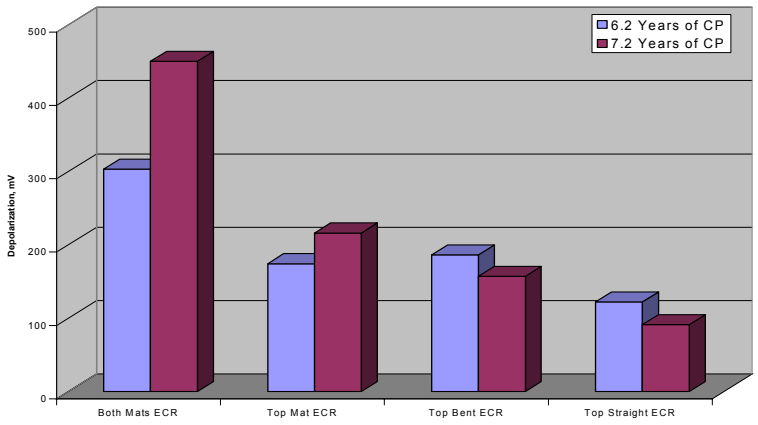

Figure E-6: Average 4-hour Depolarization Values after 6.2 and 7.2 years of CP.

Table E-3: Summary of CP Current Outputs and System Voltages.

Slab	Current Output, mA			Avg Current Density, mA/ft^2			System Voltage, volts		
	Min	Max	Avg	Total	Top Mat	Bot. Mat	Min	Max	Avg
1	2.26	3.84	2.81	1.00	2.53	1.66	1.84	9.53	4.51
2	2.42	3.59	2.86	1.00	2.53	1.66	1.57	8.59	3.62
3	0.32	1.28	0.68	0.99	3.44	1.38	1.45	8.01	3.43
4	0.31	1.10	0.62	0.99	2.84	1.52	1.55	7.75	3.42

After 7.2 years of cp, the ECR's in all slabs were autopsied, including those in the control slabs. A total of 29 ECR's were autopsied. These consisted of four top bars and six bottom bars from slab 1, four top bars in slab 2, one bent top bar in slab 3, two straight top bars in slab 4, four top bars and six bottom bars in control slab 5, and two top bars in control slab 6. The top and bottom traces of each ECR were examined visually and pH tests were conducted. Each side of each ECR was visually examined for bare, mashed, blistered, or rust stained areas and a corrosion rating was assigned. The number of holidays was determined and the coating thickness was measured. Finally, adhesion tests were performed and detailed observations were made of the substrate steel and the underside of the epoxy coating.

Due to the condition of the ECR's in these slabs prior to applying cp (i.e. the ECR's had experienced varying degrees of corrosion at the time cp was applied), results from the autopsy studies did not provide any conclusive information with respect to corrosion mitigation or potential adverse consequences attributable to cp. However, other test results indicated that electrically continuous ECR can be cathodically protected, even when used in conjunction with uncoated rebar. In addition, it was found that adequate corrosion protection can be achieved at or below current densities commonly employed on concrete structures with uncoated reinforcing steel.

REFERENCES

1. Taylor, S. R., Bognaski, D. S., and Clemena, G. G., “Effect of Cathodic Protection on Epoxy-Coated Rebar,” Virginia Transportation Research Council, FHWA/VTRC 98-R5, June 1998.

2. Sagues, A A., and Powers, R. G., “Sprayed Zinc Galvanic Anodes for Concrete Marine Bridge Substructures,” Strategic Highway Research Program, Contract No. SHRP-88-ID024, 1994.

3. Clear, K.C., Hartt, W.H., McIntyre, J.F., and Lee, S.K., "Performance of Epoxy-Coated Reinforcing Steel in Highway Bridges", NCHRP Report No. 370, National Cooperative Highway Research Program, Washington, D.C., 1995.

4. Clear, K.C., “Feasibility of Cathodic Protection of Epoxy Coated Reinforcing Steel in Concrete”, Final Report, Canadian Strategic Highway Research Program, Ottawa, ON, December 1992.

5. Scannell, W.T., and Clear, K.C., "Long Term Outdoor Exposure Evaluation of Concrete Slabs Containing Epoxy-Coated Reinforcing Steel", Transportation Research Record No. 1284, Transportation Research Board, Washington, D.C., January 1990.

6. Clear, K.C., Part I “Effectiveness of Epoxy Coated Reinforcing Steel,” in “CRSI Performance Research: Epoxy Coated Reinforcing Steel,” Interim Report, Concrete Reinforcing Steel Institute, Schaumburg, IL, 1992.

7. Sohanghpurwala, A.A., and Clear, K.C., "Effectiveness of Epoxy Coatings in Preventing Corrosion of Reinforcing Steel", Transportation Research Record No. 1268, Transportation Research Board, Washington, D.C., January 1990.

8. Clear, K.C., Hartt, W.H., McIntyre, J.F., and Lee, S.K., “Performance of Epoxy-Coated Reinforcing Steel in Highway Bridges,” NCHRP Report No. 370, National Cooperative Highway Research Program, Washington, D.C., 1995.

APPENDIX F

DECISION MATRIX

PROCEDURES FOR USING THE DECISION MATRIX

Prior to using the decision matrix field evaluation must be conducted to obtain the following information:

1. Accumulated Damage
2. Chloride ion Distribution at the Steel Depth
3. Condition of the Epoxy Coated Rebars

Obtain accumulated damage information by performing visual and delamination surveys of the subject bridge structure. To obtain chloride ion content distribution at the steel depth, collect either concrete cores and/or powdered concrete samples. Prior to collecting the chloride samples, perform concrete cover survey to obtain average cover or a distribution of concrete cover in the subject element. Concrete cores and/or powdered concrete samples should be collected such that the concrete at the steel depth can be tested in a laboratory in accordance with standard test method described in 'Sampling and Testing for Chloride Ion in Concrete Raw Materials," AASHTO T 260-94. Collect cores containing two intersecting ECR to ascertain the condition of the epoxy coating. Then extract the ECR from the core and document the condition of the ECR.

Once the field and laboratory work is completed, ascertain the damage and probability for corrosion rating using the results of accumulated damage, chloride ion distribution, and condition of the ECR from the following definitions:

Damage Ratings

Negligible: Insufficient damage to warrant a repair or maintenance of the concrete component.

Crack Damage: Detectable damage is in the form of cracking.

Partial Damage: Sufficient delaminations and spalling have occurred to warrant a patch repair of the damaged areas.

Full Surface Damage: Sufficient delaminations and/or spalling has occurred to warrant a full surface repair.

Probability for Corrosion Rating

Low Probability: The concentration of chloride ions and/or carbonation at the steel depth is not sufficient to initiate and sustain corrosion of epoxy coated rebars. No failure of epoxy coating due to corrosion is observed in extracted samples.

Localized Probability: The contamination of chloride ions and/or carbonation is localized. Examples include 1) chloride exposure due to contaminated water runoff in certain sections of the concrete component; 2) chloride exposure primarily through cracks in certain sections of the component; 3) uneven distribution of chloride ions due to exposure conditions.

Medium Probability: This category applies when significant portions of the component (in the order of 20%) are contaminated with chloride ion concentration at the steel depth in excess of the threshold required to initiate corrosion and/or the number of extracted samples exhibiting failure of the epoxy coating are in the order of 30%.

High Probability: This category applies when chloride ion contamination (in excess of the threshold) and/or the failure of epoxy coating due to corrosion is/are prevalent throughout the component, i.e. in the order of 50%..

Once the damage and probability ratings are developed, the decision matrix can be used to obtain potential options for repair and rehabilitation.

To use the decision matrix, first select the appropriate table (Marine Environment or Deicing Salt Environment) based on the exposure condition. Each table is further subdivided into substructure and superstructure elements. Under each of these categories applicable reinforced concrete elements are listed.

For each type of reinforced concrete element, a subcategory of exposure conditions is defined. For each subcategory of exposure condition, four damage categories and four probability categories are used to form a decision matrix. For each cell of the decision matrix, the most appropriate or most commonly used repair and/or protection system is listed. In each instance an attempt has been made to provide an option that will provide the maximum extension in service life of the component. In many instances, more than one choice is provided.

DEFINITIONS

Service Life: time to next repair

Threshold for Corrosion Initiation:	0.71 Kg/m^3 (1.2 pcy) of chloride ions in concrete
Condition of Epoxy-Coated Rebar:	visually observable damage or presence of corrosion
Carbonation:	reduction in the pH of concrete due to reaction with air